Functional Characterization of GmmHO: a Heme Oxygenase from the Tsetse fly *Glossina morsitans morsitans*

Thesis submitted in accordance with the requirements of the University of Liverpool for the degree of Doctor in Philosophy

By

Glauber Pacelli Gomes de Lima

June 2017

Supervisors

Dr. Mark paine

Dr. Gareth Lycett

Dr Lu-Yun Lian

Declaration

This work has not previously been accepted in substance for any degree and is not being currently submitted in candidature for any degree.

Signed ……(Candidate)

Date ……

Statement 1

This thesis is the result of my own investigation, except where otherwise stated. Other sources are acknowledged and bibliography appended.

Signed ……(Candidate)

Date ……

Statement 2

I hereby give my consent for this thesis, if accepted, to be available for photocopying and for inter-library loan, and for the title and summary to be made available to outside organisations.

Signed ……(Candidate)

Date ……

"The fat body of insects is a rather ungrateful material for cytological studies."

(A. B. Dutkowski, 1974.)

Acknowledgments

I would like to state how awesome and career-changing this journey has been… Investigating the fascinating role of the heme oxygenase enzyme in such a mesmerising organism… Just amazing! Despite all difficulties along the way, I definitely fell really lucky and I have learnt a lot! However, it is very important to point out that this experience would likely not have been the same without so many great people who helped along the way and to those I am deeply thankful:

First of all, for my supervisor Dr Mark Paine for giving me the chance to perform my PhD studies under his supervision. Thank you for the guidance, patience and constantly encouraging me to think critically over these years.

To my secondary supervisors Dr. Gareth Lycett and Dr. Lu-Yun Lian, both gave insightful suggestions and provided support for the realisation of this project.

To Dr. Alvaro Acosta Serrano and his team for always contributing with great advices and opening the doors from their research group to me so I could get acquainted with the fascinating biology of tsetse flies. A special thanks for Daniel Southern for providing me flies whenever I needed!

Thanks to Dr. Ray Owens, Dr. Louise Bird, Dr. Joanne Nettleship and all OPPF people who guided me in the processes of cloning, expression and crystallization trials of heme oxygenases constructs.

My sincere acknowledgements to CNPq/Science without borders, who has funded my studies.

I wish to express my sincere gratitude to the brilliant young scientists Dr. Lee Refuse Haines and Dr. Cristina Yunta Yanes. Both of them gave me crucial scientific

insights and advice as well as great personal support and without whom this challenging project would had been much more difficult. Thank you so much guys!

This PhD would not have been as enjoyable without the great company I have had during those years, Thank you so much for Loïc Revuelta, Jacob Riveron, Grazia Stecchino, Angela Hugues, Eilidh Carrington, Chris Spencer, Adriana Adolfi, Fabricio Martins, Lucas Cunningnham, Amalia Anthousi and many other current (and former) members from LSTM. Those are people who really cheer me up when I needed and made this journey much more fun! I will miss all of you a lot!

Finally, Thanks to all my family and personal friends who gave me so much support during this PhD and never allowed me to give up when things got difficult. I will be forever grateful to Andy Bolton, Terezinha Souza, Felipe Vasconcelos and so many more. In particular, I am grateful to my parents Giovanni Pacelli and Elizabeth Gomes as well as to my husband who always have been so patient and caring and give me the reasons to persisting in achieving this degree. Thank you.

ABSTRACT

Hematophagous insects ingest several times their body weight with each blood meal, obtaining nutrients needed for reproduction and survival in addition to high levels of free heme. However, they survive the high toxicity imposed by free heme due to the development of heme detoxification mechanisms such as heme degradation by the enzyme heme oxygenase (HOs). Despite being present in several disease vector insects, including tsetse flies that transmit sleeping sickness, the role and biochemical features of HOs in blood feeding insects is poorly studied. Here, we have cloned and expressed HO from the tsetse fly *Glossina morsitans morsitans* to determine whether the enzyme was active, unveil its biochemical features and develop specific antibodies to investigate HO distribution in this insect. HPLC analysis of midgut contents from *G. m. morsitans* was performed to track the degradation of heme and conversion to biliverdin during the first 6 days following a single blood meal, showing that whilst heme concentration roses to 3 mM at 48 hours after a single blood meal, the maximum concentration reached by biliverdin is 0.5 μM after 96 hours, suggesting that despite HO being active in the insect, it may play a minor role in heme degradation. Comparison of recombinant HOs suggests that the heme oxygenase from *G. m.morsitans* (GmmHO) degrades heme slower and presents distinct spectroscopic features to HOs from other hematophagous insects and humans. However, it is similar to that observed in *D. melanogaster*. Confocal analysis of immunostained tissues and western blotting using antibodies raised against recombinant enzymes have been used to track the tissue distribution of GmmHO, demonstrating that the enzyme is ubiquitously expressed in the insect, particularly in the nuclei from oenocytes, liver-like cells involved in cuticle synthesis. Such results were supported by analysis of mRNA levels, which showed higher expression levels in reproductive tissues (6.5 fold), digestive tract (2.0 fold) and fat bodies/oenocytes (1.7 fold), evincing a role in reproduction. Time series analysis of HO mRNA levels after a single blood meal revealed that GmmHO is an early blood meal induced gene in digestive tract (3.4 fold) and fat bodies/oenocytes (2.2 fold), confirming a role in the defence against heme toxicity in the digestive tract as well as unveiling possible roles in the catabolism of lipids. Thus, this work has confirmed the presence and activity of HO in a hematophagous insect and revealed both biochemical and functional aspects of the enzyme, shedding new light on the role of HO in hematophagous insects.

LIST OF CONTENTS

Acknowledgements……..…IV

Abstract……....VI

LIST OF FIGURES……..……X

LIST OF TABLES……..……XIV

LIST OF ABBREVIATIONS……..……..……..……XV

CHAPTER 1 – INTRODUCTION

1.1 Background……..……..……..……..……1

1.2 Human African trypanosomiasis……..……..……..……1

1.3 Tsetse fly biology..……..……..……2

1.4 Oenocytes……..……..……..……6

1.5 Hematophagy and heme toxicity……..……..……6

1.6 Heme detoxification mechanisms……..……..……9

1.7 Heme oxygenases……..……..……12

1.8 Research aims……..……..……..……15

CHAPTER 2 – CLONING AND EXPRESSION OF HEME OXYGENASE FROM GLOSSINA MORSITANS MORSITANS.....16

2.1 Introduction……..……..……..……16

2.2 Material and methods……..……..……18

2.2.1 TseTse Fly mantainance ……..……..……18

2.2.2 Bionformatics methods ……..……..……..... 18

2.2.3 Agarose gel electrophoresis……..……..……..……19

2.2.4 RNA extraction, cDNA synthesis and Genomic DNA……..……19

2.2.5 DNA sequencing ……..……..……19

2.2.6 Design of primers for GmmHO cloning.....20

2.2.7 Digestion with restriction enzyme and DNA ligation.....20

2.2.8 Transformation of *Escherichia coli* cells.....21

2.2.9 Plasmid purification by Miniprep.....22

2.2.10 Preparation of growth media 22

2.2.11 Cloning of GmmHO in pColdII 22

2.2.12 Cloning and expression screening of GmmHO constucts using in-fusion technology.....25

2.2.13 Protein expression of GmmHO constructs in *E. coli*.....26

2.2.14 Creation of bacterial cell lysate for protein purification.....27

2.2.15 Transformation and expression of insect cells.....27

2.2.16 Purification Strategies of GmmHO constructs 28

2.2.17 Purification of constructs by Nickel Affinity cromatography.....28

2.2.18 Cleavage of fusion tags by digestion enzyme.....29

2.2.19 Separation of MBP-tag and recombinant GmmHO by MBP-affinity chromatography.....29

2.2.20 Size exclusion chromatography..... 30

2.2.21 Quantification of protein content by Bradford method 30

2.2.22 Protein electrophoresis 30

2.2.23 Western blotting.....32

2.2.24 Crystallization trials of GmmHO constructs.....32

2.2.25 Attempt to clone GmmCPR.....32

2.3 Results.....36

2.3.1 Identification and sequence analysis of GmmHO 36

2.3.2 Cloning of GmmHO 44

2.3.3 Cloning and expression of GmmHOΔ250 ……..48

2.3.4 High thought expression of GmmHO ……..53

2.3.5 Crystalization trials of GmmHO…..……..58

2.3.6 Antibody generation and validation …..……..60

2.4 Discussion ……..62

CHAPTER 3 – BIOCHEMICAL CHARACTERIZATION OF *GLOSSINA MORSITANS MORSITANS* HEME OXYGENASE (GMMHO)….65

3.1 Introduction…….65

3.2 Material and methods……67

3.2.1 Dissection of Tsetse fly and preparation of samples……...67

3.2.2 Quantification of biliverdin and heme in tsetse fly digestive tube contents by HPLC-reserse phase chromatography….67

3.2.3 Creation of GmmHO-heme complexes ……68

3.2.4 Spectral analysis of GmmHO complex variants…… ……68

3.2.5 Cytochrome p450 reductase ……68

3.2.6 Identification of biliverdin as a degradation product by using CPR or ascorbic acid ……69

3.2.7 Identification of iron as heme degradation product ……69

3.3 Results……69

3.3.1 Evidence of GmmHO activity in vivo ……69

3.3.2 Biochemical characterization of recombinant GmmHO ……74

3.4 Discussion…..…82

CHAPTER 4 – FUNCTIONAL MAPPING OF GMMHO……86

4.1 Introduction…….86

4.2 Material and methods……87

4.2.1 Animals and tissues handling..……87

4.2.2 Antibodies ……87

4.2.3 Determination of protein content by Bradford method ……88

4.2.4 Sample preparation for western blotting ……88

4.2.5 Protein electrophoresis and western blotting……88

4.2.6 Immunohistochemistry methods ……88

4.2.6 Fluorescent microscopy……89

4.2.7 RNA and cDNA preparation ……89

4.2.8 Quantitative PCR ……89

4.3 Results……91

4.3.1 Tissue distribution of GmmHO ……91

4.3.2 Identificaton of Oenocytes ……104

4.3.3 Effect of a blood meal on GmmHO expression ……106

4.4 Discussion……111

Chapter 5 – CONCLUSIONS AND FINAL REMARKS ……112

5.1 Heme degradation by the enzyme heme oxygenase is an active detoxification mechanism to *G. m. morsitans*……112

5.2 GmmHO shares biochemical features with *Drosophila melanogaster*……114

5.3 GmmHO is a ubiquitous gene highly expressed in oenocytes and digestive tract and may play other roles……115

5.4 Future perspectives……117

6 REFERENCES……109

LIST OF FIGURES

Figure 1.1 Reproductive and digestive organs from *G. m. morsitans* ……..5

Figure 1.2 Structure of heme B, the most common form of heme.……....8

Figure 1.3 Heme detoxification mechanisms reported in blood sucking arthropods…….....11

Figure 1.4 Heme degradation reaction carried out by the enzyme heme oxygenase……14

Figure 2.1 Multiple sequence alignment of protein HO sequences from insect and non-insect species…….38

Figure 2.2 Structure model of full length GmmHO(GmmHOFL)……..……...39

Figure 2.3 Phylogenetic relationship of heme oxygenases from several insect and non-insect species.....42

Figure 2.4 Prediction of Transmembrane domain regions for full length GmmHO… ……..……..43

Figure 2.5 Isolation of full length and truncated forms of GmmHO from tsetse female cDNA.....……..44

Figure 2.6 Diagnostic PCR of DH5α (*E. coli*) colonies transformed with full length and truncated GmmHO in pJET1.2 cloning vector.....46

Figure 2.7 PCR product amplification of GmmHO using different DNA sources …….....46

Figure 2.8 Purification of GmmHOΔ250……..……..……..49

Figure 2.9 Isolation of full length and truncated forms of GmmHO from female tsetse cDNA.....……..50

Figure 2.10 Size exclusion chromatogram of GmmHOΔ250 following Ni-NTA affinity purification…….....51

Figure 2.11 Purification of recombinant GmmHOΔ250 by size exclusion chromatography.....52

Figure 2.12 PCR screening of GmmHO constructs ……..……..……54

Figure 2.13 Ni-NTA Purified GmmHO-popinM constructs from OPPF screening in bacterial expression system……..55

Figure 2.14 Ni-NTA Purified GmmHO-popinF constructs from expression screenings in insect cells using different two volumes of viral suspension culture……56

Figure 2.15 Purification of recombinant full length GmmHO (GmmHOFL) from scale up bacterial expression …..……..57

Figure 2.16 Purification of recombinant GmmHOΔ263 construct from scale up baculovirus expression system..……..59

Figure 2.17 Western blot analysis showing specificity of anti-GmmHO polyclonal antibodies raised in hen against recombinant ΔGmmHO5……..60

Figure 2.18 Western blot analysis showing specificity of anti-GmmHO polyclonal antibodies raised in rabbit against recombinant ΔGmmHO5……..61

Figure 3.1 Digestive tract of *G. m. morsitans* five days after a single blood meal……...71

Figure 3.2 Time course of heme degradation in *G.m.morsitans* midgut content after a single blood meal…….....72

Figure 3.3 HPLC spectra of female tsetse fly digestive tract contents after a single blood meal…….....73

Figure 3.4 Absorption spectra of different GmmHOΔC250-heme complexes…… 77

Figure 3.5 Detection of catalytic activity from GmmHOΔC250…..…....78

Figure 3.6 Detection of catalytic activity from GmmHOΔ250 in the presence of MdCPR and desferrioxamine ….……...79

Figure 3.7 Assay of heme degradation by detection of biliverdin using ascorbic acid as electron donor…….....80

Figure 3.8 Assay of heme degradation by full length GmmHO in the presence of desferrioxamine…….....81

Figure 4.1 Reactivity of anti-GmmHO to tsetse fly tissues and recombinant enzymes…….... 92

Figure 4.2 Immunoblot of teneral male tsetse fly before and 72 hours after a single blood meal against anti-GmmHO antibodies raised in rabbit…….....94

Figure 4.3 Immunoblot of teneral female tsetse fly before and 72 hours after a single blood meal against anti-GmmHO antibodies raised in rabbit……95

Figure 4.4 Immunoblot of different extractions of tsetse fly tissues against anti-GmmHO antibodies raised in rabbit…..97

Figure 4.5 Immunoblot of different extractions of tsetse fly tissues against anti-GmmHO antibodies raised in chicken...99

Figure 4.6 Western blotting analysis of several sections of tsetse fly digestive tract ……..…… 101

Figure 4.7 Immunofluorescence of tsetse fly tissues marked with rabbit anti HO…….....102

Figure 4.8 Immunofluorescence of tsetse fly tissues marked with hen anti HO and rabbit anti CPR……..…… 103

Figure 4.9 immunolocalization of HO and CPR in Tsetse flies oenocytes ……..……..…….....105

Figure 4.10 Relative GmmHO mRNA expression levels in various female *G. m. morsitans* body compartments in relation to the whole body……..……..107

Figure 4.11 Expression kinetics of GmmHO gene in female reproductive tissues.…….....108

Figure 4.12 GmmHO expression in various female tsetse fly tissues in relation to the whole body…….....109

Figure 4.13 Effect of blood meal in HO expression of Tsetse fly alimentary canal ……...……..……110

LIST OF TABLES

Table 2.1 Reaction composition of DNA treatment with restriction enzymes ……20

Table 2.2 Reaction components of DNA ligation……21

Table 2..3 Primers used for GmmHO cloning ……23

Table 2.4 PCR Reaction components ……24

Table 2.5 PCR thermal cycling timetable ……24

Table 2.6 Primers used for infusion cloning screening in popinF and pOPINM vectors……26

Table 2.7 SDS-PAGE gel composition ……32

Table 2.8 GmmHOΔ263 samples submitted for crystallization……33

Table 2.9 Primers used to clone GmmCPR……34

Table 2.10 PCR thermal cycling timetable for cloning of GmmCPR……35

Table 2.11 Identity of several heme oxygenases protein sequences to GmmHO ……41

Table 2.12 GmmHO constructs used in this work…… 47

Table 4.1 qPCR primers……90

LIST OF ABREVIATIONS

aa	Amino acids
AgHO	*Anopheles gambiae* heme oxygenase
ABM	After a blood meal
APS	Ammonium persulphate
BLAST	Basic local alignment search tool
bp	(Nucleotide) base pairs
BV-IX	Biliverdin IX
BV-Ixα	Biliverdin alpha
cDNA	Complementary deoxyribonucleic acid
CO	Carbon monoxide
CPR	Cytochrome P450 reductase
DMSO	Dimethyl sulphoxide
DNA	Deoxyribonucleic acid
EDTA	Ethylenediaminetetraacetic acid
EST	Expressed sequence tag
GmCPR	*Glossina morsitans* cytochrome P450 reductase
HO	Heme oxygenase
HO-1	Human heme oxygenase 1
HO-2	Human heme oxygenase 2
HO-3	Human heme oxygenase 3
IPTG	Isopropyl-β-D-1-thiogalactopyranoside
$NADP^+$	Nicotine adenine dinucleotide phosphate (oxidised form)
NADPH	Nicotine adenine dinucleotide phosphate (reduced form)
NCBI	National Center for Biotechnology Information
Ni-NTA	Nickel-nitrilotriacetic acid
NMR	Nuclear magnetic resonance imagery
OD	Optical density
PCR	Polymerase chain reaction
qPCR	Quantitative or real time Polymerase chain reaction
SDS-PAGE	Sodium dodecyl sulphate polyacrylamide gel electrophoresis
TAE	Tris-Acetate-EDTA buffer

CHAPTER 1 - INTRODUCTION

1.1 Background

Approximately one million deaths are caused every year by vector borne diseases such as dengue fever, malaria, leishmaniosis and human African trypanosomiasis (WHO, 2016), triggering devastating social-economic impacts in the effected populations (Hunt *et al.*, 2007). Many of these diseases lack effective treatment. Thus, killing the insects that transmit the causative parasites or viruses is the primary method of disease control (Lemon, 2008). Despite the effectiveness of WHO approved insecticides in reducing the incidence of vector borne diseases such as malaria in Sub-Saharan Africa (Bhatt *et al.*, 2015), the selection pressure imposed by the massive use of insecticides has led to vector populations with increased levels of resistance to insecticides (Riveron *et al.*, 2015), putting at risk such control strategies. Thus, the pursuit for molecular targets that may allow development of new vector control strategies is strongly encouraged.

Blood feeding insects depend on hematophagy for survival and oogenesis. Through this feeding habit these insects gain a significant nutritional intake rich in haemoglobin, whose proteolysis results in the release of globin and free heme (Briegel & Lea, 1975). At high concentrations, free heme is highly toxic, causing oxidative stress through generation of reactive oxygen species (ROS) which may result in oxidative damage to lipids, proteins and DNA and alteration in permeability of cell membrane (Schimitt *et al.*, 1993; Chou & Fitch, 1981; Graca-Souza, 2006). To overcome this threat, hematophagous insects have developed several detoxification systems of free heme, such as antioxidant enzymes, peritrophic membrane, processes of aggregation or degradation (Graca-Souza *et al.*, 2006). The later is governed by the enzyme heme oxygenase (HO), whose homologue (*Gmm*HO, Acession code GM0004329) has been identified in the *G. m. morsitans* genome.

HOs are microsomal enzymes that were first reported in the microsomal fractions of mammalian liver and spleen (Tenhunen *et al.*, 1969), and found to drive heme degradation with the resulting production of carbon monoxide, iron and biliverdin. In the presence of biliverdin reductase, biliverdin is further converted into

bilirubin. Heme degradation products with distinct modifications to those occurring in humans have since been isolated from the hematophagous insects *Aedes aegypti* and *Rhodnius prolixus* (Paiva-Silva *et al.*, 2006; Pereira *et al.*, 2007), suggesting that insect HOs possesses differences in active-site structure and mechanisms compared to mammalian HOs. However, the structure and role of heme oxygenase in these organisms have been poorly studied. Furthermore, some studies have suggested that HOs are involved on reproduction in the insect vectors *Anopheles gambiae* and *R. prolixus* (Spencer, 2016; Caiaffa *et al.*, 2010).

Thus, the goal of this study was to investigate the mechanism of heme degradation by the enzyme heme oxygenase in the blood feeding insect *Glossina morsitans morsitans*, a disease insect vector with a unique reproductive biology. This was intended to characterise GmmHO to understand its role in heme detoxification in *G. morsitans* and potential as a target for the development of new tools to improve vector control.

1. 2 Human African Trypanosomiasis

One of the most important health problems in Africa (Hotez *et al.*, 2009), human African trypanosomosis (HAT) is caused by trypanosomes transmitted by hematophagous flies from the genus *Glossina* (popularly known as Tsetse flies) during blood feeding (LEAK, 1998). This potentially fatal disease affects the human central nervous system and if not treated may cause deterioration of mental ability leading to behavioural changes such as hypersomnia, which eventually is followed by coma and death (Pentreath *et al.*, 1994; Pentreath *et al.*, 1994b).

The geographical range of the disease is restricted to sub-Sabaran Africa. Depending on the subspecies of *Trypanossoma brucei* transmitted, two pathologically distinct forms of HAT can occur. The chronic and most common form is caused by *T. b. gambiense* in western and central Africa. The acute form is caused by *T. b. rhodeniense* in eastern and southern Africa (Brun *et al.*, 2010). Additionally, a third form of African Trypanosomiasis known as Nagana or animal Trypanosomiasis is caused by infections of *T.b.brucei* in cattles, strongly affecting the agricultural development in Sudan and West Africa (Wilson, 1963)

During the twentieth century, three major epidemics of HAT have affected the continent (Steverding, 2008), killing 250.000 people during the first one between 1900-

1920 (Fevre *et al.*, 2004). However, massive efforts have led to a significant decrease in the number of HAT cases during the past 10 years (WHO, 2003), bringing down the number to less than 10,000 annual cases (Franco *et al.*, 2014). Bran *et al.*, (2010), however, point out that the status of HAT should not be a reason to underestimate the social economic impacts caused by the disease. Currently, it is estimated that approximately 70 million people live in areas of risk of HAT infection (Simarro et al, 2012). Thus, a significant obstacle for the health and economic development of the populations living in the endemic areas (Barret *et al.*, 2003).

Currently, there are 5 drugs that are used for the treatment of HAT (WHO, 2017), three of which were created over 50 years ago. All current drugs are compromised by toxicity, adverse effects and drug resistance (Fairlamb, 2003). Thus, innovative and cost effective strategies for a sustainable control of HAT have been strongly encouraged (Aksoy *et al.*, 2008)

1.3 Tsetse Fly Biology

The members of Genus *Glossina* (tsetse flies), are the insect vectors responsible for transmitting the trypanosomes that cause HAT and animal trypanosomiasis. These flies can be grouped according to their habitat (Wanwiri & Changasi, 2016) in riverine, savannah or forest-dwelling types. Different tsetse fly species differ in their ability to acquire, develop and transmit distinct trypanosome species, which determines which form of the disease they can transmit (Geiger *et al.*, 2005). The chronic form of HAT is caused by *T. b. gambiense,* whose main vectors are the riverine type *G. palpalis and G. fuscipes*. The acute form of HAT is caused by *T. b. rhodeniense*, transmitted by the savannah fly *G. m. morsitans* (Bouteille & Buguet, 2012). Recently, the sequencing of the complete genome of *G. m. morsitans* was accomplished (Attardo *et al*, 2014), allowing further gene functional studies in this important insect vector species.

Both male and female tsetse flies are obligate blood feeders. The organization of the digestive tract (Figure 1.1) of tsetse flies has a similar organization to other members of the Muscidae family, being divided into morphologically distinct regions (Billingsley, 1990). These include the anterior midgut (AM), bacteriome (BT, previously known as mycetome), secretory midgut (SM) and posterior midgut (PM). In the

secretary midgut, water is removed from the blood meal and blood digestion takes place (Leak *et al*., 2008; Cheeseman & Gooding, 1985).

The size of the blood meal varies accordingly to sex and dietary status, and average ~26 mg for laboratory males (Loder, 1997). Amino acid residues and heme are the main components of blood digestion. The former are used to synthetize fat reserves (Loder, 1997; Loder *et al.*, 1998). High concentrations of heme are excreted by the insect, which makes 6% of the main components of the insect dry faeces. It is not clear, however, if heme is excreted as a monomer, polymer or even as a heme degradation product.

Tsetse flies have a unique system of reproduction compared with other insects. Their mode of reproduction is adenotrophic viviparity, a system in which the embryo and larvae are developed inside the female uterus, nourished by milk-like proteins synthetized by specialised organs called milk glands (Hagan, 1951; Ma *et al.*, 1975). As a way to allow the grow and intrauterine nourishing of larvae, tsetse flies as well as other members of the superfamily Hippoboscoidea adapted by reducing the size of their ovaries (Figure 1.1). In contrast to the dozens of ovarioles that are present in other diptera, tsetse flies have only 2 ovarioles per ovary, while expanding the milk glands and reproductive tract (Benoit *et al.*, 2015). This type of reproduction however, allows each female give birth to one larvae at each gonotrophic cycle, which last about 10 days counting intrauterine embryogenesis and larval development (Sanders & Dodd, 1972; Tobe & Langley, 1978). Due to this physiological trait, this unique reproductive strategy yields much fewer progeny compared with other hematophagous insects and has been proposed as a key target for the development of strategies to control tsetse fly populations (Benoit *et al.*, 2015).

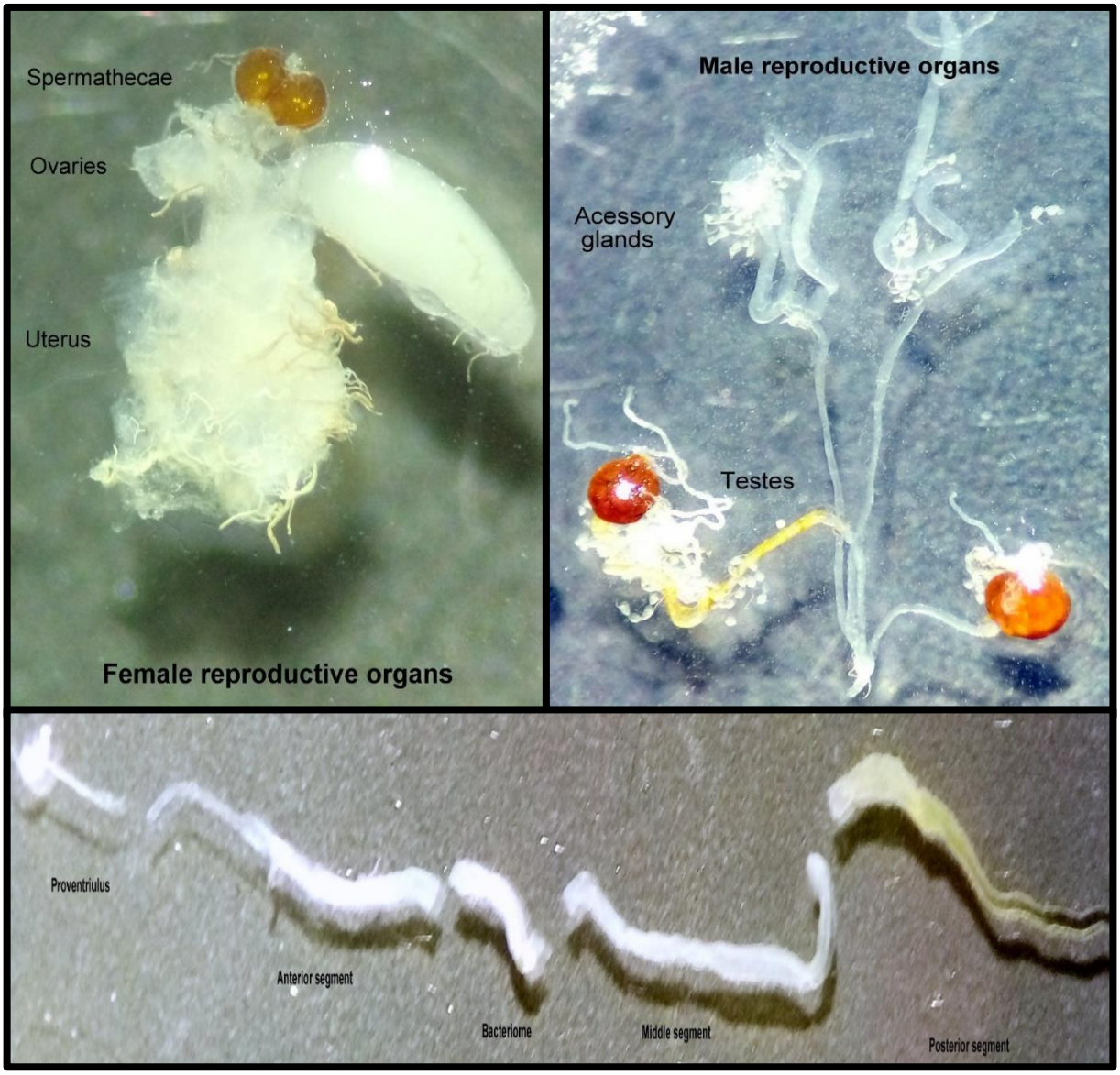

Figure 1.1 – Reproductive and digestive organs from *G. m. morsitans*. (A) Female reproductive tissues (B) Male reproductive tissues (C) Digestive tract

1.4 Oenocytes

Oenocytes are insect cells of ectodermal origin (Wheeler & Morton, 1892). They are generally associated with the fat body or abdomen but their size and anatomical location vary depending on the insect species (Martins & Ramalho-Ortigao, 2012). In *D. melanogaster,* they have been shown to express lipid-metabolizing proteins, indicating a role in the regulation of lipid metabolism equivalent to those of mammalian liver cells (Gutierrez *et al.*, 2007). However, other studies have implicated key roles in the synthesis of cuticle lipids (Lockey, 1988) and detoxification of xenobiotics (Clark & Dahm, 1973).

Early work by Tobe *et al.* (1973) has revealed cytological changes in milk gland, fat body and oenocytes of *G. austeni* that shows that during various phases of of the female reproductive cycle, the milk glands go through a cycle of secretion of milk-like proteins that nourishes the larvae. Additionally, the authors described that among fat body cells, there are smaller and rounder structures rich in tyrosine that they proposed to be oenocytes. Despite being morphologically different from higher diptera, those cells presented characteristics common to other oenocytes such as large and poliploid nuclei and dense cytoplasm (Perez, 1910; Wigglesworth, 1965). In *G. m. morsitans*, such studies have not been carried out however due to the close phylogenetic relationship, it is assumed oenocytes in *G. m. morsitans* are morphologically similar to *G. austeni*.

1.5 Hematophagy and Heme Toxiciy

Hematophagy is a key event in blood-feeding insects, arising independently numerous time during evolution in arthropods (Ribeiro, 1995). During a blood meal, blood feeding insects can ingest twice to several times their own unfed weight in blood, acquiring nutrients needed for oogenesis and survival (Lehane, 2005). It is during blood feeding that aetiological agents of vector borne diseases are transmitted.

According to Weed *et al.*, (1962) haemoglobin corresponds to 95% of dry weight in erythrocytes, the most abundant blood cells. Because of haemoglobin proteolysis, high levels of free heme are released into the insect digestory tract. Like others tetrapyrroles, heme (Figure 1.2) is a molecule formed by four pyrroles (5-membered hydrocarbon rings containing nitrogen) linked by unsaturated methane

groups. Due to the presence of several double bonds, it strongly absorbs light. A remarkable difference to other tetrapyrroles is that in heme, the four nitrogens are linked to an iron group in their core, which can present two different oxidation states (Smith and Witty, 2002). As a prosthetic moiety of several hemoproteins (or heme-containing proteins) this versatile compound is involved in a wide range of physiological event events such as oxygen transport (Klotz and Klotz, 1955), electron transfer (Tijet *et al.*, 2001) and catalysis (Yuda *et al.*, 1996).

Due to its molecular characteristics, however, heme in its free form is highly toxic, potentially leading to undesirable effects in cells. Free heme can be toxic by two main mechanisms. Firstly, acting as prooxidant activity by forming reactive oxygen species (ROS) through Fenton reaction (Ryter & Tirell, 2000; Gozzelino, 2016) and secondly, by causing physical disturbance of phospholipid bilayers (Schmitt *et al.*, 1993), resulting in cytotoxicity and damage to biological molecules. For instance, at concentrations higher than 1 μM, heme is considered toxic to human cells (Sassa, 2004). Thus, taking into consideration that blood feeding insects feed on high volumes of blood, the release of high concentrations of heme poses a toxic threat to hematophagous organisms. As a way to evade such threats, blood feeding arthropods have evolved a series of heme detoxification mechanisms (Figure 1.3). These include the control of ROS by antioxidant enzymes, binding of free heme by means of heme-binding proteins, polymerization of heme in hemozoin-like structures, trapping of heme by peritrophic matrix and heme degradation by the enzyme heme oxygenase (Graca-Souza *et al.*, 2006).

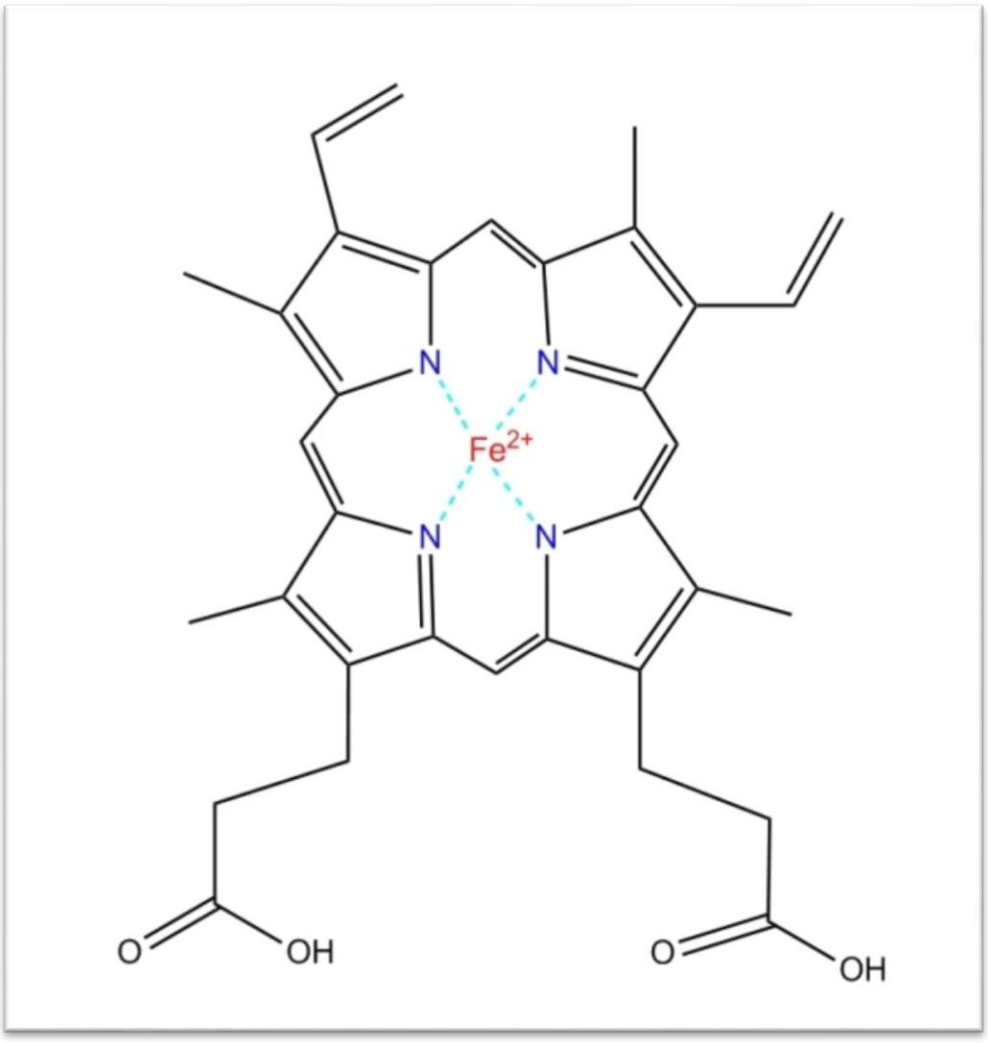

Figure 1.2 – Structure of heme B, the most common form of heme

1.6 Heme Detoxification Mechanisms

Despite its potential for vector control, a limited number of studies have targeted mechanisms of heme detoxification in hematophagous insects. To date, most studies have focused on the kissing bug *Rhodnius. prolixus*, the vector of Chaga`s disease and *Aedes aegypti,* the main vector of dengue fever and zika.

In *Ae. aegypti*, the type I peritrophic matrix (PM) as well as being a physical barrier against damage caused by the abrasion of particles of food, it also acts as a chemical defence by binding heme in similar levels to those acquired during a blood meal (Pascoa *et al.*, 2002). This trait was later showed to be due to mucin-like proteins present in the insect PM, which have a dual function in binding chitin as well as being able to bind high concentrations of heme (Devenport *et al.*, 2006).

The kissing bug *R. prolixus* lacks a perithophic matrix, but has an equivalent structure called the perimicrovillar membrane. Unlike *Ae. aegypti* this structure not only binds heme, but also promotes heme aggregation into hemozoin in the gut lumen of *R. prolixus* (Oliveira *et al.*, 1999; Silva *et al.* 2007). The hemozoin granules formed are dark-brown crystalline structures that are harmless to the insect and easier to be secreted, similar to the hemozoin observed in Plasmodium parasites. The peritrophin formation is expected to be a first line defense against toxic amounts of free heme in *R. prolixus.*

Another heme controlling mechanism present in arthropods is played by heme binding proteins (HBPs). HBPs have mostly been detected in the hemolymph of *R. prolixus* (Dansa-Petretski *et al.*, 1995) and from the tick *Boophilus microplus* (Lara *et al.*, 2003). Whilst the ability to bind heme does not necessarily implies that the prooxidant potential of heme is being stopped (Vincent *et al.*, 1989), when associated with heme, HBPs are able reduce its potential to generate ROS (Dansa-Petretski *et al.*, 1995; Maya-monteiro *et al.*, 2004) and direct heme to tissues where it is reutilized for embryogenic development (Braz *et al.*, 2002) or hemoprotein synthesis (Maya-Monteiro *et al.*, 2000).

With regards to the pathway of heme degradation by HO in arthropods, the isolation of heme degradation products from the digestive tract of *Ae. aegypti* (Pereira *et al.*, 2007) and *R. prolixus* (Paiva-Silva *et al.*, 2006) indicates the enzyme is active in these insects. However the distribution and biochemical features of those enzymes have yet to be established.

To date, the mechanisms of heme detoxification have been poorly studied in Tsetse flies. Earlier studies conducted by Bursell (1966) that compared concentrations of nitrogenous products of *G. morsitans* excretions with human blood composition concluded that heme obtained from haemoglobin digestion is not absorbed or degraded by the fly. Instead it is quantitatively excreted. However, as mentioned earlier, the methods used for quantification of heme in that study make it difficult to say whether the heme in excreted in its monomer or conjugated, hemozoin-like form.

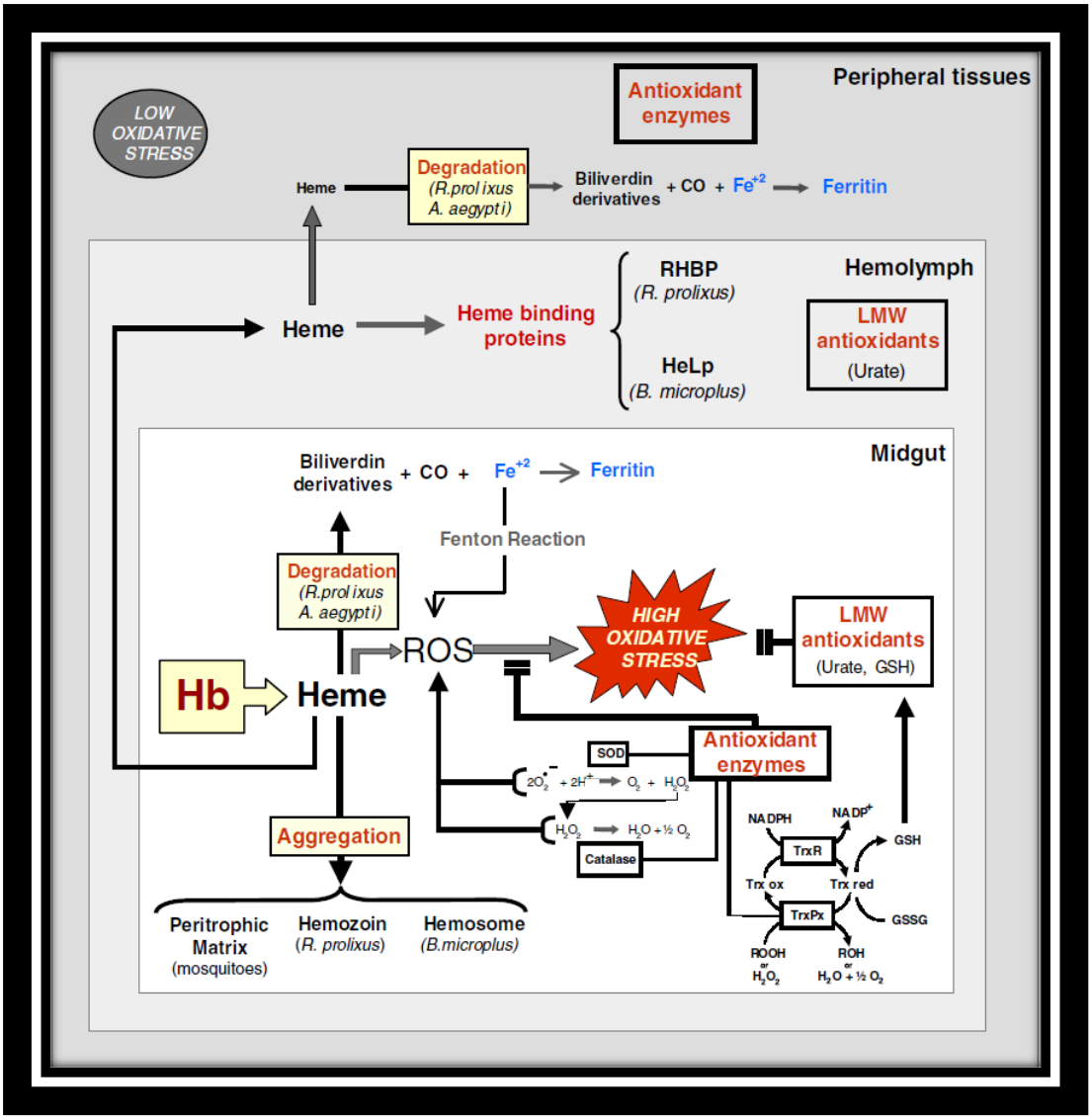

Figure 1.3 – Heme detoxification mechanisms reported in blood sucking arthopodes (figure adapted from Graca-souza *et al.*, 2006)

1.7 Heme oxygenases

One of the mechanisms proposed for the detoxification of blood derived heme in hematophagous insects is the enzymatic degradation governed by the enzyme HO (Figure 1.4). In mammals, these enzymes were initially believed to belong to the P450 family (Tenhunen *et al.*, 1969), and later reclassified as a heat shock protein (HSP) (Keyse & Tyrell, 1989). This group of enzymes presents a signature primary sequence "QAFICHFYNI/V" (Maines, 1988) that is common to all HOs reported by far (Maines & Gibbs, 2005). Humans possess two homologues of HO (HO-1 and HO-2) that differ in their inducibility, roles and tissue distribution (Maines and Gibbs, 2005; Chen *et al.*, 2003). The presence of a third homologue was described by McCoubrey Jr *et al.* (1997) but later reclassified as a HO-2 derived pseudogene (Hayashi *et al.*, 2004).

HOs were first reported as microsomal enzymes present in mammal's liver and spleen (Tenhunen *et al.*, 1969). It is now known that HOs are widely distributed among many other organisms such as plants, bacteria and invertebrates (Gohya *et al.*, 2006; Zhang *et al.*, 2004; Zhu *et al.*, 2000). In the presence of HO, the α-methane carbon bridge of free heme is oxidised, degrading it into carbon monoxide, iron and biliverdin IX. In order to degrade free heme, HO requires three molecules of molecular oxygen (O_2) and seven electrons, commonly supplied by NADPH in a reaction driven by NADPH cytochrome P450 oxidoreductase (CPR). In plants, however, the reducing equivalents are supplied by NADH via ferrodoxin (Yoshida and Migita, 2000).

In mammals biliverdin IX alpha is further converted by the enzyme biliverdin reductase (BVR) into the major bile pigment bilirubin (Kutty & Maines, 1981), improving its solubility and antioxidant potential. It is important to point out that BVR is absent in insects, thus the final stages of heme breakdown and pigment formation are different. Specifically, amino acids are added to biliverdin, presumably to increase solubility for excretion and antioxidant potential In *Ae. aegypti* (Pereira *et al.*, 2007) and *R. prolixus* (Paiva-Silva *et al.*, 2006) the heme degradation products biglutaminyl-biliverdin IXα and dicysteinyl-biliverdin IXγ were isolated respectively from these blood feeding insects. While in *Ae. aegypti* the isomer is formed by additions of glutamine residues to biliverdin IX alpha, in *R. prolixus* the modification occurs in the porphyrin ring before it is cleaved by the enzyme. Those modifications are remarkably distinct from those observed in other HOs and suggest differences in the mechanism of degradation by HOs in insects.

Heme coordination is an important aspect for the activity of heme containing proteins. In the case of HOs, the heme is both a substrate and a prosthetic moiety necessary for its own oxidation. In a HO-heme complex, the heme iron molecule is typically oriented in a six-coordinated way, allowing catalysis at the sixth site (Schuller *et al.*, 1999). In part, this is reflected by the fact most HOs generate the same biliverdin isomer (biliverdin IXα) as a heme degradation product, however, the flexibility of the residues is also important in this differentiation. Some HOs are an exception to this rule and are able to produce other isomers. One example is the enzyme cloned from the fruit fly *D. melanogaster* (Zhang *et al.*, 2003), in which EPR analysis revealed that the heme iron in the DmHO-heme complex presented a five-spin coordination, allowing the production of alpha, beta and delta isomers of biliverdin. This was the first insect HO characterized, presenting unique features such as slower heme degradation rate and heme iron that does not participate in the binding of the heme moiety to the enzyme.

Recently, Spencer (2016) cloned and biochemically characterized the HO from the malaria vector *An. gambiae* (AgHO), showing *in vitro* that the enzyme could catalyse the degradation of heme to biliverdin, thus releasing CO and iron, the three major products of heme degradation. This was achieved in in the presence of insect and human CPR, and the dissociation constant (K_d) for heme was similar to HOs from human and from the bacteria *C. diphtheria*. Additionally, the author described that the use of HO inhibitors resulted in the diminishing of oviposition, indicating an involvement of HOs in reproduction. Taking in consideration that the reproductive traits of *G. m. morsitans* and *An gambiae* are so distinct, it would be interesting to investigate the role of HO in reproduction as well as its biochemical features compared to AgHO.

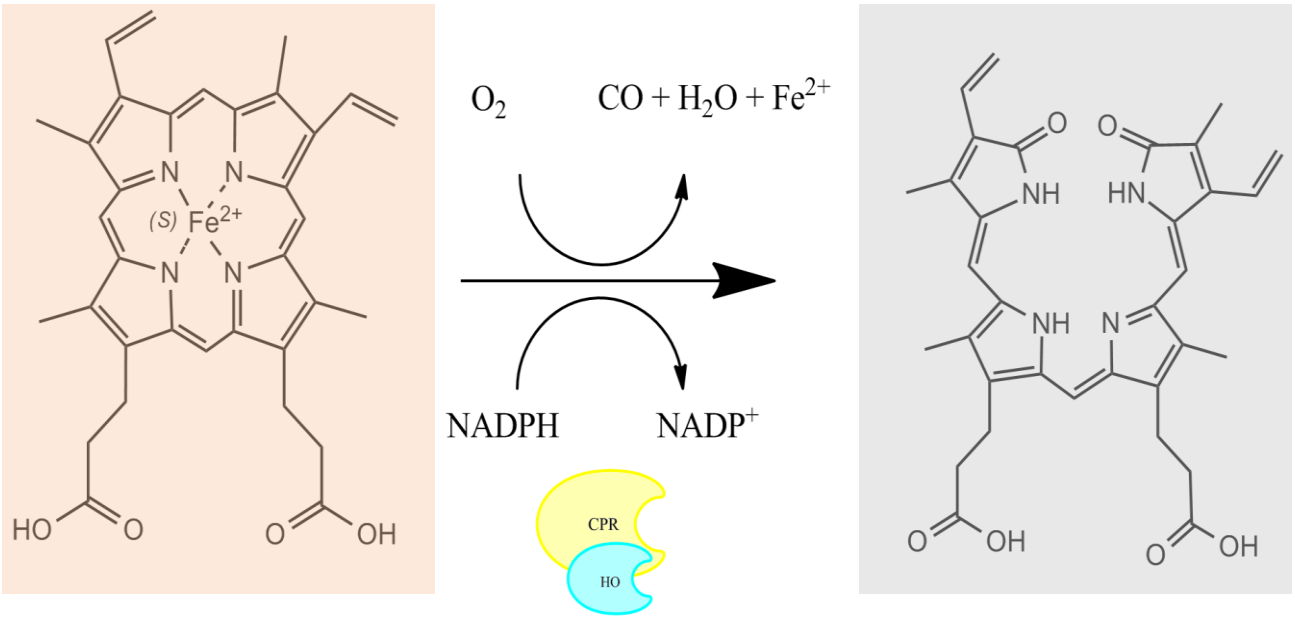

Figure 1.4 – Canonical reaction of heme degradation carried out by the enzyme heme oxygenase. To carry out the reaction, heme oxygenase requires three molecules of molecular oxygen (O_2) and seven electrons, commonly supplied by NADPH cytochrome P450 oxidoreductase (CPR).

1.8 Research aims

HO is present in the genome of the tsetse fly *G.m.morsitans* , the major African vector of HAT. However, to date GmmHO has not been cloned or functionally characterised, although it may play an important physiological role in heme catabolism. Recent work with *An. gambiae* HO has also suggested possible roles in reproduction. The main aim of this thesis was to clone and characterise GmmHO in order to determine its functional role in *G. m. morsitans*, in particular its relationship with heme detoxification. These studies are also intended to reveal the physiological significance of HOs to hematophagous insects and the potential use of this pathway as a target for the development of new technologies for vector control.

The following research questions were addressed in this thesis:

1) Does *G. m. morsitans* express an active HO?
2) How does GmmHO compare with other HOs in terms of biochemical features?
3) Where is HO located in *G. m. morsitans*?
4) What physiological role(s) does GmmHO play in *G. m. morsitans* ?

CHAPTER 2 – CLONING AND EXPRESSION OF HEME OXYGENASE FROM *GLOSSINA MORSITANS MORSITANS*

2.1 – INTRODUCTION

In recent years, the search for new strategies to control vector borne diseases has been strongly encouraged. Blood feeding is a key event in hematophagous insect's biology, however, many details have yet to be unveiled. For example, very little is known about how blood feeding insects are able to deal with the remarkably increased levels of heme in their digestive tract following a single blood meal.

Isolation of specific by-products from heme oxygenase-driven heme degradation in the alimentary canals of the hematophagous insects *Aedes aegypti* (Pereira *et al.*, 2007) and *Rhodnius prolixus* (Paiva-Silva *et al.*, 2006) suggests that heme oxygenases (HOs) are playing an important role in the heme detoxification process of blood feeding insects. However, it is still unclear to what degree HOs are responsible for depleting heme levels in those organisms and what mechanistic differences exists in comparison to mammalian HOs.

Heme oxygenases have been cloned from mammals, plants and bacteria (Yoshida & kikushi, 1977; Zhu *et al.*, 2000; Schuller *et al.*, 2001; Gohya *et al.*, 2006). In those organisms, soluble HO was obtained in either its full length or truncated forms missing the carboxy-terminal transmembrane domain (Gohya *et al.*, 2006; Tenhunen e*t al.*, 1969; *Zhu et al.*, 2000). A soluble truncated HO construct was cloned from *Drosophila melanogaster* and expressed in bacteria (Zhang *et al.*, 2004). This recombinant enzyme showed unique features when compared to mammal HOs such as slow iron release in the last heme degradation step and formation of non-alpha forms of biliverdin.

Glossina morsitans morsitans is one of the three tsetse fly species responsible for transmiting HAT (Human African Trypanosomiasis). Its complete genome sequencing was recently accomplished (Attardo *et al.*, 2014) allowing further studies in the *G. morsitans morsitans* biology. Just like the HOs from other hematophagous

species, very little is known about heme oxygenase of *G. m morsitans* (GmmHO). The aim of this chapter was to clone and express recombinant GmmHO to initiate the structural and functional characterisation of the enzyme.

2.2 – MATERIAL AND METHODS

2.2.1 TseTse Fly maintenance

G. m. morsitans flies (Westwood) were provided from by an established colony at the Liverpool School of Tropical Medicine. At the insectary, the flies were maintained at a relative humidity of 65-75% and ambient temperature of 27°C ± 2°C and three times a week they were feed on sterile, defibrinated horse blood (TCS Biosciences). Experimental flies were collected 0-24 hours after emergence, frozen and used for RNA extraction.

2.2.2 Bioinformatics methods

The available mRNA sequences of Heme oxygenase (HO, FBgn0037933) and NADPH-Cytochrome p-450 reductase (CPR, FBgn0015623) from *Drosophila melanogaster* available in Flybase, were used to search for homologous sequences in *G. m. morsitans* genome by performing BLAST searches in Vectorbase. The same procedure was applied in either Vectorbase or NCBI databases in order to find HO and CPR sequences homologues from *Aedes aegypti, Anopheles gambiae, Apis melifera, Corynebacterium diphtheria, Culex quinquefasciatus, G. fuscipes fuscipes, G. palpalis palpalis, Musca domestica, Rattus novergicus, Rhodnius prolixus, Synechocystis sp, Stomoxys calcitrans* and *Homo sapiens*. Using EMBL-EBI online platform (http://www.ebi.ac.uk/), those HO sequences were used for comparison of protein sequence by multiple sequence alignment using ClustalW Omega method (Goujon *et al.*, 2010; Sievers *et al.*, 2011; McWilliam *et al.*, 2013) and phylogenetic relationship, this data was then used to build and edit a phylogenetic tree at Trex online platform (http://www.trex.uqam.ca). Additionally, pairwise sequence alignment with GmmHO (GM004329-RA) (Vectorbase) in NCBI was carried out in order to reveal the degrees of identity to *G. m. morsitans* HO homologue.

A homology model of GmmHO was created in the SWISS-MODEL server workspace (https://swissmodel.expasy.org/interactive). A total of 132 templates were found however only 70 of those were used for compared building of a GmmHO model. The top templates used were crystal structures from *H. sapiens* HO-2 (2rgz.1.A, 2rgz.1.A and 2rgz.1.A), *Chlamydomonas reinhardtii* (4raj.1) and Synechocystis sp. (1wow.1). The images were then created and manipulated to highlight the functional residues using PyMOL software (Schrodinger, 2015). A prediction for transmembrane

helices domains in GmmHO was also performed by using TMHMM server according to methods described in Krogh *et al.* (2001) and Sonnhammer *et al.* (1998).

2.2.3 Agarose gel electrophoresis

All gels were made using Tris Acetate-EDTA (TAE) buffer with 1.5 % agarose and 0.5mg/mL ethidium bromide. To each 3µL of DNA samples a volume of 1 µL of DNA loading time (6x) was added. A total volume of 15 µL of DNA sample/DNA loading mixture was then added per well. A DNA ladder was added in at least one well per gel (GeneRuler 1kB, Hyperladder I or Hyperladder IV, depending on availability and expected fragment size) and the set gels were submerged in TAE. Samples were run at 90 – 120 V for as long as required for appropriate resolution. At the end of running procedure, the gels were visualised with a UV-transilluminator.

2.2.4 RNA extraction, cDNA synthesis and Genomic DNA

Total RNA was extracted from unfed female specimens of *G.m. morsitans* using the RNAqueous® Micro Kit from ThermoFisher Scientific following the provided protocol. An aliquot of the RNA (~1 µg) was then used for cDNA synthesis, using the Superscript IV First Strand Synthesis kit from Thermofisher Scientific, with strict adherence to their manufacturer's intructions. The concentration and quality of both RNA and cDNA was estimated with a NanoDrop ND1000 Spectrophotomer (ThermoFisher Scientific).

Genomic DNA from *G. m. morsitans, G. fuscipes fuscipes, G. palpalis palpalis*, and *Stomoxys calcitrans* were kindly provided by Dr. Lee Haines from Liverpool School of Tropical Medicine. The gDNA extracts were used for comparison of conservation of HOs among those species and for confirmation of the presence of an intron in the GmmHO gene. PCRs were run with GmmHO primers in the same conditions as described in session 2.2.12.

2.2.5 DNA sequencing

DNA sequencing was executed externally by the University of Sheffield's DNA sequencing service and by Source BioScience. Everything to be sequenced was sent in duplicate, with the appropriate forward and reverse primer pairs. Sequencing primers were the initial PCR primers in the case of PCR amplicons, and plasmid primers in the case of cloned or subcloned plasmid constructs.

2.2.6 Design of primers for GmmHO cloning

To design cloning primers for GmmHO, the nucleotide sequence of *G. m. morsitans* HO gene coding (GM004329-RA) (Vectorbase) was used as a guide. The primer design followed the rules generally applied for primers design. Firstly, to make sure the primers were specific to the HO sequence, the primers were kept to 18-30 base pairs long. Secondly at least 2 out of the 5 last nucleotides in the 3' end of the primers were either guanine or cytosine, to promote specific binding due to the stronger hydrogen bonding between those bases. The melting temperature was generally kept between 52-58°C and with a maximum difference of 2°C between primers. Finally, the oligonucleotide sequences were submitted for prediction of secondary structures formation in an online database (https://www.idtdna.com/site). Extra base pairs were added according to specific requirements for cloning in specific plasmids.

2.2.7 Digestion with restriction enzyme and DNA ligation

Before ligation in the expression vector, PCR products were digested with the appropriate Fast Digest enzymes (ThermoFisher Scientific). Following instructions from manufacturer, the reaction mixture as shown in table 2.1 were incubated at 37ºC for 1 hour. The enzymes were heat inactivated at 65ºC for twenty minutes.

Table 2.1 – **Reaction composition of DNA treatment with restriction enzymes**

Component	Volume (µL)
DNA (up to 1 µg)	2
Restriction enzyme 1	1
Restriction enzyme 2	1
Fast digestion 10x buffer	2
Free nuclease water	16
Total	20

Plasmid inserts were prepared for ligation by creating sticky ends, i.e. performing restriction digests according to the MCS of the plasmid. Plasmids were linearized using the same restriction enzymes. The ligation reaction was catalysed by T4 DNA ligase (ThermoFisher Scientific), using the reaction mixture outlined in Table 2.2 using a 1:5 molar ratio of vector:insert DNA. The ligation solution would be incubated at room temperature for 30 min and then used for transformation.

Table 2.2 – Reaction components of DNA ligation

Component	Volume (µL)
10x T4 DNA ligase buffer	1
Plasmid DNA	1
Insert DNA	1-2[a]
T4 ligase	1
Water	Up to 10 µL
Total volume	10

[a]DNA volume would be dependant of the concentration

2.2.8 Transformation of *Escherichia coli* cells

Three different strains of *E. coli* were used according to the purpose or plasmid used: DH5α (LifeTechnologies) for sub-cloning in pJET1.2 (ThermoFisher Scientific), BL-21 (LifeTechnologies) for protein expression in pCold-II vector (TaKaRa Bio - Clontech) and BL-21*(DE3) (LifeTechnologies) for pOPIN vectors (provided by OPPF – Oxford Protein Production Facility). All cells were purchased from Thermofisher Scientific. 50-100ng of plasmid DNA was added to a single vial containing 50uL competent cells. Cells were mixed by gentle tapping, and then incubated on ice for 30 minutes. Cells were transformed via heat shock in a water bath prewarmed to 42°C for 30 seconds. The cells were then immediately returned to ice for 10 minutes and then a volume of 250µL of SOC medium was added. Then, then cell mixture was incubated at 37°C, shaking at 200rpm for 90 minutes. The grown mixture was then pipetted onto an LB agar plate containing 100µg/mL of ampicillin, and incubated overnight at 37°C.

2.2.9 Plasmid purification by Miniprep

For preparations of mini preps was used the QIAprep Spin miniprep Kit (Qiagen plasmids) and the purification process was carried out using their proprietary buffers, tubes and protocols. Bacteria with plasmids to be isolated were picked from single colonies and grown overnight at 37^{o}C in 5mL LB broth containing the appropriate antibiotic. Bacteria were then pelleted by centrifugation at 5000rpm for 6 minutes before being resuspended with in 250µL buffer P1 and transferred to a 1.5mL Eppendorf tube. After resuspension and centrifugation steps with supplied buffers accordingly as described instructions, the spin column was moved to a fresh 1.5mL Eppendorf tube. 50µL buffer EB was added, and the column was rested for three minutes. Isolated plasmid was recovered by centrifuged at 13,000g for a final 60 seconds. Plasmid concentrations were estimated by Nanodrop spectroscopy.

2.2.10 Preparation of growth media

Luria-Bertani (LB) broth was made with 10g tryptone, 10g NaCl and 5g yeast extract, dissolved in 1L H_2O. Terrific broth (TB) was made with 12g tryptone, 24g yeast extract, 2.2g KH_2PO_4, 9.4g K_2HPO_4 and 4mL glycerol, dissolved in 996mL H_2O. LB agar plates were made with 10g tryptone, 10g NaCl, 5g yeast extract and 15g agar, dissolved in 1L H_2O.

Once dissolved, all media and the glassware were stored in and/or were grown in were autoclaved to ensure sterilisation. Care was taken to ensure that autoclaving occurred as soon as possible after the media was dissolved, such that bacterial growth was prevented. Antibiotic was added to the media when it had reached a temperature of 50^{o}C or lower. LB agar was poured into plastic agar plates after having had antibiotic added, but before the liquid had begun to solidify.

2.2.11 Cloning of GmmHO in pCold-II

A truncated (GmmHOΔC250) and the full length (GmmHOFL) coding sequences of GmmHO were amplified from female tsetse cDNA using the primers listed in Table 2.3. Polymerase chain reactions were typically carried out in a 20µL reaction volume with the composition outlined in Table 2.4, under the conditions described in table 2.5. The enzyme system used was Phusion HF (ThermoFisher Scientific). Following the PCR reaction, 3µl of PCR products were separated on 1.5%

agarose gel stained with ethidium bromide (0.5µg/µl) and then visualised using transilluminator to confirm product sizes.

The PCR products were then inserted into the pJET1.2 holding vector (ThermoFisher Scientific) following specific instructions from manufacturer and used for transformation of *E. coli* (DH5α). The cells were incubated overnight at 37°C, miniprepped and sent for sequencing before transformation of expression cells.

Following sequence confirmation, full length GmmHOFL was excised from the pJET 1.2 holding vector using restriction enzymes *XhoI* and *NdeI*. The reaction mixture was then incubated with linearized pCold-II and ligated using T4 ligase. The mixture was used to transform BL21 *E. coli* following procedure described in session 2.2.8.

Table 2.3 – Primers used for GmmHO cloning

Primer	Forward sequence (5' - 3')	Reverse sequence (5' - 3')	Size (bp)
Full length	GGGAATTCCATATGGCA ACTGCTAAGGAAAATA	CCGCTCGAGTCAAC GTCTTGCTAATTTAA TTGC	822
Truncated	GGGAATTCCATATGGCA ACTGCTAAGGAAAATA	CCGCTCGAGTCAA TTAGCTCGATTAAC ACCTTTACC	750
pJET1.2	CGACTCACTATAGGGA GAGCGGC	AAGAACATCGATTT TCCATGGCAG	-
pCold-II	ACGCCATATCGCCGAA AGGR	TGGCAGGGATCTT AGATTCTG	-

Table 2.4 – PCR reaction components

Component	Volume (µL)	Concentration
Nuclease-free water	Complete to 20	-
5x HF buffer*	4	1x
10 mM dNTPs	0.4	200 µM each
10 µM forward primers	0.5	0.25 µM
10 µM reverse primers	0.5	0.25 µM
DMSO	0.6	3%
Template DNA	1	1-5 ng/ µL
Phusion DNA polymerase	0.2	0.02 U/ µL

Table 2.5 – PCR thermal cycling timetable for cloning of GmmHO

Cycle stage	Temperature (ºC)	Time (s)	Cycles
Initial denaturation	98	30	1
Denaturation	98	10	
Annealing	60	20	35*
Extension	72	60	
Final extension	72	10	1
Hold	4	∞	-

*The number of cycles refer to denaturation, annealing and extension steps.

2.2.12 Cloning and expression screening of GmmHO constructs using In-fusion cloning technology

In order to express soluble forms of GmmHO for both biochemical and structural studies, a high-through cloning and expression screening of several constructs of the HO with an array of truncations in the C-terminal transmembrane domain was performed using ligation independent pOPIN In-Fusion™cloning system. This system allows cloning of genes without the need of the ligation step, by performing PCRs using gene specific primers with 15bp extensions homologous to the vector ends, generating products that can be fused to the desired In-fusion vector by incubating those with an In-fusion enzyme. Those procedures were accomplished at the Oxford Protein Production Facilites (OPPF – University of Oxford) following standards OPPF protocols (Bird, 2012). pOPIN vectors contain promoters for *E. coli*, baculovirus and mammalian cell expression, thus allowing rapid and reliable cloning and expression of recombinant proteins linked to a variety of affinity purification tags in multiple expression hosts (Berrow *et al.*, 2007).

Primers are detailed in Table 2.6. PCR products were analysed using agarose gel electrophoresis. Miniprep of full length GmmHOFL in pJET1.2 holding vector was used as templates for PCR amplification using KOD Hot Start DNA polymerase. The resultant PCR products were then purified using AMPure XP Magnetic Bead Purification. Because the templates were held in pJET1.2, which has the same antibiotic resistance marker as pOPIN-M (ampicillin), the reaction products were DpnI treated to eliminate false positives with ampicillin selection on agarose plates. The purified inserts were next cloned into linearized pOPIN-F and pOPIN-M vectors using lyophilised InFusion recombinase by mixing followed by incubation at 42°C for 30 minutes. These newly created plasmids were then immediately used to transform OmnimaxII *E. coli* cells. These cells were grown overnight at 37°C on LB agar containing ampicillin, X-Gal and IPTG.

Two positive white colonies were picked per construct and used to inoculate Power Broth and grown overnight at 37ºC, shaking at 220rpm. These cultures were used for Miniprep and for creation of glycerol stocks. The Minipreps were verified using PCR with KOD Hot Start DNA Polymerase before transformation in *E. coli* or insect cells.

Table 2.6 – Primers used for infusion cloning screening in popinF and popinM vectors

Construct	FWD	REV	Size (bp)
GmmHO∆C274	AAGTTCTGTTTCAGGG CCCGGCAACTGCTAA GGAAAATAAAGATG ACGTAGAACCAG	ATGGTCTAGAAAGCTTTATC AACGTCTTGCTAATTTAAT TGCAAAATAAATGC	**849**
GmmHO∆C269	AAGTTCTGTTTCAGGG CCCGGCAACTGCTAAG GAAAATAAAGATGACGT AGAACC	ATGGTCTAGAAAGCTTTATT TAATTGCAAAATAAATGCTA ACAAAGAATAAGACGACAA T	**834**
GmmHO∆C263	AAGTTCTGTTTCAGGGC CCGGCAACTGCTAAG GAAAATAAAGATGAC GTAGAACC	ATGGTCTAGAAAGCTTTA GCTAACAAAGAATAAGAC GACAATGGCCAGTTTCC	**816**
GmmHO∆C255	AAGTTCTGTTTCAGGG CCCGGCAACTGCTAAG GAAAATAAAGATGACGT AGAACC	ATGGTCTAGAAAGCTTTA GGCCAGTTTCCTAATAT TAGCTCGATTAACACC	**792**
GmmHO∆C250	AAGTTCTGTTTCAGGGC CCGGCAACTGCTAAGGA AAATAAAGATGACGTA GAACC	ATGGTCTAGAAAGCTTTA ATTAGCTCGATTAACACC TTTAACCGAACGC	**777**
pOPINF	AAGTTCTGTTTCAGGGCCCG	ATGGTCTAGAAAGCTTTA	**+225**

2.2.13 Protein expression of GmmHO constructs in *E. coli*

Two GmmHO constructs were chosen for scaled-up bacterial protein expression: full length GmmHOFL (in pOPINM vector) and truncated GmmHO missing 23 residues from the C-terminal transmembrane domain (GmmHO∆C250, in pCold-II vector). Both procedures started with a fresh transformation of BL-21 (for protein expressed in pCold-II) or BL21 (for protein expressed in pOPIN-M) *E. coli* cells (LifeTechnologies). Single transformed colonies were used to inoculate 10mL TB containing ampicillin at a concentration of 100µg mL^{-1}.

After an overnight incubation at 37ºC with shaking at 180rpm, the 10mL culture was used to inoculate 1L of TB with antibiotic (100 µg/ mL ampicillin) in a 2L

Erlenmeyer flask. The culture was incubated at 37ºC with shaking at 180 rpm for approximately 5 hours. The optical density (OD) at 600nm was followed in an Epoch spectrophotometer. Once the culture reached an OD_{600} of 0.3 – 0.5 Abs, the shaking incubator's temperature was reduced to that required for expression (25ºC for pOPIN-M constructs, 15ºC for pCold-II construct) with shaking reduced to 160 rpm. Once this temperature was reached by the incubator, the OD was checked again and an aliquot separated to be used as a control (not induced). Once the OD of the culture had reached 0.7 Abs, the culture was induced by addition of IPTG to a final concentration of 0.5mM. The culture was incubated further for another 24h. Bacteria were harvested by centrifugation at 8000rpm for 10 minutes.

2.2.14 Creation of bacterial cell lysate for protein purification

Following centrifugation of 1L protein expression, the supernatant (media) was discarded and the pellet immediately stored at -80ºC until use. Before purification, the pellets were resuspended in 25mL ice cold lysis buffer 50mM Tris-HCl pH8.0; 250mM NaCl with 1X EDTA-free protease inhibitor mix (Roche, 1 tablet per 50mL) and 5U/mL DNAseI. 0.1% Triton X-100 was used to improve solubility as high levels of precipitation were observed despite all steps being performed on ice. The pellets were sonicated on ice at an amplitude of 60-80% for twenty seconds, then left to stand for ten seconds. The process was repeated for a period of seven minutes. The lysate solution created were then centrifuged at 17000 rpm for 30 minutes, after which time the supernatant was collected for purification by the appropriate method to each construct.

2.2.15 Transformation and expression of insect cells

Following the cloning and expression screening of GmmHO construct candidates in bacteria, the same plasmids were used for expression screening in insect cells – due to the ability of those plasmids to be able to express proteins in different hosts (bacterial, insect or human). For that, the plasmids containing the different inserts were used for transformation of baculovirus, which were then used for transfection of Sf9cells (Invitrogen), a clonal isolate of cells prevenient from the insect *Spodoptera frugiperda*. The specific protocols and materials used for cell maintenance, bacmid preparation, transfection, viral amplification and expression testing were performed as described in OPPF standard protocols (Netteship, 2016)

Among the constructs tested in the screening, GmmHOΔC263 (in pOPINF) was selected for scaled up expression in insect cell via baculovirus.

2.2.16 Purification Strategies of GmmHO constructs

The purification strategy of GmmHO constructs differed according to their affinity tag and application (see table 2.12):

GmmHOFL, which was expressed using pOPIN-M vector is a fusion protein of full length GmmHO linked in the N-terminal to maltose binding protein (MBP) and 6-histidine (his-tag or MAHHHHHHSSG) fusion tag by a C3 protease cleavage site (LEVLFQGP↓). Thus, the strategy consisted of resuspension of bacterial pellet in lysis buffer and purification by Ni-NTA affinity chromatography (as described in session 2.2.17), due to the presence of the histidine tag. This step was then followed by incubation of eluted fraction with a digestion enzyme for cleavage of fusion tag (session 2.2.18) and finally, separation of MBP-His fusion tags and GmmHOFL recombinant protein by means of affinity purification using Dextrin-Sepharose affinity chromatography (session 2.2.19), which MBP-HIS fusion tag would bind to.

The GmmHOΔC263 construct was expressed using pOPINF vector with an excisable his-tag thus it was purified by Nickel-affinity chromatography (as described in session 2.2.17), followed by incubation with digestion enzyme (session 2.2.18).

Due to the fact that GmmHOΔC250 construct was expressed in the pCold-II plasmid, it does not possess an amino acid sequence that allows removal of His-tag by a specific tag cleavage protease, thus for purification of this recombinant protein, an affinity chromatography step was enough for biochemical analysis purposes. However, for production of antibodies or crystallization trials, a higher degree of purification was needed and therefore, an additional step of size exclusion chromatography (2.2.20) was executed.

2.2.17 Purification of constructs by Nickel Affinity chromatography

Ni-NTA agarose purification columns were created by adding 2mL shaken Ni-NTA resin into a plastic elution column containing a filter disc. The ethanol solution runs through the column, leaving a Ni-NTA column with 1mL resin bed volume. This column was then rinsed with 20mL dH_2O, followed by 20mL wash buffer (50mM Tris-HCl pH8.0; 150mM NaCl; 30mM imidazole; 0.1% Triton X-100).10 mL of supernatant

from pellet lysis (see section 2.15) were then applied to the resin, which was sealed at the bottom. The lid was replaced, and the resin/supernatant mixture was incubated, shaking at 4ºC for two hours. The column was affixed to a clamp stand and held over a falcon tube, the lid and stopper were removed, and the flow through was collected.

The resin was then washed with 10mL of wash buffer the flow through fraction was collected in a separate tube. This step is repeated, with the flow through collected in another separate tube. To elute the recombinant proteins from the resin, 10mL of elution buffer (50mM Tris-HCl pH8.0; 150mM NaCl; 400mM imidazole 0.1% Triton X-100) was used. 1 mL aliquots were collected in 10 separate Eppendorfs and applied (10 µL) to an SDS-PAGE gel to assess purity and presence of the protein of interest. The aliquots that showed expression of the desired recombinant protein in their protein profile were pooled and used for the following steps.

2.2.18 Cleavage of fusion tags by digestion enzyme

When required, a fraction of fusion-tagged recombinant enzyme eluted from Ni-NTA purification step (~1 mg) was submitted for excision of fusion tags. For that, the PreScission 3C protease (GE-Healthcare) was employed. The Human Rhinovirus (HRV) 3C protease enzyme is able to specifically cleave between the glutamine and glycine residues in the cleavage recognition site (LEVLFQGP↓), present in recombinant proteins expressed in pOPIN vectors. The amount of protease (2U for each 100 µg of fusion recombinant protein), buffers, buffer exchange, overnight incubation at 4ºC and enzyme inactivation and removal were performed following specific instructions provided by GE healthcare.

2.2.19 Separation of MBP-tag and recombinant GmmHO by MBP-affinity chromatography

After the cleavage of recombinant protein, a mix recombinant GmmHO and fusion tags were then separated by MBP-affinity chromatography using a Dextrin-Sepharose High Performance media (GE Healthcare). For that, the mixture was buffer exchanged to the appropriated work buffer (20 mM Tris-HCl, 200 mM NaCl, 1 mM EDTA, pH 7.4), and eluted a 10 mM maltose solution, as recommended by the guidelines provided by GE. The eluted fraction with maltose in which the MBP tags would bind to the media was discarded and the washed fraction containing untagged GmmHO was tested used for biochemical activity.

Aliquots were collected from all the purification steps and analysed by SDS-gel electrophoresis.

2.2.20 Size exclusion chromatography

For size exclusion chromatography, a semi preparative size exclusion chromatography column (Hiload Superdex S-200 - GE Healthcare) coupled to AKTA system was used. After several washing steps with 100 mM Tris-HCl, 300 mM NaCl pH 7.5, a volume of 2 mL of sample (1 mg of eluted fraction from Ni-NTA affinity chromatography) in the same buffer was applied onto the column and the chromatography was run at a rate of 1 mL/min. Aliquots of 1.5 mL were automatically collected by the collector system. The tubes containing the sample of interest were analysed by SDS protein gel and the fractions of interest would be pooled together.

2.2.21 Quantification of protein content by Bradford method

For quantification of protein concentration of the samples the Bradford method was performed (Quick Start™ Bradford assay, BioRad) in wells in a 96-well plate. For that, a standard curve of BSA (0.1 – 1.0 mg mL^{-1} protein) was built by adding to each well 5 µL of each standard, 45µL distilled water and 200µL of Quick Start™ Bradford reagent. 5µL of the protein sample to be quantified was added to empty wells on the plate. In cases where the protein concentration was completely unknown, the sample was diluted 1 in 5, 1 in 10 and 1 in 20, to try and ensure that the absorbance value obtained for the sample wells could be located in the linear portion of the standard curve generated by the BSA standards. The BSA standards were used to generate a standard curve, which was used to calculate the protein concentration, in mg mL^{-1} of the samples. All the groups were prepared in triplicate.

2.2.22 Protein electrophoresis

SDS-PAGE gels were made by first allowing a 12.5% acrylamide resolving gel to set, then pouring a 3% acrylamide stacking gel on top. The resolving gel was made using the reactants described in Table 2.7. After mixing, these reactants had 100µL fresh 0.1g mL^{-1} ammonium persulfate (APS) and 10µL TEMED added to catalyse polymerisation. The solution was poured between two pairs of glass plates up to 1.5cm below the top, and 100µL 2-propanol was pipetted onto the solution. The 2-propanol is immiscible with the gel solution, and floats on top of it, thereby making the resolving

gel flat on top. The gel was allowed to set by leaving it to stand at room temperature for 1 hour.

The stacking gel was made using the reactants described in Table 2.7. Again, after mixing these reactants had 50µL fresh 0.1g mL^{-1} APS and 5µL TEMED added. The 2-propanol was poured off from the resolving gel, and the stacking gel solution was poured in. Gel combs were slotted into the top of the glass plate cassettes so that wells would be formed. The stacking gel was left to stand for 30 min.

After having set, gels to be run were placed in a gel tank, clamped in place, and then submerged in SDS-PAGE running buffer (made from a dilution of 10x stock, the stock was 144g glycine, 30.2g Tris base and10g SDS, dissolved in 1L H_2O). All protein samples to be run were of a volume of 25µL, mixed with 25µL 2X Laemmli buffer (950 µL BioRad premixed 2X Laemmli buffer, 50µL β-mercaptoethanol) in micro centrifuge tubes. These sample tubes were incubated at 95^oC for 10 minutes in order to denature the protein samples. When using a 10 well comb, up to nine protein samples can be run on one gel and at least one is loaded with 6 µL with molecular marker (PageRuler$^+$ Prestained Protein ladder from ThermoFisher Scientific). 20 µL of each denatured protein sample was pipetted into each well. The gel was subjected to a voltage of 60mV until the dye front had moved into the resolving gel, after which time the voltage was increased to 90mV. The gel was allowed to run until the dye front reached the bottom of the gel (~1h).

Table 2.7 – SDS-PAGE gel composition

Resolving gel		Stacking gel	
Component	**Volume**	**Component**	**Volume**
30% acrylamide bis	4.16mL	30% acrylamide bis	0.625mL
H_2O	3.14mL	H_2O	3.0mL
1.5M Tris HCl, pH 8.8	2.50mL	0.5M Tris HCl, pH 6.8	1.25mL
10% SDS	100µL	10% SDS	50µL

2.2.23 Western blotting

After the end of the electrophoresis, the samples were transferred onto BioTrace polyvinylidene diflouride (PVDF) membrane at 90 V for 45 minutes. The membrane was then incubated overnight at 4°C in blocking buffer (PBS/0.1% (v/v) Tween 5% (w/v) and 5% skimmed milk powder). After several washes in washing buffer (PBS/0.1% (w/v), Tween 20), the membrane strips were probed overnight at room temperature with either anti-HO or anti-CPR antibodies. After several washes, the strips were incubated with a 1:10,000 dilution of secondary antibody at room temperature for 1 hour. After several washes, the strips were incubated with SuperSignal West Dura (Pierce, UK) peroxidase buffer and luminol/enhancer solution at a 1:1 ratio, and developed by chemiluminescence for the necessary time.

2.2.24 Crystallization trials of GmmHO constructs

Two of the GmmHO constructs (GmmHO∆C263 and GmmHO∆C250) expressed in this project were chosen for crystallization trials. This step was carried out at OPPF-UK facilities under the supervision of Dr. Joanne Nettleship.

Following purification of GmmHO∆C263 (summarized in session 2.2.16) from insect cells, the protein fractions obtained from size exclusion chromatography were

pooled and split in half. One half was concentrated to 8.5 mg/ml and to the other half 3C protease was added for tag removal and it was left at 4 °C overnight. Crystallisation was set (Table 2.8) up with JCSG+, PACT, Morpheus, Wizard3+4 and Index at 18 °C following specific OPPF guidelines.

For GmmHOΔC250, a pCold-II plasmid containing the insert was sent for OPPF and the expression in *E. coli* and crystallization procedures were carried out in those facilities by Dr. Cristina Yunta Yanes following the same protocols described in OPPF guidelines applied for GmmHOΔC263.

Table 2.8 – GmmHOΔ263 samples submitted for crystallization

Protein	Barcode	Screen	Conc. (mg/ml)
GmmHOΔC263 (His tagged)	441305052231	JCSG+	8.5
	441305052194	PACT	
	441305052200	Morpheus	
	441305052217	Wizard 3+4	
	441305052224	Index	
	441305045004	Salt RX	

2.2.25 Attempt to clone GmmCPR

In an effort to have an appropriate electron partner for GmmHO biochemical characterization, attempts were made to clone and express the NADPH Cytochrome P450 Reductase from *G. m. morsitans* (GmCPR; entry GMOY007231 in VectorBase) in its full length and truncated (without the C-terminal transmembrane domain) versions. Following the same rules for primer design described in session 2.2.6, primers were designed for the cloning and expression of GmmCPR (Table 2.9) in pCold-II plasmid. PCR conditions were set as described in table 2.10.

Table 2.9 – Primers used to clone GmmCPR

Primer	Forward sequence (5' - 3')	Reverse sequence (5' - 3')	Size (bp)
Full length	CCGCTCGAGATGACTGATGAGAAAATCGAAAACG	CCCAAGCTTCTACCCACATATGTAAAAGTGGC	1,878
Truncated	CCGCTCGAGATGACTGCAGCAGTTACAGAAAATTCG	CCCAAGCTTCTACCCACATATGTAAAAGTGGC	1,704
pJET1.2	CGACTCACTATAGGGAGAGCGGC	AAGAACATCGATTTTCCATGGCAG	-
pCold-II	ACGCCATATCGCCGAAAGGR	TGGCAGGGATCTTAGATTCTG	-

Table 2.10– PCR thermal cycling timetable for cloning of GmmCPR

Cycle stage	Temperature (ºC)	Time (s)	Cycles
Initial denaturation	98	30	1
Denaturation	98	10	
Annealing	60	20	35*
Extension	72	60	
Final extension	72	10	1
Hold	4	∞	-

*The number of cycles refer to denaturation, annealing and extension steps.

2.3 – RESULTS

2.3.1 Identification and sequence analysis of GmmHO

Blast searches showed that *G. m. morsitans* possesses a single putative heme oxygenase homologue (Accession number GMOY004329), here named GmmHO. The gene (902bp) contains a single intron and two exons. The coding sequence was predicted to be 822 base pairs long, coding for a 31,93 kDa protein comprised of 273 amino acid residues.

The protein sequence was compared to several putative and confirmed sequences of heme oxygenases from other organisms by Clustal Omega multiple sequence analysis (Figure 2.1), showing a conserved HO sequence arrangement. Sequence alignment indicated that GmmHO contains a large catalytic domain at the N-terminus and a small hydrophobic domain at the C-terminus. This structural arrangement is similar to *D. melanogaster* and mammalian HOs, but different from bacterial, algal, and cyanobacterial HOs which lack the hydrophobic domain.

A GmmHO structural model was built (Figure 2.2), which shows overall structural similarity with mammalian HO-1 (Schuller *et al.*, 1999). With regards heme binding, His25 acts as the proximal ligand of the heme iron in rat HO-1 (ref). In human HO-1, crystal structures have shown that the backbone atoms of the two glycine residues, Gly139 and Gly143 contact the iron are involved in heme binding. These two residues are highly conserved in HOs. In the GmmHO sequence, His-29, equivalent to the proximal iron ligand His-25 in human HO-1 is present. Similarly, Phe-37 in human HO-1 is involved in the interaction with the α-meso edge of heme (Schuller *et al.*, 1999). An equivalent Phe-233 is found in GmmHO, and is conserved in DmHO, AgHO and most other species (Zhang *et al.*; Spencer, 2016)

However, while Gly-161 equivalent to human Gly-139 is present, human HO-1 Gly-143 is replaced by Leu-163 in GmmHO. In DmHO, Gly-139 is similarly replaced by alanine (Zhang *et al.*, 2004). Site-directed mutagenesis of Asp-140 in human HO-1 has previously shown that this residue plays a role in the activation of oxygen (Lightning, 2001; Fujii *et al.* 2001). This residue is replaced by Leu-134 in GmmHO. Similarly in DmHO Gly139 is replaced by Ala (Zhang *et al.*, 2004). Taken together,

the sequence and modelling data suggests that the overall structure of GmmHO is similar to that of mammalian and other HOs. However the differences in some key amino acids that interact with heme may indicate differences in the structure of the heme pocket.

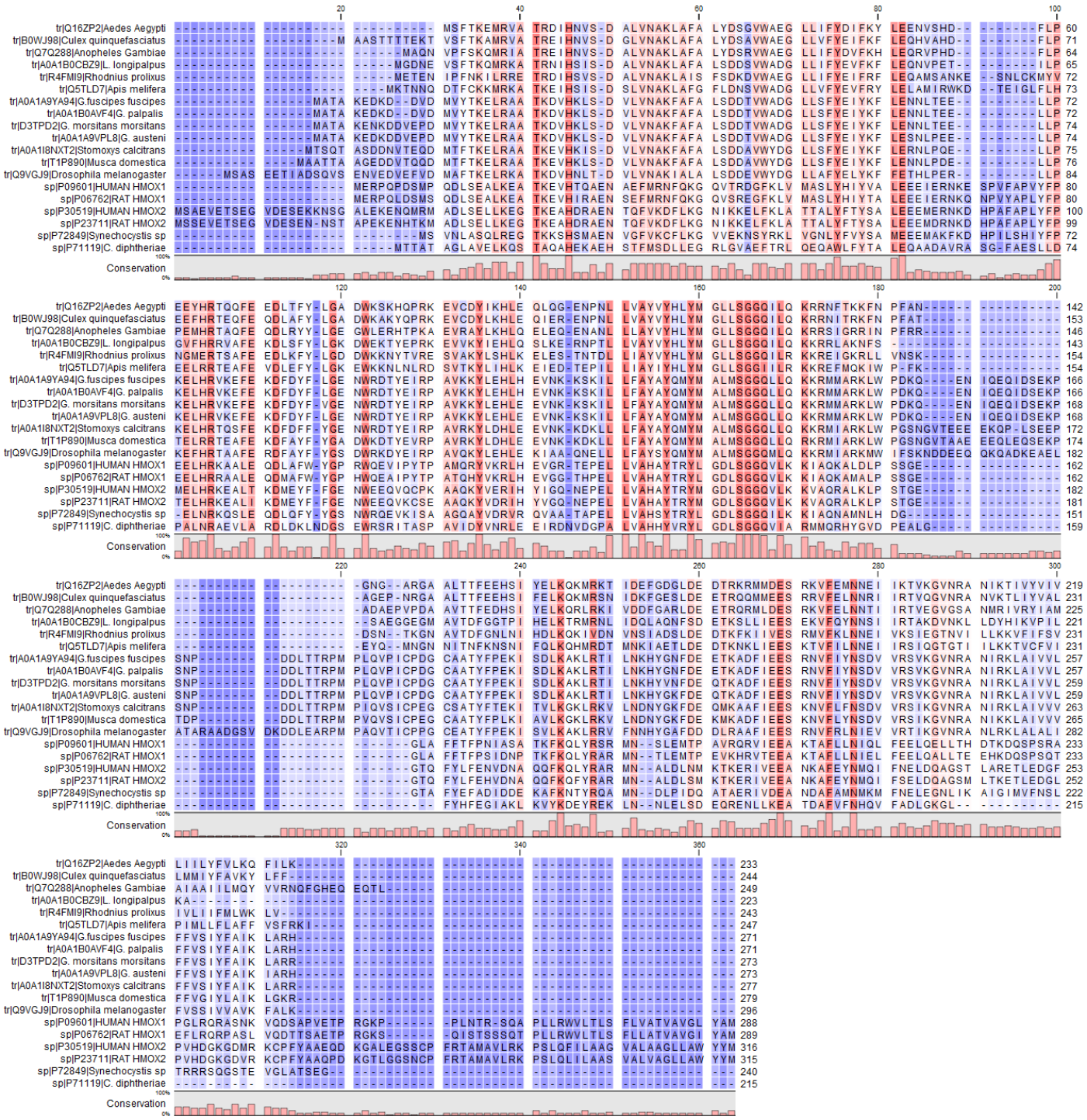

Figure 2.1 Multiple sequence alignment of protein HO sequences from insect and non insect species. Background colouring indicates residues conservation from low (blue) to high (red). The species compared were *Aedes aegypti, Anopheles gambiae, Apis melifera* , *Corynebacterium diphtheria, Culex quinquefasciatus, G. fuscipes fuscipes* (0), *G. palpalis palpalis, G. austeni, Musca domestica, Rattus novergicus* HO-1 and HO-2, *Rhodnius prolixus, Synechocystis sp Stomoxys calcitrans* and *Homo sapiens* HO-1 and HO-2.

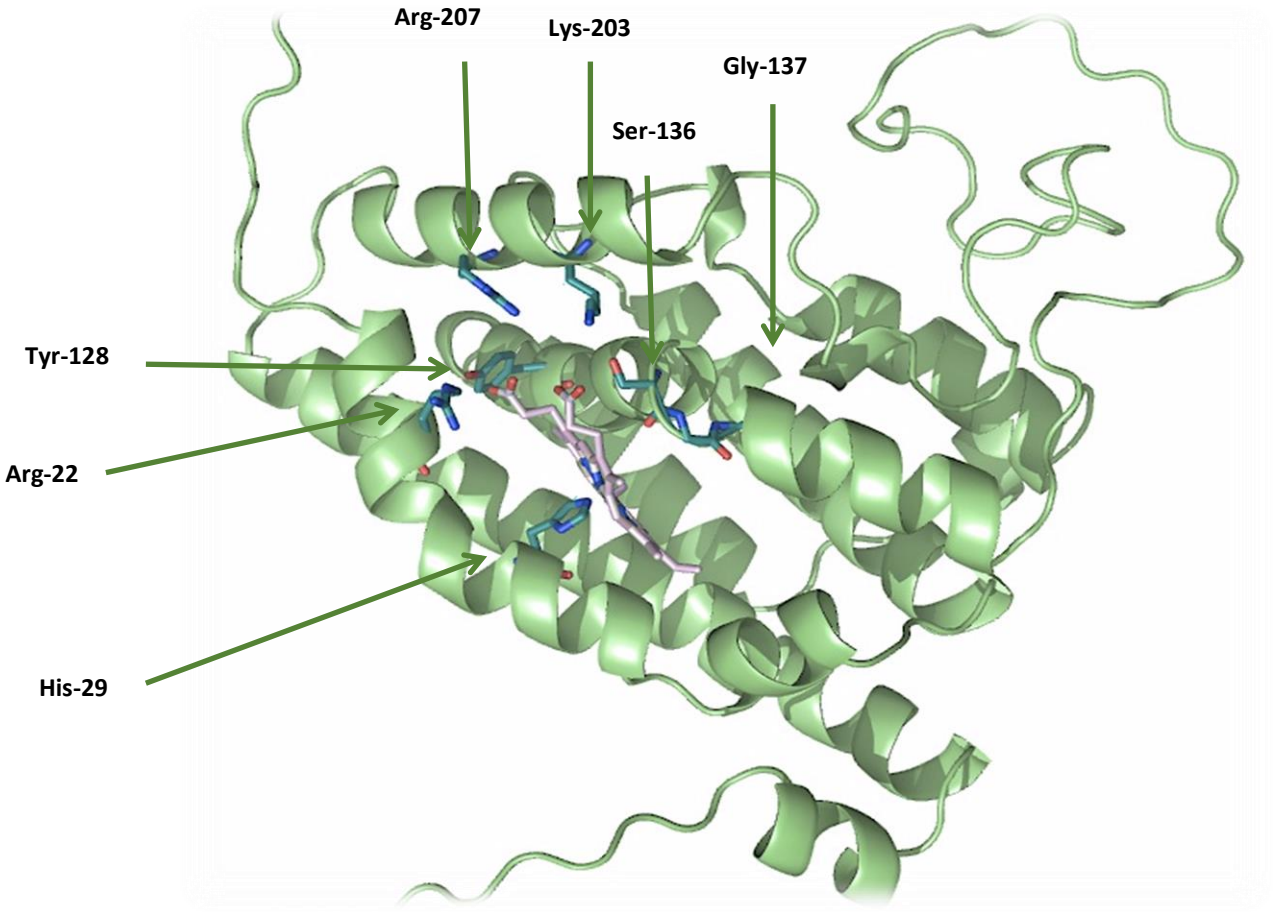

Figure 2.2 Structure model of full length GmmHO (GmmHOFL). The theoretical protein structure model of G. m. morsitans HO (GmmHO) was built based in empirical models of other heme oxygenases available. The top templates used were crystal structure from *H. sapiens* HO-2 (2rgz.1.A, 2rgz.1.A and 2rgz.1.A), *Chlamydomonas reinhardtii* (4raj.1) and Synechocystis sp. (1wow.1). The green arrows indicate which residues are potentially involved in heam-binding.

Interestingly, some residues conserved in *D. melanogaster, M. domestica, S. calcitrans* and the *Glossina* genus were different from the highly conversed ones in the other organisms. These include Gly-161 and Leu-163. Table 2.11 shows the sequence identity of HO homologues from other insects and from well characterized HOs from mammals, plant and bacteria to GmmHO. It was notable that all insect species analysed this far appear to contain a single HO gene. This differs with humans and other mammals, which are reported to contain at least two isoforms each. As expected, the highest levels of identity were found with other tsetse fly species *G. austeni* (97.4%), *G. fuscipes fuscipes* (97.4%) and *G. palpalis* (97.4%), confirming the high level of conservation of those enzymes in the genus *Glossina*. Besides, high identities were found to the stable fly *Stomoxys calcitrans*, to the house fly *Musca domestica* (74%) and to fruit fly *Drosophila melanogaster* (63%), phylogenetically the most related insect species to *G. morsitans morsitans*. Relatively low (36.7 %) identity was found with *Anohopeles gambiae*, the only other HO characterised from a blood feeding insect (Spencer, 2016) a possible indication that hematophagus HOs do not have distinguishing functional features. The phylogenetic relationships among the HOs can also be seen in Figure 2.3.

Transmembrane region predictions showed that GmmHO has one potential transmembrane domain in the C-terminal between residues 254 and 271 (Figure 2.4). Similar feature has been observed in other HOs, such as human HO-1 and HO-2 and in *D. melanogaster*. A series of nucleotide primers were designed for cDNA cloning and PCR amplification of full length and truncated forms of GmmHO lacking portions or the transmembrane domain. Since hydrophobic transmembrane sequences are not generally involved in catalytic function and can lead to solubility issues in recombinant proteins, removal of the transmembrane region was done to enhance the production of soluble HO for crystallisation.

Table 2.11 Identity of heme oxygenases protein sequences from several species to GmmHO.

Species	Identity to GmmHO
Glossina austeni	97.4
Glossina fuscipes fuscipes	97.4
Glossina palpalis gambiensis	97.4
Stomoxys calcitrans	77.5
Musca domestica	74.4
Drosophila melanogaster	62.1
Culex quinquefasciatus	42.1
Lutzomyia longipalpis	42.4
Aedes aegypti	39.5
Rhodnius prolixus	35.9
Anopheles gambiae	36.7
Human HO1	32.4
Human HO2	41.4
Rat HO1	30.1
Rat HO2	41.4
Synechocystis sp.	31.2
Corynebacterium diphtheriae	32.3

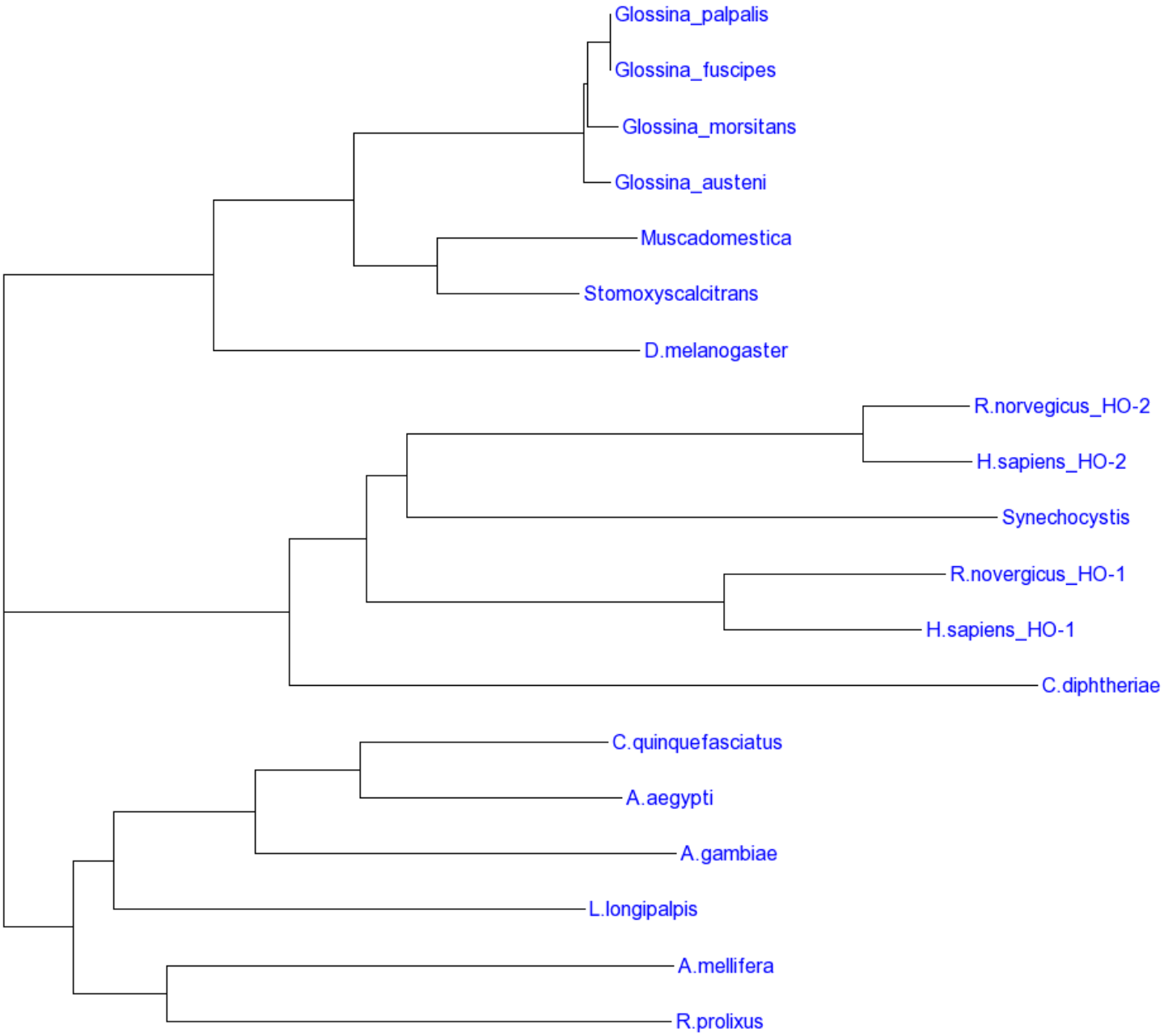

Figure 2.3 Phylogenetic relationship of heme oxygenases from several insect and non-insect species. The species and respective distance values were *Aedes aegypti* (0.124), *Anopheles gambiae* (0.19978), *Apis melifera* (0.24033), *Corynebacterium diphtheria* (0.355), *Culex quinquefasciatus* (0.11737), *G. fuscipes fuscipes* (0), *G. palpalis palpalis* (0), *G. austeni* (0.01274), *Musca domestica* (0.09501), *Rattus novergicus* HO-1(0.10445), HO-2 (0.05127), *Rhodnius prolixus* (0.23901), *Synechocystis sp* (0.2803), *Stomoxys calcitrans* (0.06744) and *Homo sapiens* HO-1(0.10445) and HO-2 (0.05127). The distance values asigned represent number of substitutions as a proportion of the length of the alignment.

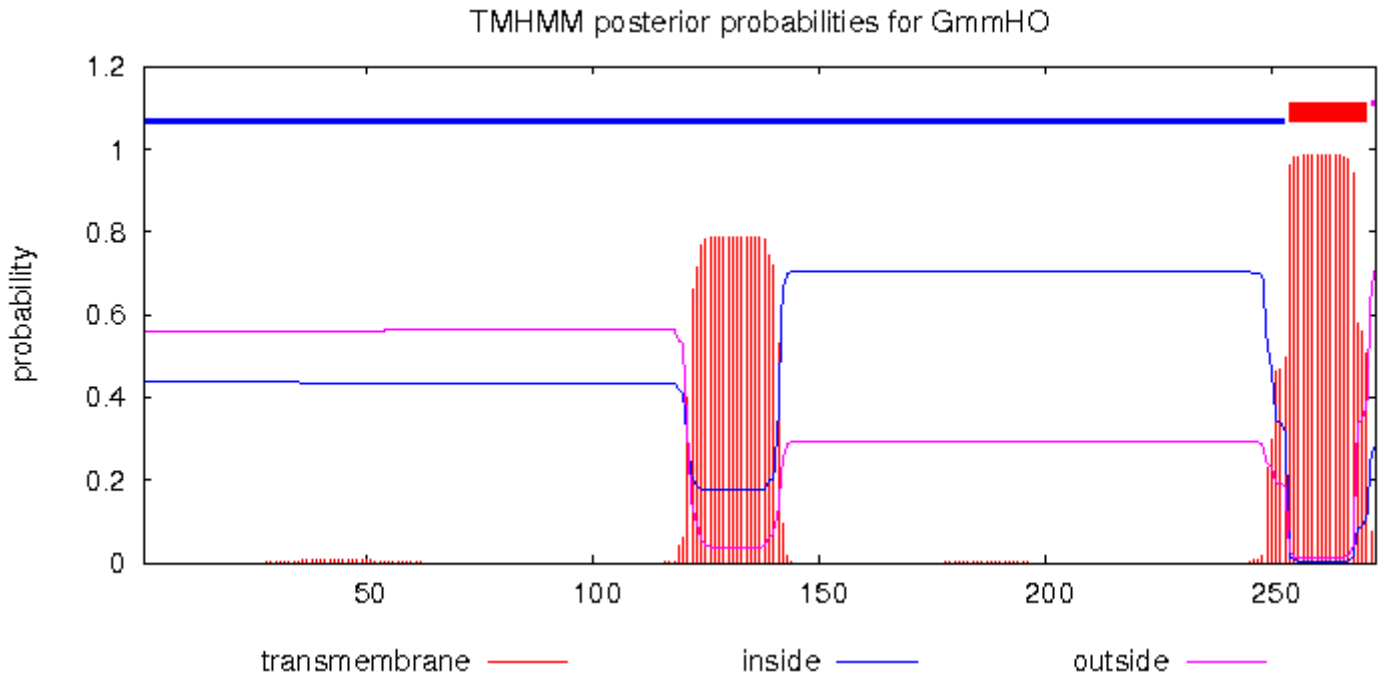

Figure 2.4 Prediction of transmembrane regions for full length GmmHO. The transmembrane domain prediction of GmmHO was performed using TMHMM method (Sonnhmer et al, 1998). As indicated by the red bold line, the residues 254-271 are predicted to constitute a transmembrane helix and was used as a guide to design primers targeting truncations for the expression of soluble recombinant GmmHO constructs.

2.3.2 Cloning of GmmHO

Based on the sequence found in databases (VectorBase, GMOY004329), complementary primers to the 5' and 3' ends of GmmHO were designed to clone full length and truncated forms lacking the nucleotides correspondent to the C-terminal transmembrane domain. As shown in Figure 2.5, when using cDNA from unfed female *G. m. morsitans*, the PCR products amplified had the expected size for both truncated (790bp) and full length (862bp) forms. No extra bands were detected suggesting that designed primers were specifically amplifying the HO gene fragment.

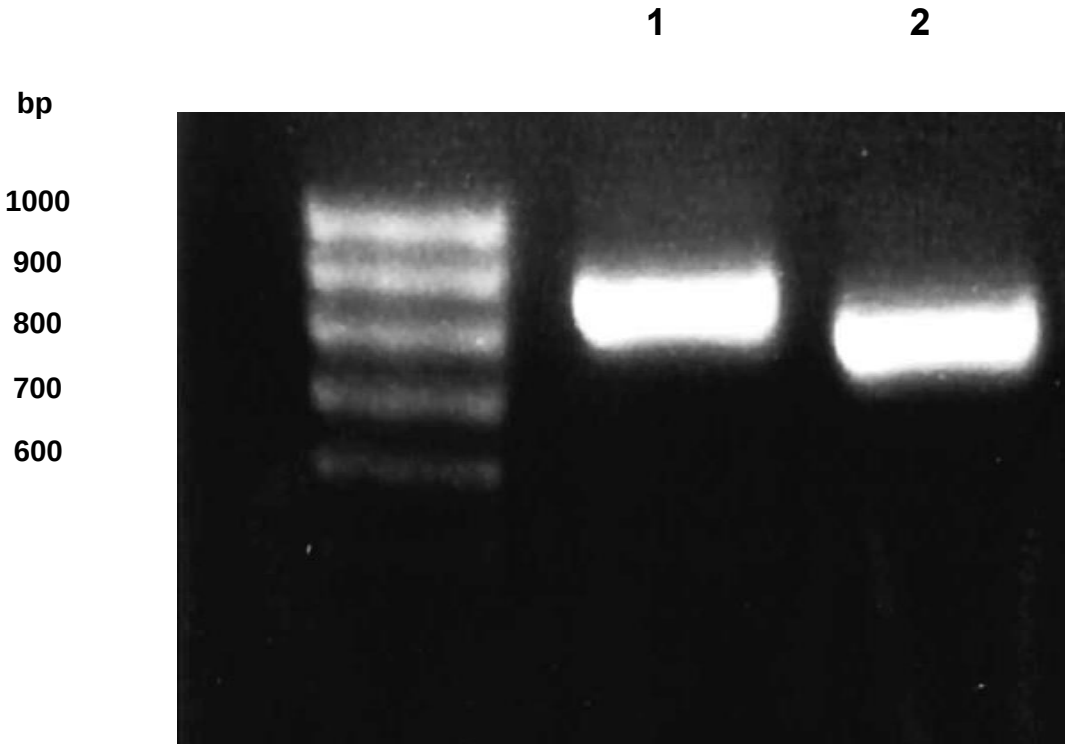

Figure 2.5 – Isolation of GmmHOFL (1, full lenght) and GmmHO∆C250 (2, truncated) forms of GmmHO from tsetse female cDNA. Gels contained with 1.5 % agarose and 0.5mg/mL ethidium bromide. A total volume of 15µL of each sample with 6x dye was added per well, along with 6µL Hyperladder IV. Samples were run at 100 V for 45 min.

The sequence of the primers used for cloning in pJET1.2 holding vector were adapted for cloning into the expression vector pCold-II by adding restriction sites for the enzymes *XhoI* and *NdeI*. As seen in Figure 2.6 both forms were successfully cloned; it is noticeable that most colonies were transformed with truncated constructs but only two of the colonies were positive for full length primers.

Sequence analysis revealed that most colonies matched the one available in the database (VectorBase, GMOY004329). These were sub cloned in *E. coli* expression vectors for functional characterisation or crystallography purposes (Table 2.12). However, it was notable that approximately 10% of the clones produced a proline to serine substitution at amino acid position 171. Since this was a consistent nucleotide change, and Pfu polymerase was used for PCR, which has a very low error rate, this result suggests the presence of a possible polymorphic variant. As this not part of the predicted heme binding pocket, the mutation is not expected to have a functional impact, although this was not examined.

For comparison, full length primers were used for amplification of products from *G. m. morsitans* cDNA and gDNA templates as well as gDNA from two other species of Tsetse fly (*G. fuscipes fuscipes and G. palpalis gambiense*) and the stable fly *Stomoxys calcitruns.* Two clones (FM985191.1 and BX557197.1) from the expressed sequence tag (EST) library that matched the GmmHO sequence were also used as positive controls. As expected, the PCR products generated from *G. morsitans* gDNA was slightly bigger than the ones from EST library and Tsetse cDNA (Figure 2.7), confirming the presence of an intron as described in database. The gDNA from the two *Glossina* species were amplified but not *S. calcitrus*. This indicates a high conservation of HO sequence among *Glossina* species that doesn't appear to extend to the other species tested.

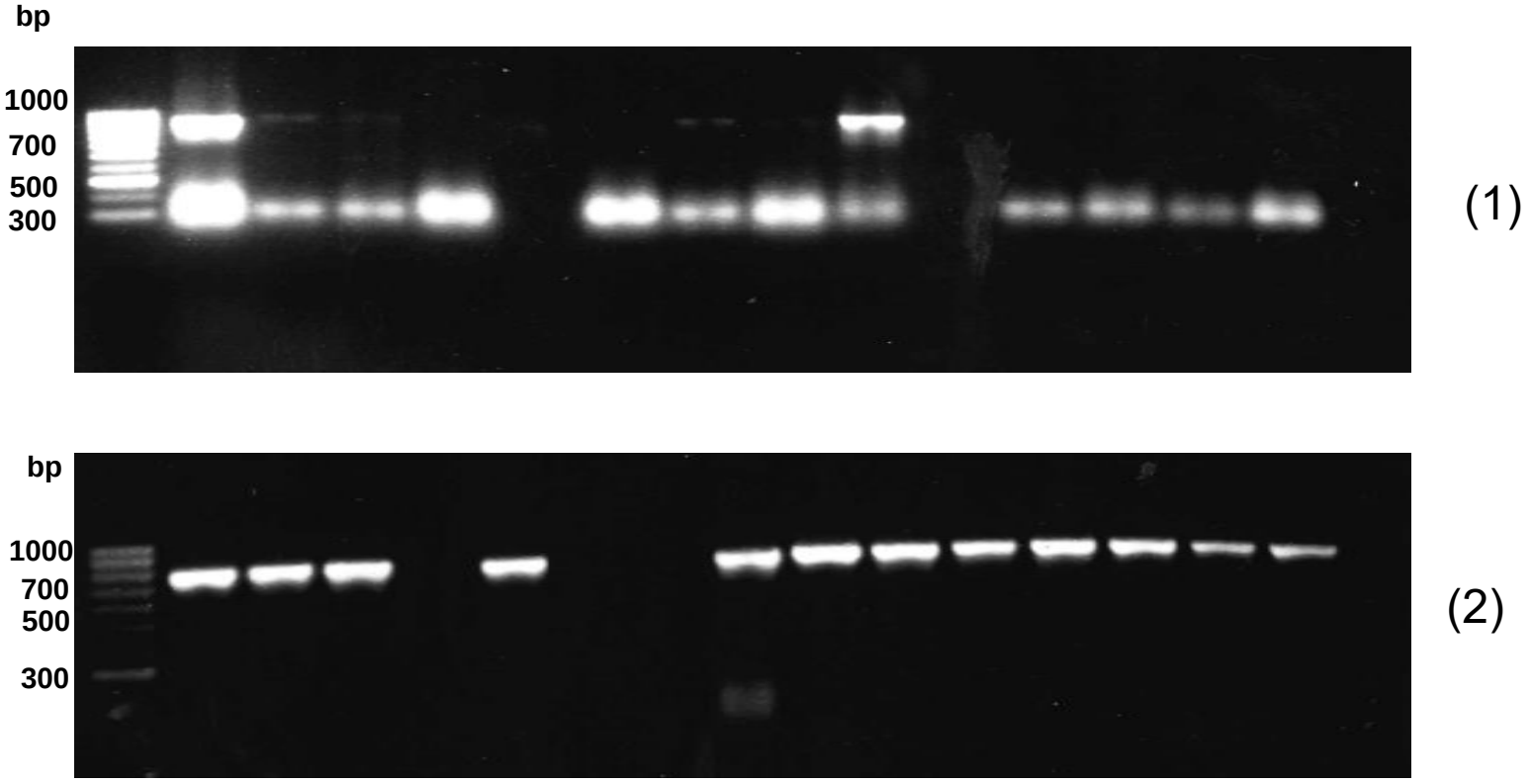

Figure 2.6 – Diagnostic PCR of DH5α (*E. coli*) colonies transformed with GmmHOFL (1) and GmmHO∆C250 (2) in pJET1.2 cloning vector. Gels contained with 1.5 % agarose and 0.5mg/mL ethidium bromide. A total volume of 15µL of each sample with 6x dye was added per well, along with 6µL Hyperladder IV. Samples were run at 100 V for 45 min.

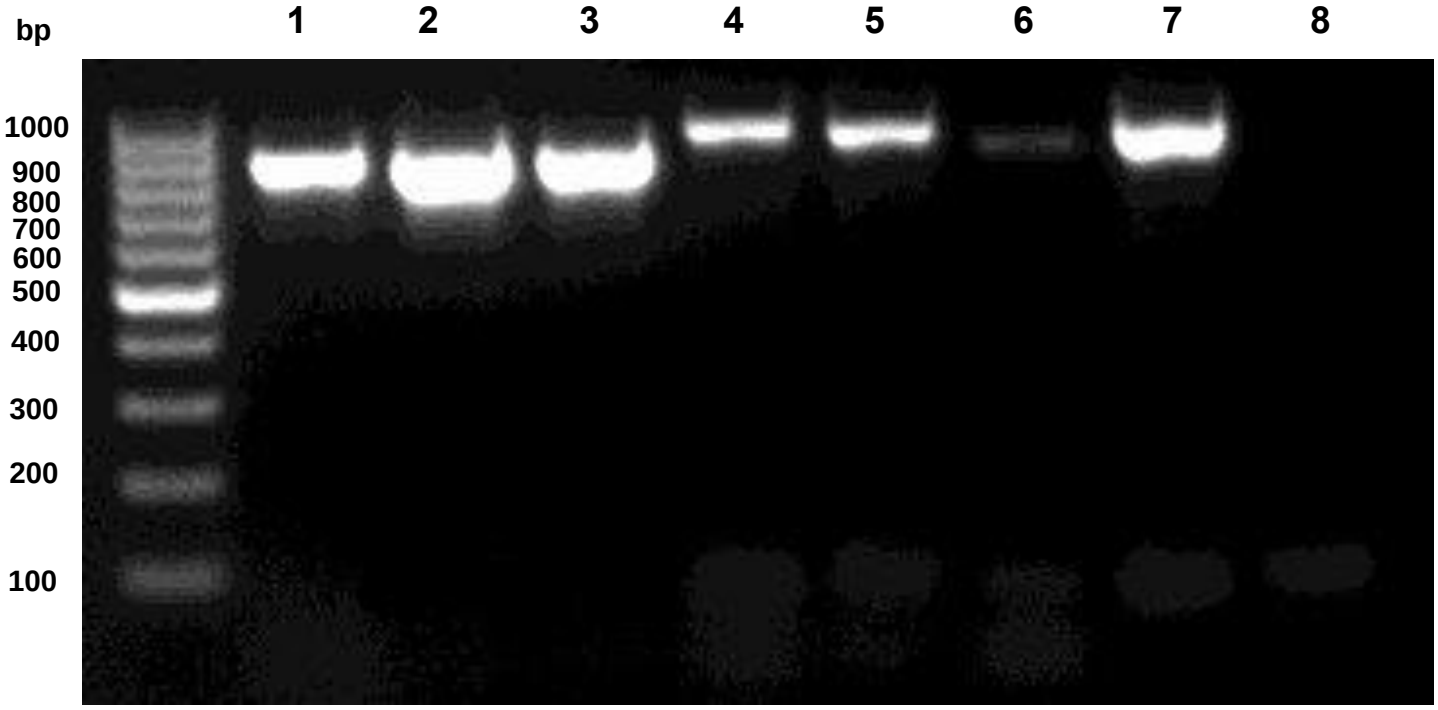

Figure 2.7 – PCR product amplification of GmmHO using different DNA sources (1) Tsetse cDNA (2) EST clone BX557197.1 (3) EST clone FM9851911 (4) *G. morsitans morsitans* gDNA (5) *G. palpalis* gDNA (6) *S. calcitrans* gDNA(7) *G. fuscipes* gDNA (8) negative control. Gels contained with 1.5 % agarose and 0.5mg/mL ethidium bromide. A total volume of 15 µL of each sample with 6x dye was added per well, along with 6 µL Hyperladder IV. Samples were run at 100 V for 45 min.

Table 2.12 – GmmHO constructs used in this work.

Construct	Residues nº	Vector	Tag	MW with tag (kDa)	MW without tag (kDa)	Expression system	Aim	Purification yield (mg/l culture)
GmmHOFL (full lenght)	273	pOPINM	N-his$_6$-MBP-3C	31.93	76.53	*E. coli*	BC	2.27
GmmHOΔC263	263	pOPINF	N-his$_6$-3C	30.70	75.3	Insect cells via baculovirus	BC, CT	1.19
GmmHOΔC250	250	pCold-II	N-his$_6$	Not cleavable	30.03	*E. coli*	BC, CT, AP[123]	8.6

[1,2,3]BC: biochemical characterization; CT: Crystalization; AP: Antibody production

2.3.3 Cloning and expression of GmmHOΔC250

To express a soluble form of the enzyme for biochemical characterization, a pJET1.2:GmmHOFL clone was used as a template to clone GmmHOΔC250 into the expression vector pCold-II. *E. coli* strain DH5α was transformation with the construct and verified by sequencing before transformation in *E. coli* BL21 (DE3) for expression.

A time course of protein expression showed an increase in expression at 24 and 48 hours after IPTG induction as well as the subsequent purification of GmmHOΔC250 48 hours after IPTG induction (Figure 2.8.) Due to the high degree of contamination, the eluted fractions (Figure 2.9) were pooled and subjected to size exclusion chromatography (Figure 2.10). SDS-PAGE analysis of eluted fractions (Figure 2.11) confirmed the removal of higher molecular weight contaminating proteins and the production of pure GmmHOΔC250 (>95%) of the expected molecular weight (~29 kDa). The purified GmmHOΔC250 was used for antibody production. For biochemical analysis, the eluted fraction resultant from the first chromatography step were used.

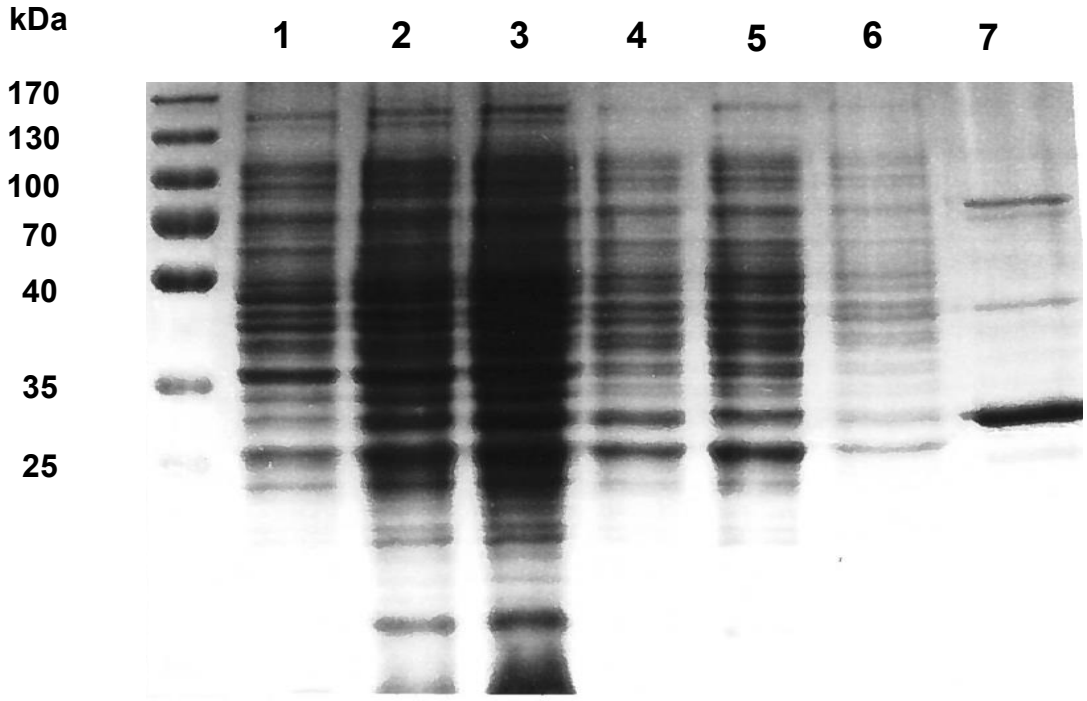

Figure 2.8 – Purification of GmmHO∆C250. Acrylamide gel (12.5%) showing purification steps of recombinant GmmHO∆C250. (1) Before induction; (2) 24 hours after induction; (3) 48 hours after induction; (4) lysate before chromatography (5) Washed fraction; (6) Flow thought fraction; (7) Eluted GmmHO∆C250. The samples with mixed with reducing Laemmli sample buffer and incubated at 95^{o}C for 10 minutes before loading 20 µL of each denatured protein sample (10 µg) in each individual lane the gel along with 6 µL of molecular marker (PageRuler^{+} Prestained Protein ladder from ThermoFisher Scientific). The gel was subjected to a voltage of 60mV until the dye front had moved into the resolving gel, after which time the voltage was increased to 90mV. The gel was allowed to run until the dye front reached the bottom of the gel (~1h).

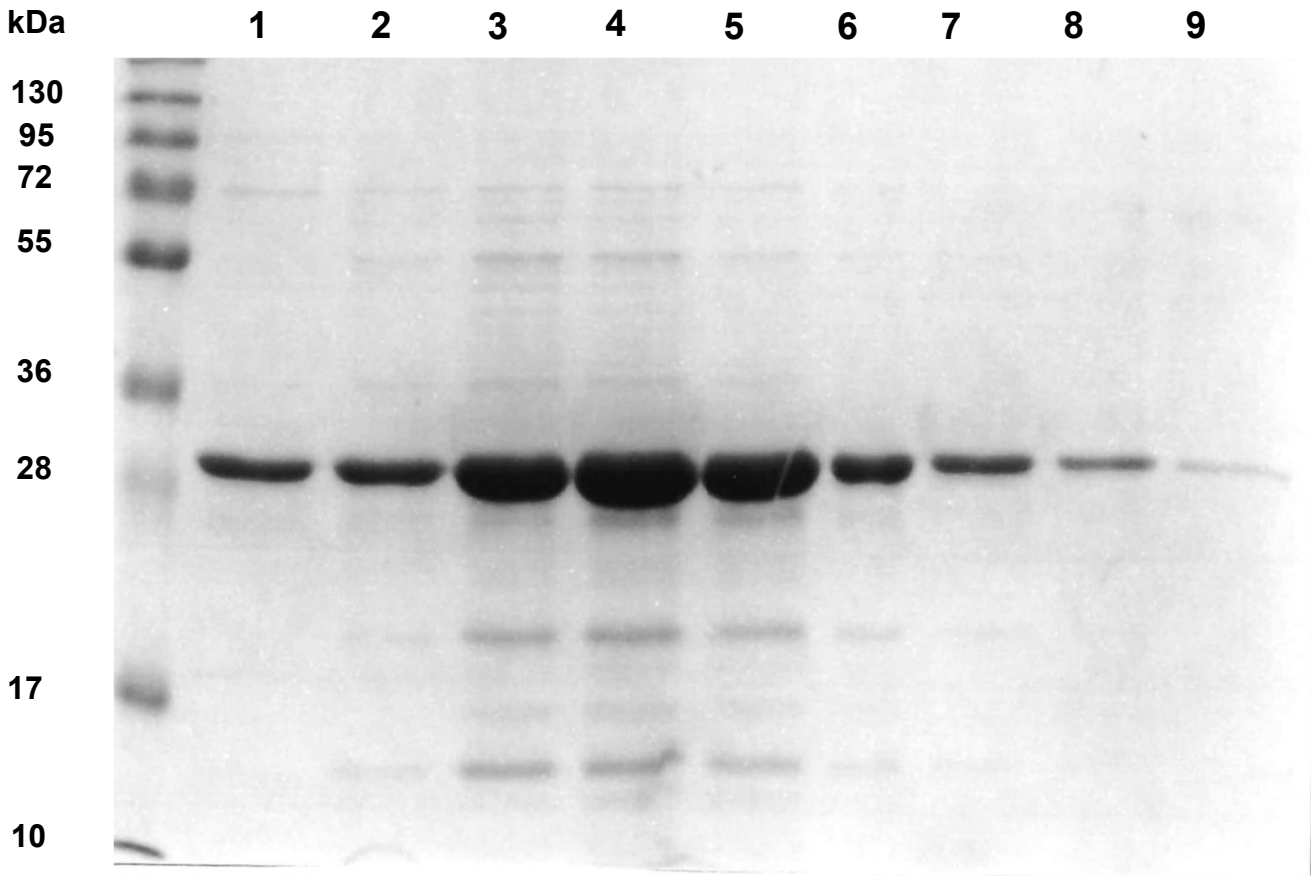

Figure 2.9 – Protein profile of eluted fractions from purification of recombinant GmmHO∆C250 by Ni-NTA affinity chromatography. Acrylamide gel (12.5%) showing eluted fractions (1-9). During the procedure 1 mL from each fraction was collected in individual tubes and used for protein electrophoresis. The samples with mixed with reducing Laemmli sample buffer and incubated at 95^{o}C for 10 minutes before loading 20 µL of each denatured protein sample (10 µg) in each individual lane the gel along with 6 µL of molecular marker (PageRuler^{+} Prestained Protein ladder from ThermoFisher Scientific). The gel was subjected to a voltage of 60mV until the dye front had moved into the resolving gel, after which time the voltage was increased to 90mV. The gel was allowed to run until the dye front reached the bottom of the gel (~1h).

(1)

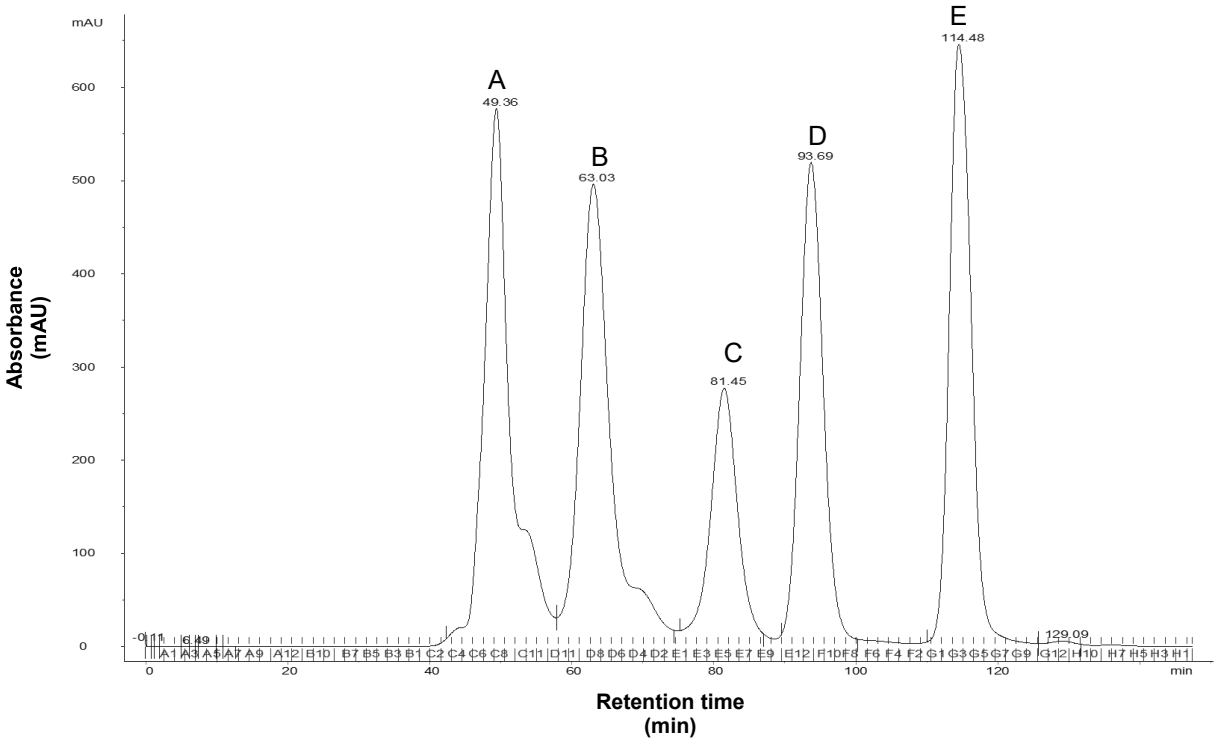

(2)

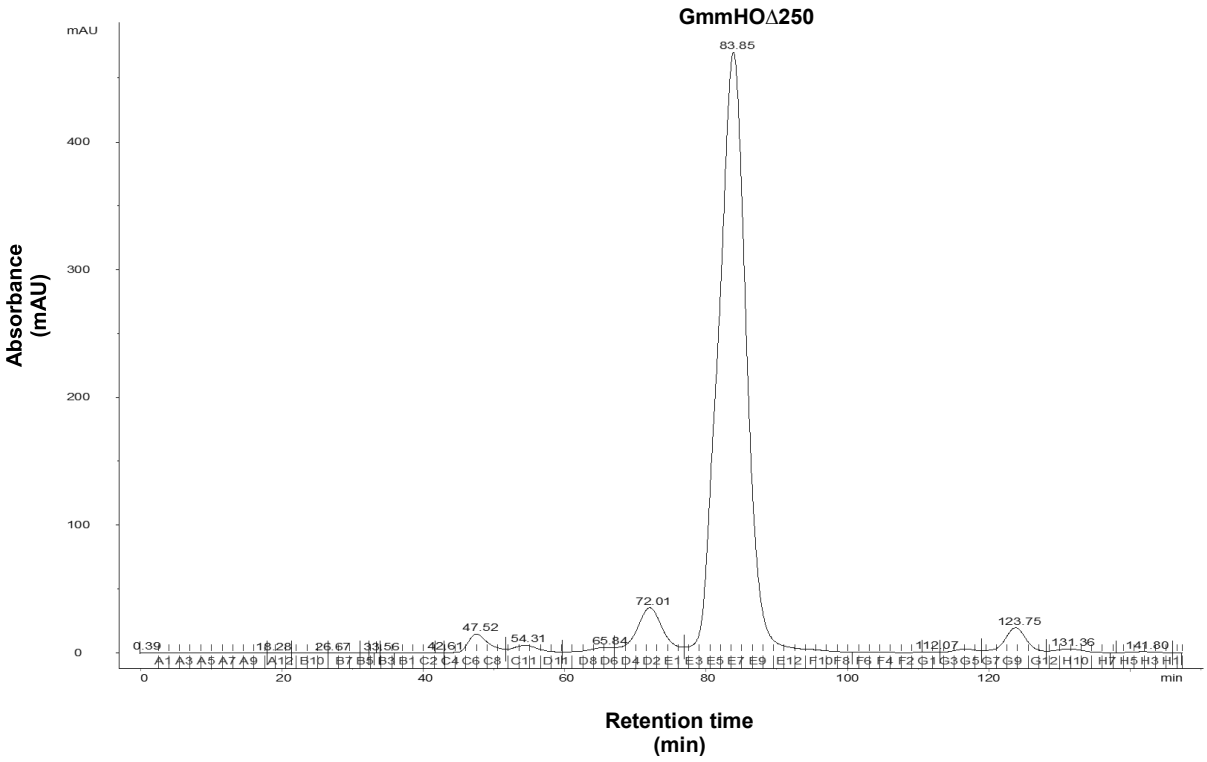

Figure 2.10 – Size exclusion chromatogram of GmmHOΔ250 following Ni-NTA affinity purification. (1) Molecular standards: [A] Thyroglobulin – 660 kDa, [B] Bovine Y-globulin – 158 kDa, [C] Chicken ovoalbumin – 44 kDa, [D] Equine myogloblulin – 17 kDa, [E] Vitamin B – 1.3 kDa (2) Recombinant GmmHO. 5 mg of the sample was applied to a 120 mL column in 100 mM Tris-HCl, 300 mM NaCl pH 7.5. A vlolume of 1.5 mL of each fraction was collected.

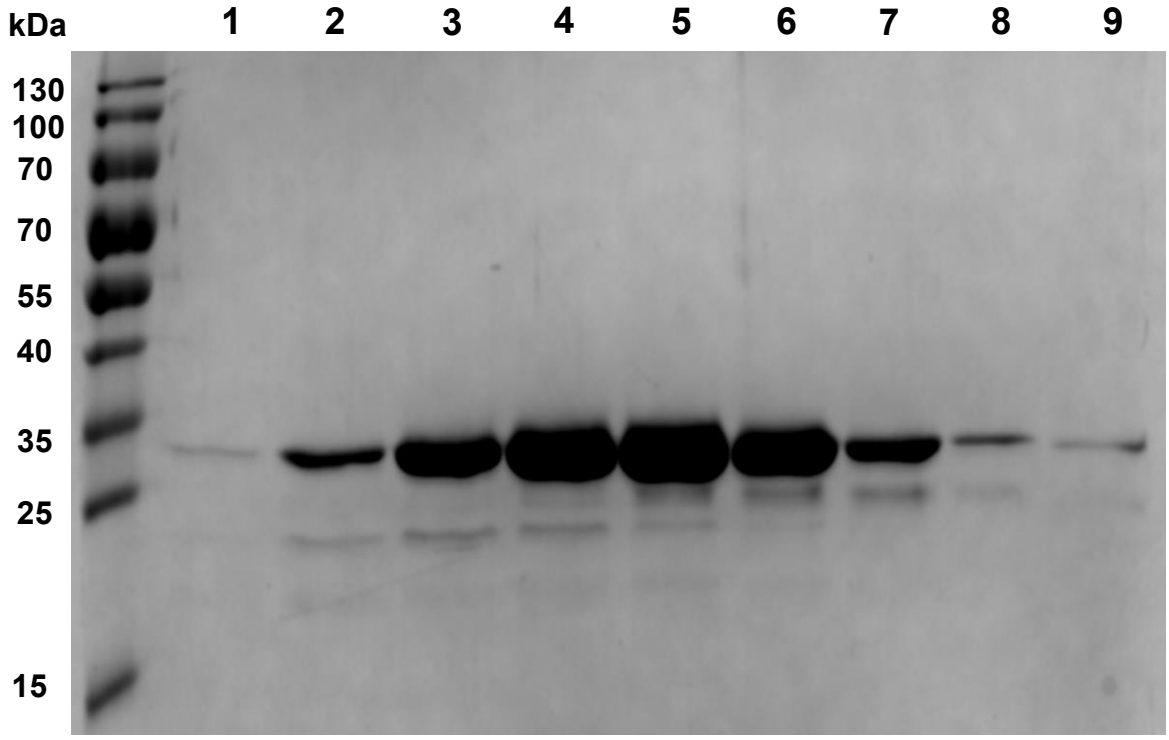

Figure 2.11 – Purification of recombinant GmmΔC250 by size exclusion chromatography. Acrylamide gel (12.5%) showing eluted fractions (1-9). The samples with mixed with reducing Laemmli sample buffer and incubated at 95°C for 10 minutes before loading 20 µL of each denatured protein sample (10 µg) in each individual lane the gel along with 6 µL of molecular marker (PageRuler+ Prestained Protein ladder from ThermoFisher Scientific). The gel was subjected to a voltage of 60mV until the dye front had moved into the resolving gel, after which time the voltage was increased to 90mV. The gel was allowed to run until the dye front reached the bottom of the gel (~1h).

2.3.4 High thought expression of GmmHO

The pJET1.2 vector holding full-length GmmHO (Figure 2.5) was used as template and the PCR products cloned into pOPIN-F and pOPIN-M expression vectors (Figure 2.12). Following which, the constructs were screened for expression in bacteria and insect cells. This resulted in the successful expression of several GmmHO-pOPIN-M constructs in bacteria (Figure 2.13) and GmmHO-pOPIN-F in insect cells (Sf9) (Figure 2.14). The highest levels of soluble recombinant GmmHO were associated with higher levels of membrane anchor truncation.

Based on the recombinant protein yield (Table 2.12), full length (GmmHOFL) and truncated GmmHO lacking 10 residues in the C-terminal constructs (GmmHOΔC263) were chosen for scaled up expression in *E. coli* and insect cells, respectively. Due to the presence of 3C cleavage site in both plasmids, the fusion tag from the recombinant proteins were excisable by enzymatic treatment with HRV 3C protease.

Figure 2.15 shows the purification steps of full length GmmHOFL expressed with maltose binding protein (MBP) tag. In this case, the protein eluted from Ni-NTA column (Figure 2.15, lane 1) was treated with the protease (Figure 2.15, lane 2) and subsequently applied to a Dextran-Sepharose column. The eluted fraction (MBP), (Figure 2.15 lane 5) was discarded and the flow thought containing the recombinant enzyme (Figure 2.15, lane 3) was recovered and used for biochemical analysis.

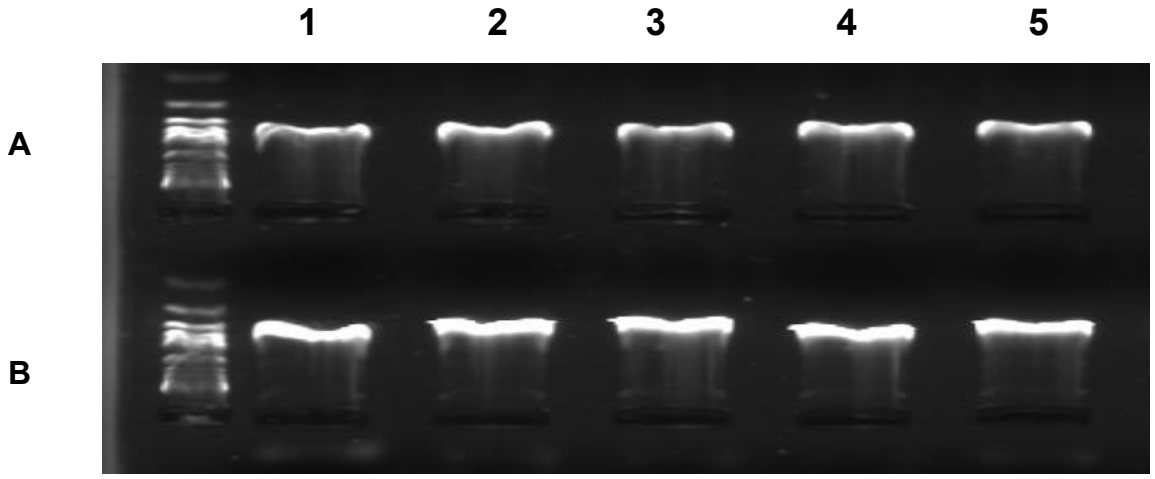

Figure 2.12 PCR screening of GmmHO constructs in pOPINF (A) and pOPINM plasmids (B). (1) GmmHO∆274 (2) GmmHO∆269 (3) GmmHO∆263 (4) GmmHO∆255 (5) GmmHO∆250 Gels contained with 1.5 % agarose and 0.5mg/mL ethidium bromide. A total volume of 15uL of each sample with 6x dye was added per well, along with 6uL Hyperladder IV. Samples were run at 100 V for 45 min.

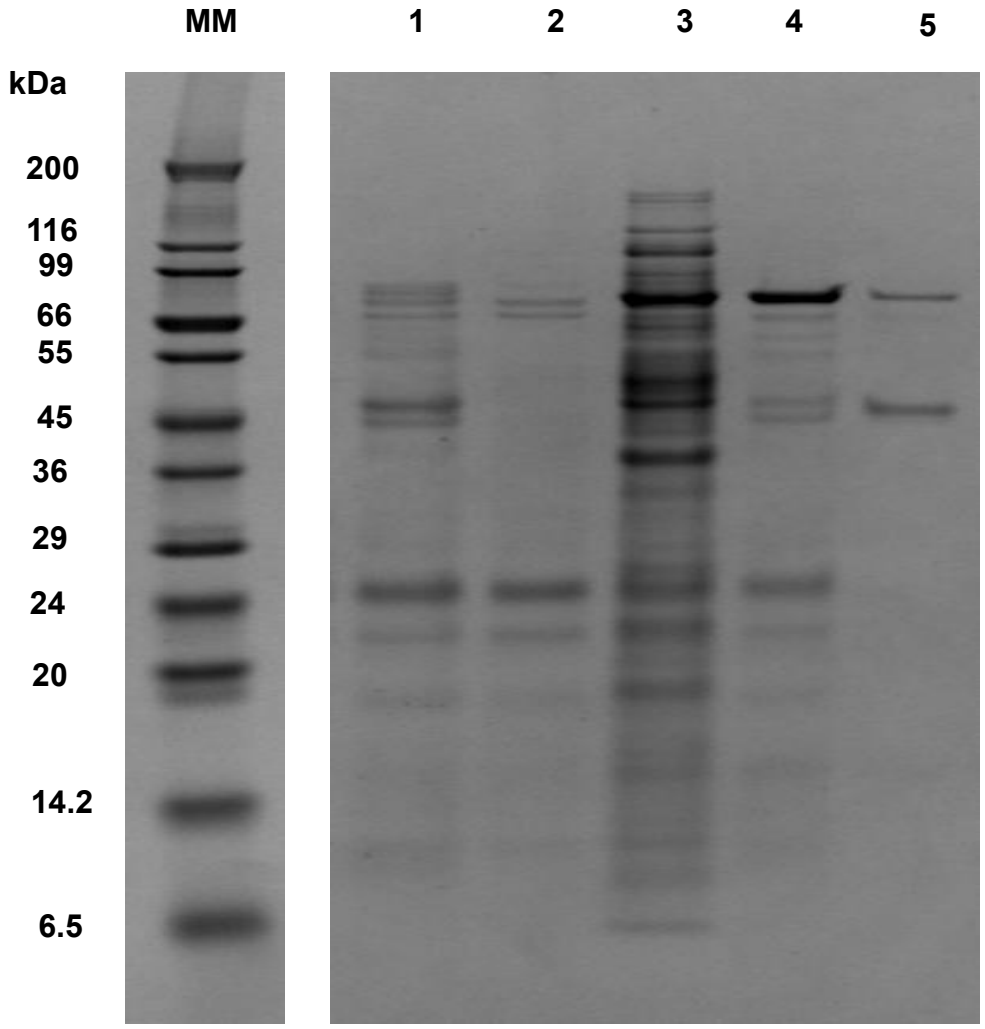

Figure 2.13 Ni-NTA Purified GmmHO-popinM constructs from OPPF screening in bacterial expression system (1) GmmHOΔC274, (2) GmmHOΔC269, (3) GmmHOΔC263, (4) GmmHOΔC255, (5) GmmHOΔC250. The samples with mixed with reducing Laemmli sample buffer and incubated at 95^{o}C for 10 minutes before loading 20 µL of each denatured protein sample (10 µg) in each individual lane the gel along with 6 µL of molecular marker (SigmaMarker™wide range, SIGMA-ALDRICH). The gel was subjected to a voltage of 60mV until the dye front had moved into the resolving gel, after which time the voltage was increased to 90mV. The gel was allowed to run until the dye front reached the bottom of the gel (~1h). Samples and molecular marker are shown as separated gels due to the high number of samples that were loaded in the same gel, however they run at the same time.

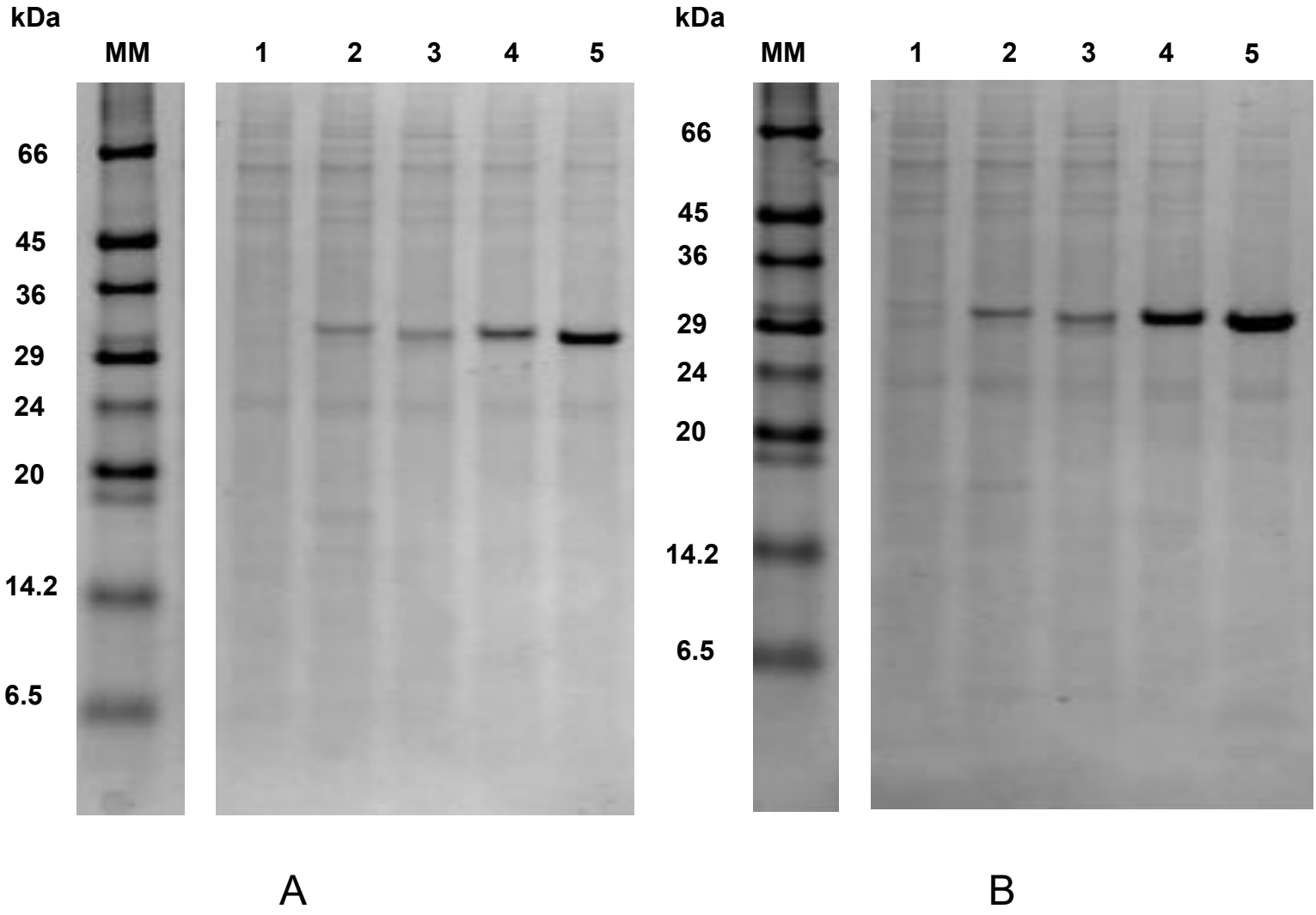

Figure 2.14 Ni-NTA Purified GmmHO-popinF constructs from expression screenings in insect cells using different two volumes of viral suspension culture. (1) GmmHOΔC274 (2) GmmHOΔC269 (3) GmmHOΔC263 (4) GmmHOΔC255 (5) GmmHOΔC250. Insect cells were transfected with 2 different volumes of baculovirus suspension transformed with the plasmids: 3 µL and 30 µL. After resuspension of pellets, the samples were mixed with reducing Laemmli sample buffer and incubated at 95^{o}C for 10 minutes before loading 20 µL of each denatured protein sample (10 µg) in each individual lane the gel along with 6 µL of molecular marker (SigmaMarker™ low range, SIGMA-ALDRICH). The gel was subjected to a voltage of 60mV until the dye front had moved into the resolving gel, after which time the voltage was increased to 90mV. The gel was allowed to run until the dye front reached the bottom of the gel (~1h). Samples and molecular marker are shown as separated gels due to the high number of samples that were loaded in the same gel, however they run at the same time

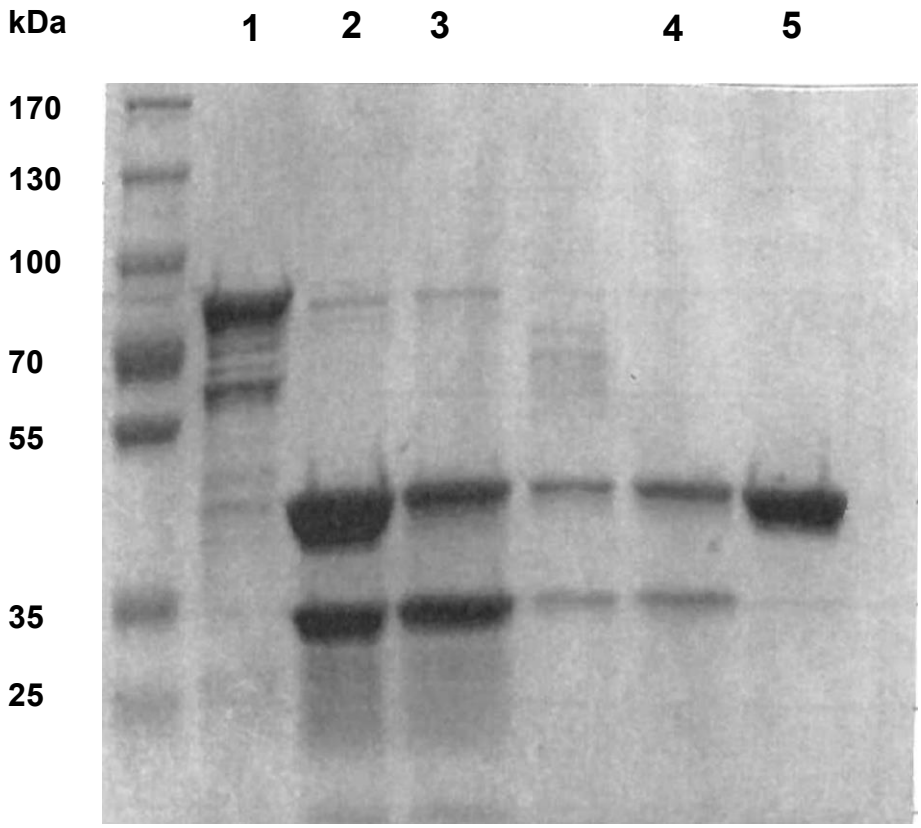

Figure 2.15 – Purification of recombinant full lenght GmmHO (GmmHOFL) from scale up bacterial expression – Acrylamide gel (12.5%) showing purification steps of recombinant GmmHO1. (1) Eluted fraction from Ni-NTA chromatography ; (2) After enzymatic treatment with 3C protease; (3) Flow through; (4) Washed fraction; (5) Eluted MBP fraction. The samples with mixed with reducing Laemmli sample buffer and incubated at 95^{o}C for 10 minutes before loading 20 µL of each denatured protein sample (10 µg) in each individual lane the gel along with 6 µL of molecular marker (PageRuler^{+} Prestained Protein ladder from ThermoFisher Scientific). The gel was subjected to a voltage of 60mV until the dye front had moved into the resolving gel, after which time the voltage was increased to 90mV. The gel was allowed to run until the dye front reached the bottom of the gel (~1h).

2.3.5 Crystalization trials of GmmHO

For GmmHO∆C263 expressed in insect cells, the His-tagged recombinant HO was purified over a Ni-NTA column (Figure 2.16, lane 1). Half the protein was treated with C3, however, loss of the affinity tag resulted in a high degree of protein precipitated (Figure 2.16, line 3). Thus, the remaining His-tagged GmmHO∆C263 was concentrated and submitted for crystallisation trials using several crystallization screen kits (Table 2.8). Regarding to GmmHO∆C250, which does not have a signalling sequence for cleavage of tag, did not need to go through enzymatic treatment and following purification in Ni-NTA column and size exclusion chromatography (data not shown), was used for crystallization following the same procedures applied for GmmHO∆C263.

However, despite extensive optimisation of buffer conditions for both constructs, no crystals were obtained and further work on protein crystallisation was halted.

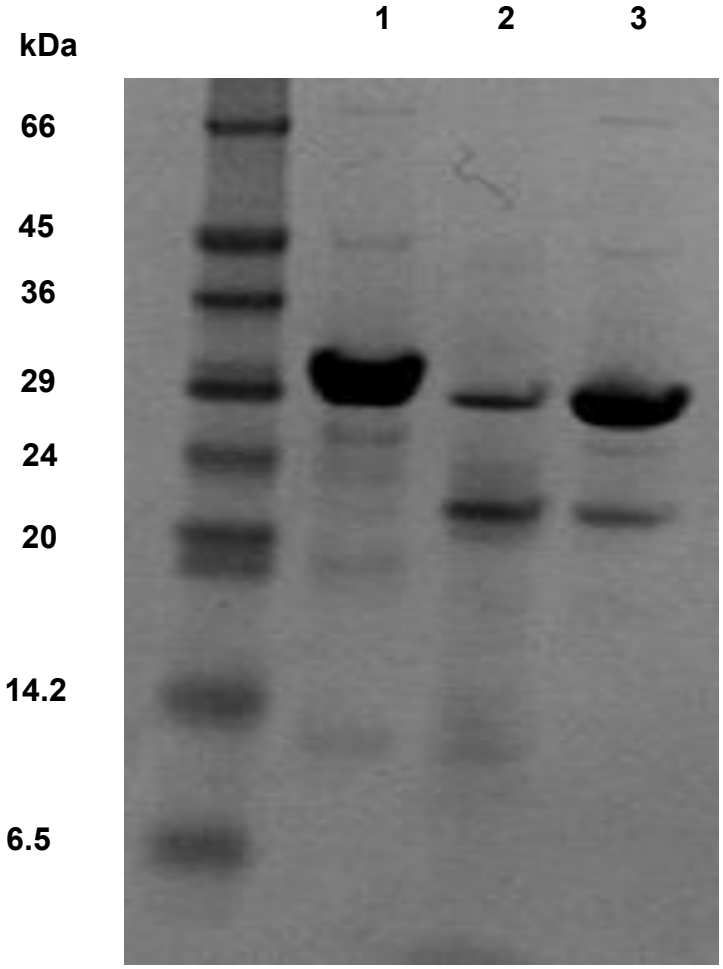

Figure 2.16 Purification of recombinant GmmHO∆C263 construct from scale up baculovirus expression system. Acrylamide gel (12.5%) showing purification steps of recombinant GmmHO1. (1) Eluted fraction from Ni-NTA chromatography; (2) Soluble recombinant GmmHO3 after enzymatic treatment; (3) Precipated GmmHO after enzymatic treatment. The samples with mixed with reducing Laemmli sample buffer and incubated at 95^{o}C for 10 minutes before loading 20 µL of each denatured protein sample (10 µg) in each individual lane the gel along with 6 µL of molecular marker (SigmaMarker™ low range, SIGMA-ALDRICH). The gel was subjected to a voltage of 60mV until the dye front had moved into the resolving gel, after which time the voltage was increased to 90mV. The gel was allowed to run until the dye front reached the bottom of the gel (~1h).

2.3.6 Antibody generation and validation

Using western blotting techniques, the polyclonal anti-GmmHO antibodies raised in chicken and rabbit were tested for specificity against purified GmmHO (>95%). (Figures 2.17 and 2.18). Chicken GmmHO antiserum detected 0.16 µg GmmHO, which was ~100 fold weaker than rabbit antiserum, which detected 1.6 ng. However, the chicken anti-GmmHO produced much less background protein binding against *E. coli* extracts compared with the rabbit anti sera (Figure 2.18).

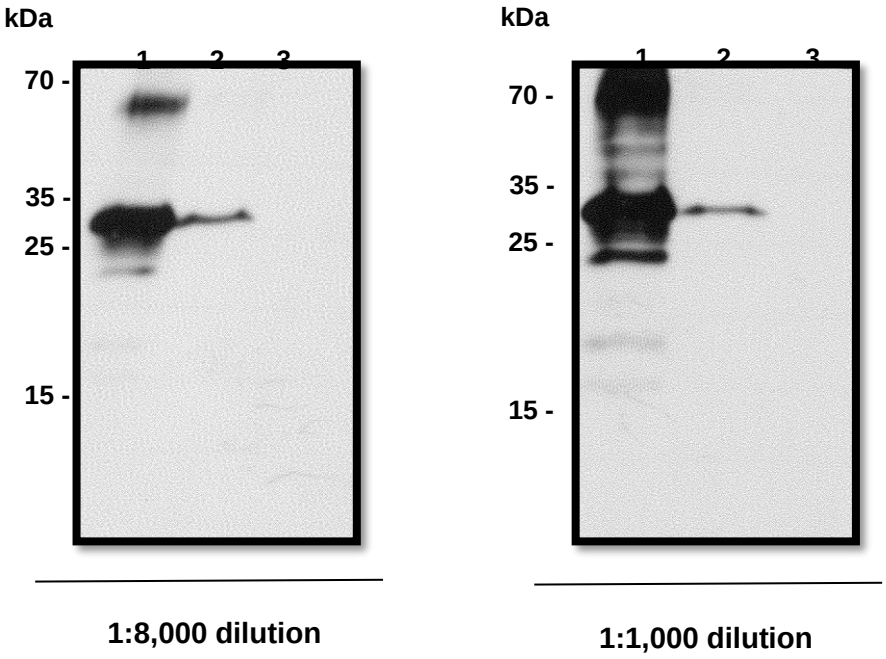

Figure 2.17 – Western blot analysis showing sensitivity of anti-GmmHO polyclonal antibodies raised in hen against recombinant ΔGmmHO5. In the acrylamide gel (12.5%) were applied serial dilutions of ΔGmmHO5: (1) 1.6 µg (2) 0.16 µg and (3) 0.016 µg, along with 6 µL of molecular marker (PageRuler+ Prestained Protein ladder from ThermoFisherScientific). The gel was subjected to a voltage of 60mV until the dye front had moved into the resolving gel, after which time the voltage was increased to 90mV. After that, the samples were transferred onto (PVDF) membrane at 90 V for 45 minutes. The membrane were then incubated for 2 hours in 5% skimmed milk powder at 4°C. The following day the membranes were probed at room temperature with different dilutions (1:8,000 and 1:1,000) of anti-GmmHO polyclonal antibodies raised in hen, washed with PBS and then incubated with a 1:10,000 dilution of rat anti-hen secondary antibody at room temperature for 1 hour. After several washes, the strips were incubated with SuperSignal West Dura (Pierce, UK) peroxidase buffer and luminol/enhancer solution at a 1:1 ratio, and developed by chemiluminescence for 1 minute

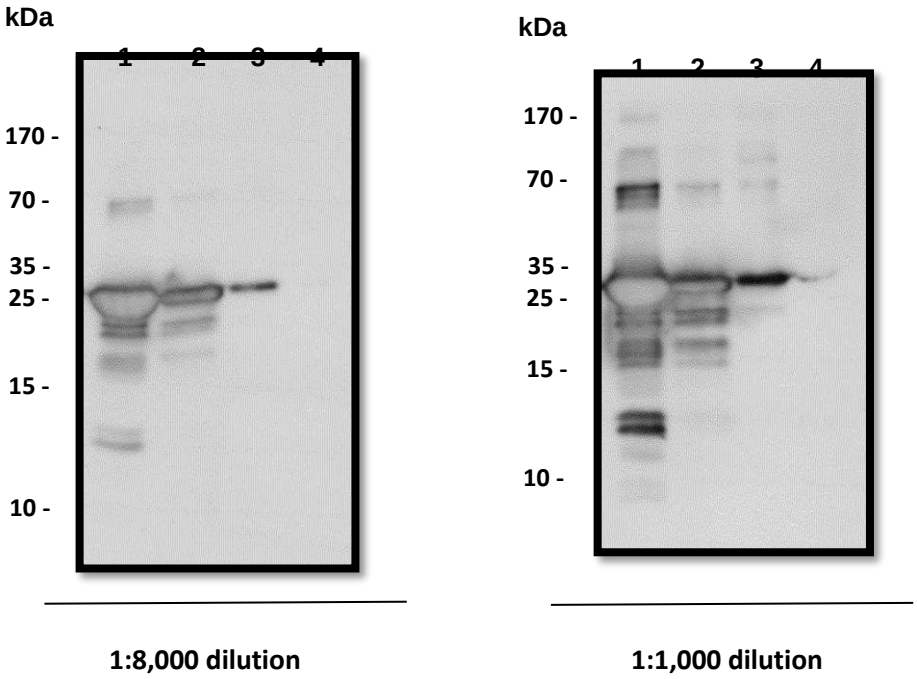

Figure 2.18 Western blot analysis showing sensitivity of anti-GmmHO polyclonal antibodies raised in rabbit against recombinant ΔGmmHO5. In the acrylamide gel (12.5%) was applied dilutions of ΔGmmHO5: (1) 1.6 µg (2) 0.16 µg, (3) 0.016 µg and (4) 0.0016 µg. In the acrylamide gel (12.5%) were applied serial dilutions of ΔGmmHO5: (1) 1.6 µg (2) 0.16 µg and (3) 0.016 µg, along with 6 µL of molecular marker (PageRuler^{+} Prestained Protein ladder from ThermoFisher Scientific). The gel was subjected to a voltage of 60mV until the dye front had moved into the resolving gel, after which time the voltage was increased to 90mV. After that, the samples were transferred onto (PVDF) membrane at 90 V for 45 minutes. The membrane were then incubated for 2 hours in 5% skimmed milk powder at 4°C. The following day the membranes were probed at room temperature with different dilutions (1:8,000 and 1:1,000) of anti-GmmHO polyclonal antibodies raised in rabbit, washed with PBS and then incubated with a 1:10,000 dilution of goat anti-rabbit secondary antibody at room temperature for 1 hour. After several washes, the strips were incubated with SuperSignal West Dura (Pierce, UK) peroxidase buffer and luminol/enhancer solution at a 1:1 ratio, and developed by chemiluminescence for 1 minute

2.4 DISCUSSION

This chapter describes the cloning, heterologous expression and purification of three constructs of recombinant heme oxygenase homologue from *G. m. morsitans* (GmmHO), as well as the production of GmmHO antibodies for immunolocalization in Chapter 4.

Although GmmHO was present in the *G. morsitans* genome database (VectorBase, GMOY004329), the enzyme has not been cloned or characterised. Thus, the coding sequence for GmmHO was amplified by PCR female tsetse fly cDNA and cloned into a series of expression vectors for enzyme production and characterisation. Sequencing results revealed an exact match with the database sequence however a proline to serine substitution at amino acid position 171 was also found in some clones. To date, we have not tested this mutant clone and therefore we have no evidence if it would cause any effect in protein folding and activity.

The genome sequence of GmmHO indicates the presence of a 60 bp intron. The presence of an intron (~60bp) in the genomic sequence was confirmed (Figure 2.7) by comparing PCR products from cDNA and gDNA templates. High similarity between HOs from organisms belonging to the same genus (Table 2.1) was implied from amplification of HOs from *G. fuscipes fuscipes and G. palpalis gambiense* using the GmmHO primers (Figure 2.7).

In general, both sequence and structure of HOs are very conserved, mostly comprised of α-helices motifs. Studies on human and bacterial HO (Hirotsu *et al.*, 2004; Schuller *et al.*, 1999) have displayed that heme is sandwiched between a proximal and a distal helix. In GmmHO, some of the classical HO residues in the proximal helix are conserved such as Thr-21, His-29 and Phe-233. However, in distal helix the highly conserved sequence ^{139}Gly-Asp-Leu-Ser-Gly-Gly^{144} (in human HO1) were replaced by ^{133}Ala-Leu-Met-Ser-Gly-Gly^{138}(in GmmHO). Those three glycine residues have been shown to provide enough flexibility to the distal helix in human HO1 (Schuller *et al.,*1999), allowing backbone atoms from Gly-139 and Gly-144 to directly contact heme. In particular, a substitution of glycine by alanine in this region is highly unusual and could potentially impact the flexibility and binding of the distal

helix to heme. Furthermore, a region comprising of coiled coil motif (Glu-155 to Pro-178) is present in *Glossina* species as well as in *D. melanogaster* and *Musca domestica* and absent in mammals. Only the biochemical characterization and structural studies of recombinant GmmHO will provide insights on the impact of such differences in primary structure.

As well as other HOs, the GmmHO possesses a carboxyterminal transmembrane domain. Truncation of the transmembrane domain is a widely-used strategy for cloning and heterologous expression of HOs, improving its solubility without compromising its folding and activity (Wilks *et al.*, 1995; Zhang *et al.*, 2004; Vukomanovic *et al.*, 2010). Thus, several truncated versions of GmmHO were constructed to optimise the expression of functional recombinant enzyme. Despite the successful cloning and expression of several constructs only three constructs were chosen for scaled-up expression: the full length (GmmHOFL), and constructs lacking 10 residues (GmmHOΔC263) and 23 residues (GmmHOΔC250). Whilst it is assumed that the cytosolic region of HOs is the catalytic domain involved in heme binding and oxidation, truncated forms of human HO were less active than the full-length enzyme (Huber III & Backes, 2007), indicating that the C-terminal transmembrane tail might be needed for maximal HO catalytic activity. Whether the same pattern applies to *G. m. morsitans* HO, will be addressed by biochemical comparison of its full length and truncated forms in chapter 3.

GmmHOΔC250 (missing the whole TM domain) was produced in *E. coli* (BL21) using pCold-II, an expression vector with a *cspA* promoter responsible for driving the overexpression of target genes upon induction of low temperature (<15°C). Despite the effective expression of several genes (>30) using plasmids from pCold series described by Qing *et al.* (2004), issues with recombinant protein solubility expressed under this technology have been argued (Rosano & Ciccarelli, 2014). In the specific case of GmmHOΔC250, high levels of precipitation were observed (data not shown) even though the purification steps were performed at low temperature. However, this was also observed for GmmHOΔC263 construct, which was expressed in pOPIN-M (Figure 2.16), which suggests that this characteristic would be innate to the enzyme nature.

The constructs GmmHOFL and GmmHO∆C263 (Figures 2.12 to 2.16) on the other hand were cloned in pOPIN plasmids based in the Infusion cloning system, designed for high throughput expression and purification of recombinant proteins using bacterial, insect or mammalian cells, and an array of excisable fusion tags (Berrow *et al.*, 2007). GmmHO∆C263 and GmmHO∆C250 was both submitted for crystallisation experiments under several conditions however by date those efforts were unsuccessful as no crystals were formed.

In terms of protein purity, Figure 2.8 and 2.9 shows that Ni-NTA purified GmmHO∆C250 had trace high molecular mass contaminants, likely to be derived from *E. coli*. However, these were removed by size exclusion chromatography and the resulting purified GmmHO∆C250 used for antibody production (Figures 2.10 and 2.11). Some low molecular weight protein bands were still visible, which confirmed as GmmHO∆C250 degradation products by mass spectrometry (data not shown).

GmmHO antibodies were raised in chickens and rabbits. Western blotting analysis showed that the anti-GmmHO antibodies raised in rabbit were ~100 times more sensitive than chicken antisera in recognizing recombinant GmmHO (Figure 2.17 and 2.18), thus used for immuno-histological mapping of the tissue distribution of GmmHO in tsetse flies as described in Chapter 4.

CHAPTER 3 - BIOCHEMICAL CHARACTERIZATION OF *GLOSSINA MORSITANS MORSITANS* HEME OXYGENASE (GMMHO)

3.1 INTRODUCTION

Following a blood meal, blood digestion takes place in the insect digestive tract. Haemoglobin is a major component of blood and its degradation leads to the release of high concentrations of globin and heme. Heme is an essential and ubiquitous molecule (Beale and Yeh, 1999) as a prosthetic group for hemoproteins involved in several biological processes such as oxygen transport by haemoglobin and electron transport by cytochromes (Kumar & Bandyopadhyay, 2005). However, in free form at concentrations above 1 μM it is highly toxic due to its ability to catalyse the generation of reactive oxygen species (ROS) through the Fenton reaction (ref). Free heme can thus cause damage to DNA (Ishkawa *et al.,* 2010), interfere with lipid organization (Miller *et al.*, 1997) and lead to cell lysis (Schmitt et al, 1993). Relatively little is known about how those organisms defend themselves from such a threat. However, heme degradation driven by the enzyme heme oxygenase (HO) is a possible protective mechanism since it catalyses the release of iron from the porphyrin ring and produces an equimolar ratio of carbon monoxide and biliverdin IXα (Sassa, 2004).

In mammals biliverdin IXα is further converted by the enzyme biliverdin reductase (BVR) in the major bile pigment bilirubin (Kutty & Maines, 1981). This enzyme is absent in insects. Instead, distinct modifications steps not seen in mammals have been observed in those organisms, suggesting key differences in the mechanism of insect HOs. Whilst the product of heme degradation in R. prolixus is dicysteinyl-biliverdin IXα, in Ae aegypti is biglutaminyl-biliverdin IXα (Pereira *et al.,* 2007; Paiva-Silva *et al.,* 2006). Due to its characteristic green colour, those biliverdins can be seen by naked eye in the digestive tract of hematophagous insects just a few hours after a single blood meal, serving as an indication of in vivo HO activity

HOs are considered a particularly distinct group of hemoproteins due to the fact they use heme porphyrin both as a prosthetic active centre and substrate (Beale and Yeh, 1999). In other hemoproteins such as cytochrome P450s heme is normally permanently bound as the catalytic centre of the active site. To degrade heme, require

molecular oxygen and electrons provided by a source of reducing equivalents, generally derived from NADPH or NADH. Electron transfer from NADPH via NADPH cytochrome P450 oxido-reductase (CPR) occurs in mammals (Yoshida and Kikushi, 1977), while electron transfer from NADH via ferredoxin (Fd) occurs in in plants, bacteria and protozoa (Cornejo, 1998; Wilks and Schmitt, 1998; Okada, 2009).

The reaction catalysed by HOs consists of several steps in which the intermediates forms have been well characterized in mammals (Yoshida *et al.,* 1980; Omata & Noguchi, 1998; Liu at al., 1997; Hirotsu *et al.*, 2004). In insects, recombinant *Drosophila melanogaster* HO (DmHO) produces three different biliverdin isomers (α, β, δ). This distinguishes it from other known HOs, which only produce biliverdin-α. It further differs to mammalian HOs in having a slower degradation rate, and the iron of heme not being involved in binding heme to the enzyme (Zhang *et al.*, 2004). More recently, AgHO from the blood feeding *Anopheles gambiae* has been characterised. (Spencer, 2016). In contrast to DmHO, several characteristics are shared with human HO-1 such as similar mode of binding and absorption spectra. Thus, although only a small number of insect HOs have been characterised, distinctive traits are observed that distinguish them from mammalian HOs and to each other, which might relate to blood feeding.

This chapter describes the biochemical characterisation of recombinant GmmHO and verifies its ability to degrade heme to produce the three reaction products associated with HO mediated heme degradation: biliverdin, carbon monoxide and ferrous iron.

3.2 MATERIAL AND METHODS

3.2.1 Dissection of Tsetse fly and preparation of samples

G. m. morsitans (Westwood) male flies (~120) were obtained from an established colony at the Liverpool School of Tropical Medicine around 0-6 hours following emergence, separated in individual groups cages (~15 flies each) and maintained at optimum conditions (RH 65-75%; 27°C ± 2°C) until dissection. At 24-30 hours after emergence they were fed on sterile, defibrinated horse blood (TCS Biosciences) and at different time points (24, 36, 48, 60, 72, 84 and 96 hours) after a single blood meal each individual group cage was dissected. For that, the flies were kept on ice for 10-15 minutes before their entire digestive tract was dissected in PBS pH 7.4 using dissecting tweezers and then transferred to brown 1.5 mL tubes (15 digestive tracts/groups) to protect them from light. All dissections were performed under binocular stereo light scope.

Immediately after dissections, the digestive tracts were resuspended in 200µL of PBS pH 7.4, homogenized using clean polypropylene pestle and microtube pellet mixer and centrifuged for 15 min at 15,000 g at room temperature. The pellets were discarded and the supernatant dried using Speed Vac evaporator at RT, after which they were stored in -80 freezer until use.

3.2.2 Quantification of biliverdin and heme in tsetse fly midgut contents by HPLC-reverse phase chromatography

To estimate the levels of biliverdin and heme from insect tissues, adaptations were made to the protocol described by Ryter & Tyrell (2000). The samples and serial dilutions of commercial stocks of biliverdin hydrochloride (FrontierScientific; a mixture of majority BVIXα and other BVIX isomers) and heme (Sigma-aldrich) ranging from 0.625 – 20 µM were prepared by resuspension in DMSO 100% and analysed by high pressure liquid chromatography (Agilent 1100 series HPLC) using a reverse phase chromatography column (Shimadzu CLC-ODS C18 column, 15 x 220 mm). The HPLC was set to perform a linear gradient that starts from 100% HPLC buffer A (100 mM ammonium acetate pH 5.1, 60% methanol) at the time zero and reaches 100% buffer B (100% methanol) at 14 min, and which then reverts to 100% buffer A and remains constant until the termination at 19 min. The flow rate was 1.5 ml/min and the sample

collection to 100 µL. The procedure was monitored by absorbance detector set at 405 and 650 nm. The standards were used to build a standard curve that then used to calculate the concentrations of heme and biliverdin in the insect digestive tract samples.

3.2.3 Creation of GmmHO-heme complexes

The first step for characterization of HO is to spectroscopically analyse the HO-heme complex. Classically, HOs bind to heme in a 1:1 stoichiometric ratio. To create the GmmHO-heme complex, recombinant enzyme (10 µM) was mixed with a 2-fold excess of heme (20µM). The solution was then applied to a PD Minitrap G-25 column for buffer exchange and removal of excess heme. The protein-heme complex was then concentrated to the desired concentration depending on the assay. The complexes were scanned spectroscopically from 750nm – 350nm in 90µL in a quartz cuvette.

3.2.4 Spectral analysis of GmmHO complex variants

In vivo, the iron requires electrons from NADPH (*via* CPR) in order to be reduced, however *in vitro* heme iron can be reduced artificially by creating a reducing environment and introducing carbon monoxide forming a complex of ferrous heme and carbon monoxide. The ferrous CO complex was created by adding sodium dithionite powder to an aliquot of the ferric complex (creating a reducing environment the solution was then saturated with CO by bubbling the gas through the solution).

The ferrous dioxyheme complex was created by passing the ferrous-CO complex over a sephadex G25 column removing excess reductant and carbon monoxide. All complexes were scanned spectroscopically from 750nm – 350nm in 90µL in a quartz cuvette, at a concentration of 10µM, in a buffer of 150mM NaCL, 50mM Tris, pH 7.4, 0.1% Triton x100.

3.2.5 Cytochrome p450 reductase

Recombinant MdCPR was provided by Evangelia Morou (University of Crete).

3.2.6 Identification of biliverdin as a degradation product by using CPR or ascorbic acid

Analysis of heme degradation activity by GmmHO were carried in a final volume of 90µL containing phosphate buffered saline, 10µM GmmHO/heme complex, 10µM MdCPR and 250µM NADPH. NADPH, CPR and HO were omitted from each control system. The reaction was initiated with addition of NADPH, and immediately subjected to scanning UV-Vis absorption spectroscopy in the range 350-800nm, and followed for 2 hours. A similar procedure was carried out in the presence of the 15µM ascorbic acid, an artificial electron dotation system.

When needed, the iron chelator 1 mM desferrioxamine was used in the system in order to accelerate the release of biliverdin from HO-biliverdin complex. In all cases, blanks were used and absorbance was measured every ten minutes for two hours.

3.2.7 Identification of iron as heme degradation product

The reaction mixture (100µL solution, 10µM HO-heme complex, 3µM MdCPR, 250µM Ferrozine, 300µM NADPH in a buffer of 150mM NaCL, 50mM Tris, pH 7.4, 0.1% Triton x100) was placed in a 90µL quartz cuvette. The reference cuvette contained only buffer and CPR. The reaction was initiated with addition of NADPH, and absorbance from 750nm to 350nm was immediately measured. Absorbance was measured every ten minutes for two hours. This reaction relies on 3-(2-Pyridyl)-5,6-diphenyl-1,2,4-triazine-*p*,*p'*-disulfonic acid, better known as Ferrozine. Ferrozine binds iron, producing a distinct change in absorption at 562nm.

3.3 RESULTS

3.3.1 Evidence of GmmHO activity *in vivo*

During dissections of the *G. m. morsitans* digestive tract a change of colour from red to green was observed associated with an accumulation of green pigment in the final portion of the midgut (Figure 3.1). This was strongly suggestive of biliverdin formation as a result of HO mediated heme degradation. A visual comparison of the midgut contents of a female tsetse fly up to 3 days after a single blood meal is shown in Figure 3.2A. The change in colour over this period of time can be easily seen.

HPLC analysis of female tsetse fly midgut contents between 24 to 144 hours following a single blood meal was carried out to assess changes in heme content and biliverdin production in the insect digestive tract. Midgut extracts separated by HPLC chromatography were compared against heme and biliverdin IXα standards. *G.m, morsitans* extracts contained a peak with the same retention time as commercial biliverdin IXα (RT 32.77 min). This suggests that the product of heme degradation catalysed by GmmHO, *G. m. morsitans biliverdin* (*Gmm*BV), is biliverdin IXα, although this would need to be confirmed by mass spectrometry.

As shown in Figure 3.2B there was a decrease in heme concentration over time with a concomitant increase in GmmBV peak concentration. The total heme content was ~1mM 24 hours after the blood, increasing three fold (3 mM) after 48 hr, before returning to 1 mM at 72 hr. Heme was cleared by 96 hr. By contrast, GmmBV increased steadily from 0.2 uM (24 hrs) to 0.5 uM after 96 hr. This result is strongly suggestive of HO activity. However, it was also notable that concentrations of heme were several orders of magnitude higher than GmmBV relative to the initial heme concentration (3.02 mM at 24h ABM), the peak biliverdin concentration only reached 0.67 µM on Day 4. This suggests that GmmHO activity only plays a minor role in total heme clearance from the midgut.

Figure 3.1 – Digestive tract of *G. m. morsitans* five days after a single blood meal. The insect digestive tract was dissected in PBS pH 7.4 around 120 hours after a single blood meal. The accumulation of green pigment indicative of biliderdin formation is evident in the hindgut.

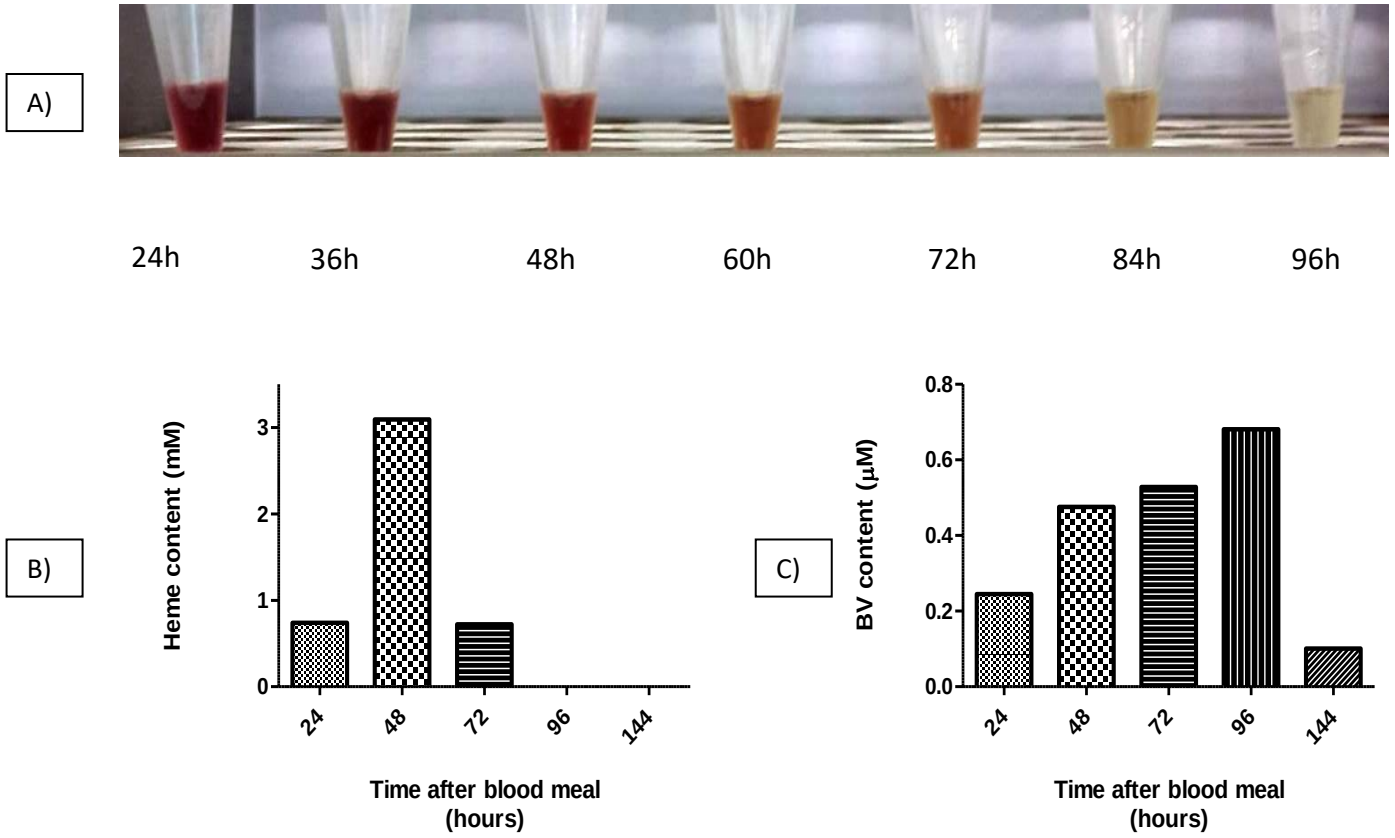

Figure 3.2 Time course of heme degradation in *G.m.morsitans* midgut content after a single blood meal. (A) Gut content extracts showing red to green pigmentation (B) HPLC analysis of heme content in Tsetse fly digestive tract (C) HPLC analysis of biliverdin IXα (BV) content in Tsetse fly digestive tract. Their entire digestive tract was dissected in PBS pH 7.4 using dissecting tweezers and then transferred to 1.5 mL tubes (15 digestive tracts/groups). The samples were dried out, resuspended in DMSO 100% and analysed by reverse phase chromatography coupled to HPLC. The analysis was performed with a flow rate of 1.5 ml/min and linear gradient that started from 100% HPLC buffer A (100 mM ammonium acetate pH 5.1, 60% methanol) at the time zero and reached 100% buffer B (100% methanol) at 14 min. The procedure was monitored by detector set at the absorbance of 405 and 650 nm and the concentration calculation was based in a standard curve built with commercial biliverdin IX isomers mixture and heme.

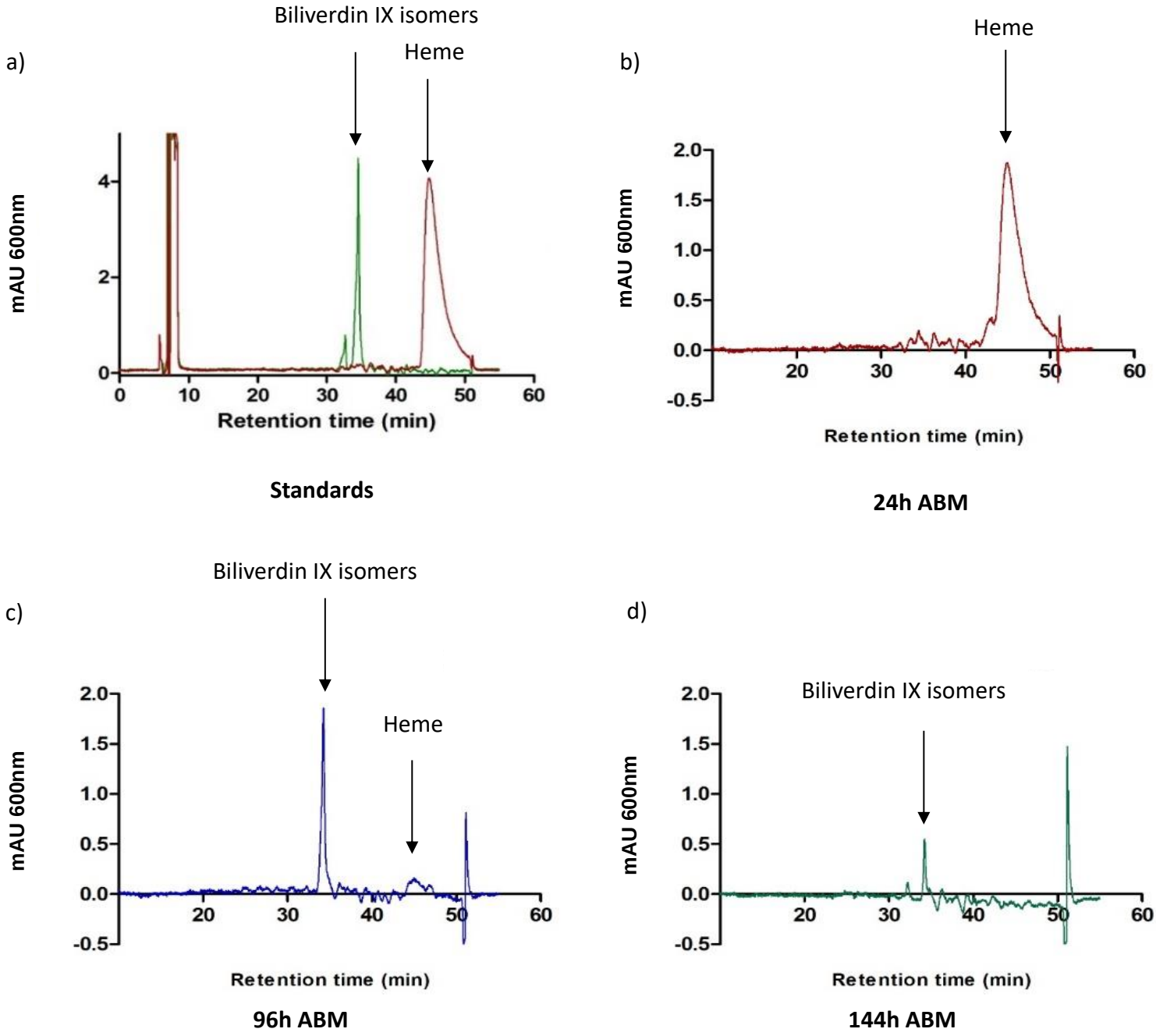

Figure 3.3 Time course of heme degradation in *G.m.morsitans* midgut content after a single blood meal. (A), gut extracts showing red to green pigmentation; (B), HPLC analysis of heme content; (C), HPLC analysis of biliverdin IXα (BV) content.

3.3.2 Biochemical characterization of recombinant GmmHO

A classical step in the characterization of heme oxygenases is the comparison spectral comparison of HO-heme complexes formed when submitted to different biochemical situations (described in session 3.2.2). This analysis provides insights into nature of the proximal ligand to heme.

To degrade heme, HO is required to bind free heme to form a HO-heme complex with iron in the ferric state (Fe^{3+}). To determine if a heme complex is formed, recombinant GmmHO was mixed with a two-fold concentration of hemin, excess heme was then removed by filtration and spectral changes recorded. As shown in Figure 3.4. a Soret peak maxima at 394 nm was observed following binding of free heme. This was similar to the reported 390nm peak absorbance maxima for *D. melanogaster* HO (DmHO) (Zhu *et al.* 2004) and 398 nm for *An. gambiae* (AgHO) (Spenser, 2016). It was slightly lower than maximal absorption peak found in rat HO (404 - 406 nm) (Yi & Ragsdale, 2007; Wang *et al.*, 2005).

The CO-bound and oxygenated forms (or oxy-form) of the GmmHO∆250-heme complex were also examined (Figure 3.3). Reduction of the ferric heme-GmmHO complex with dithionite under an atmosphere of CO gave a spectrum typical of a reduced ferrous-CO, which maximum peak of 419 nm, α peaks of 567 and β peaks of 533, comparable with DmHO (Zhu et al., 2004) and AgHO (Spencer, 2016)

The CO bound heme- GmmHO∆250 complex was passed through a Sephadex G-25 column to remove the excess reductant, producing the oxy-form. This form generated a spectrum with Soret peak of 408 nm and discreet α/β peaks at 575 and 542 nm respectively. These values are similar to those observed for rat-HO with a Soret peak of 410 and α/β peaks of 575 and 539 respectively (Takahashi *et al.*, 1994; Yoshida & Kikushi, 1979). CO bound heme-AgHO produced slightly lower values at 400nm and diminished α/β peaks (Spencer, 2016).

For heme catalysis, HOs requires oxygen and and electrons provided by NADPH via cytochrome P-450 reductase (CPR). Attempts to clone CPR from *G.m. morsitans* were unsuccessful. However, CPRs are highly conserved enzymes thus full-length housefly (*Musca domestica*) CPR (MdCPR) was used as a proxy for

electron transfer to GmmHO. In these experiments, GmmHO∆250 was mixed with MdCPR and the formation of biliverdin was tracked by measuring peak shifts between 600 to 700 nm following the addition of NADPH. Under these conditions no peak shifts were observed indicating lack of biliverdin formation (Figure 3.5a). Similarly, no peak formation was observed at 562 nm following the addition of ferrozine, which binds and reports the presence of free iron released from heme (Figure 3.5b).

Since the recombinant GmmHO∆250 lacked the carboxy-terminal membrane anchor region, thus not tethered to the membrane surface with CPR, this is likely to have reduced the GmmHO-CPR coupling efficiency. Iron chelation has also been found to enhance HO activity (Okada *et al.*, 2009) Thus, catalytical activity of GmmHO∆250 further examined in the presence of deferoxamine, an iron chelator that is known to support the completion of the heme degradation reaction by some HOs (Okada *et al.*, 2009). Following the addition of deferoxamine, spectral shifts at 650 nm were observed indicative of the formation of biliverdin (Figure 3.6a). There were no spectral shifts in absence of the GmmHO∆250-heme complex (Figure 3.6b), indicating that the biliverdin release was enzyme linked and not due to direct desferrioximine oxidation. The dependence of on an iron chelator for BR IXα formation has been observed previously for *P. falciparum* HO (PfHO) and *Arabidopsis thalania* AtHO (Muramoto *at al.*, 2002) The role of the iron chelator is believed be associated with the release of iron from the ferric-BV complex (Zhang *et al.*, 2004). In *P. falciparum*, PfHO is located in the plastid, and this may be related to the strong dependence of PfHO on iron chelators. However, GmmHO is expected to be located in the endoplasmic reticulum, thus the significance of iron chelation on the regulation of GmmHO activity is unclear.

HOs can also degrade heme in the presence of an artificial electron donor (Wang *et al.*, 2005). Thus, the heme catalysis reaction was tested using ascorbic acid as electron donor for the GmmHO-heme complex. Spectral shifts of 650 nm indicative of heme release were observed with ascorbic acid in both the presence and absence of GmmHO∆250 (Figure 3.7). However, there was a much quicker rate of heme release in the presence of GmmHO.

Finally, full-length GmmHO (GmmHOFL) was also tested for activity in the presence of deferoxamine (Figure 3.8). Interestingly, in the same conditions as

GmmHO∆250, the enzyme GmmHOFL presented a much lower activity than its truncated form. This is unexpected given that in human HO (Huber III & Backes, 2007) the presence of the transmembrane tail was shown to improve its catalytic activity

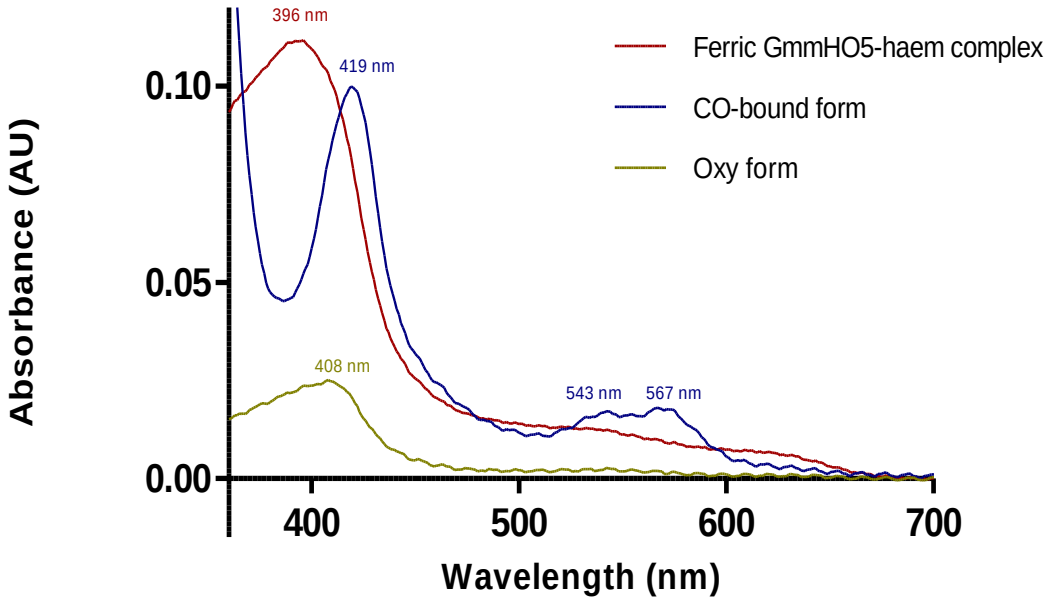

Figure 3.4 – Absorption spectra of different GmmHO∆250-heme complexes. The GmmHO-heme complexes were prepared and submitted to different biochemical situations and scanned spectroscopically from 750nm – 350nm in a quartz cuvette.

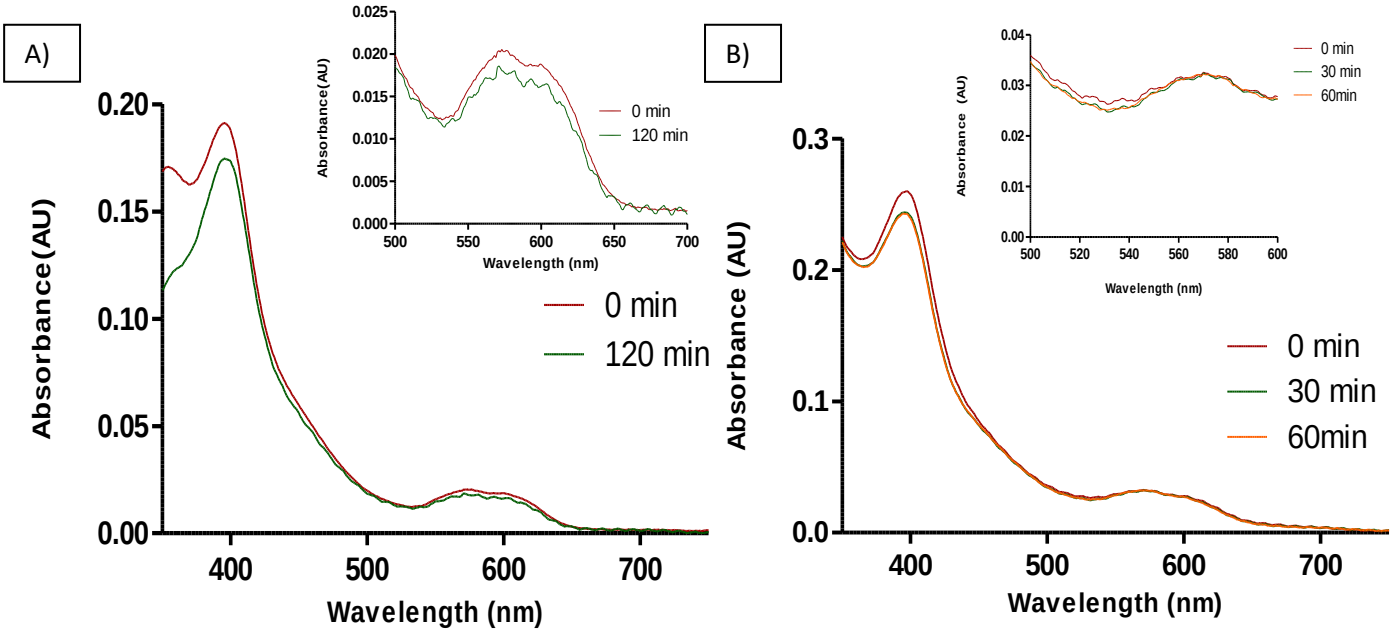

Figure 3.5 – Detection of catalytic activity from GmmHOΔ250 following release of biliverdin (A) and iron (B). The GmmHOΔ250 was mixed with a 2-fold excess of heme and then applied to a PD Minitrap G-25 column for buffer exchange and removal of excess heme. In both experiments, the same concentrations of MdCPR and NAPDH were used as electron supplier system to GmmHOΔ250. The reactions were scanned spectroscopically from 750nm – 350nm in 90µL in a quartz cuvette. In (A) the biliverdin release was monitored by following alterations in absorbance between 650-700 nm. In (B) the release of iron was monitored by following alterations in absorbance at 562 nm.

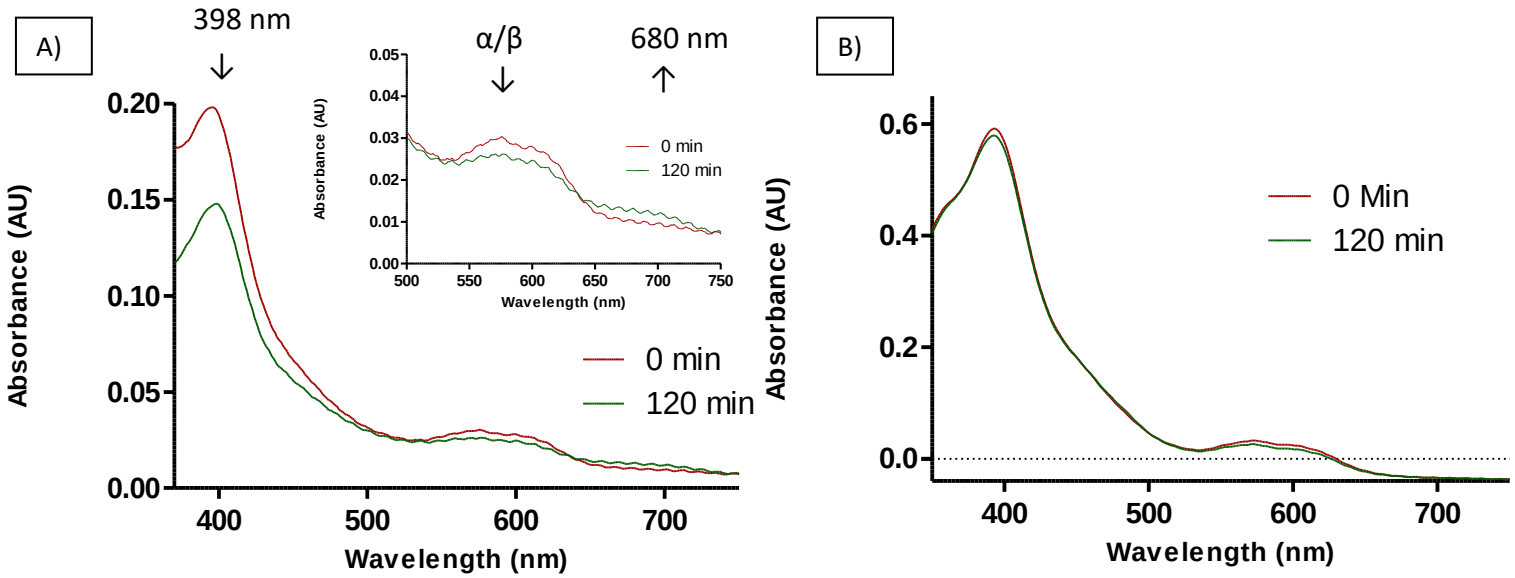

Figure 3.6 – Detection of catalytic activity from GmmHOΔ250 in the presence of desferrioxamine. Biliverdin formation is followed in the presence of (A) desferrioxamine, MdCPR-NAPDH and GmmHO-heme complex and (B) desferrioxamine and MdCPR-NAPDH (negative control). In both cases MdCPR-NAPDH was used as electron supplier The GmmHOΔ250 was mixed with a 2-fold excess of heme, then applied to a PD Minitrap G-25 column for buffer exchange and removal of excess heme. In both experiments, the same concentrations of MdCPR and NAPDH were used as electron supplier system. The reactions were scanned spectroscopically from 750nm – 350nm in 90µL in a quartz cuvette and the biliverdin release was monitored by following alterations in absorbance between 650-700 nm.

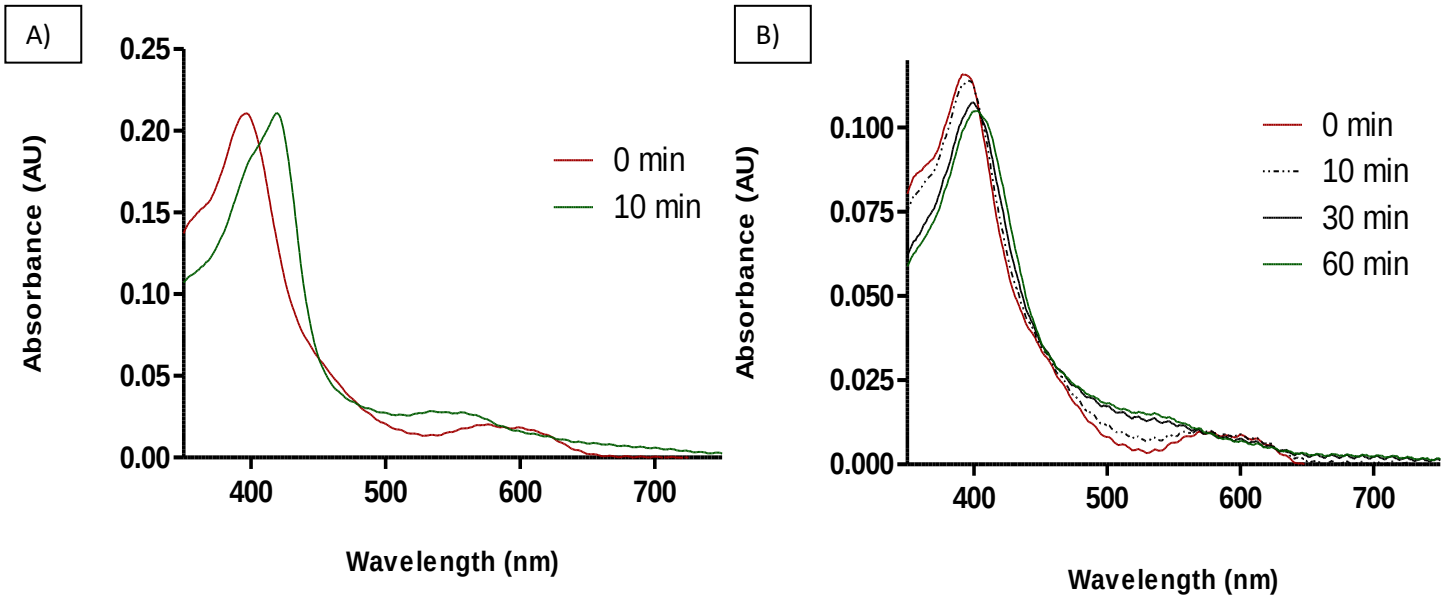

Figure 3.7 – Assay of heme degradation by detection of biliverdin using ascorbic acid as electron donor. The reactions were performed in the presence (A) and in the absence (B) of the GmmHO-heme complex. In both cases ascorbic acid system at the same concentration was used as electron supplier. The GmmHOΔ250 was mixed with a 2-fold excess of heme, then applied to a PD Minitrap G-25 column for buffer exchange and removal of excess heme. The reactions were scanned spectroscopically from 750nm – 350nm in 90µL in a quartz cuvette and biliverdin release was monitored by following alterations in absorbance between 650-700 nm.

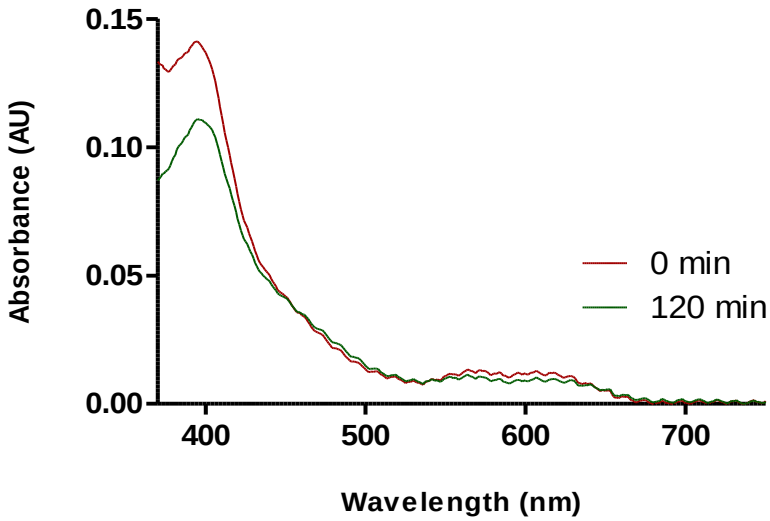

Figure 3.8 – Assay of heme degradation by full length GmmHO in the presence of desferrioxamine. GmmHOFL was mixed with a 2-fold excess of heme, then applied to a PD Minitrap G-25 column for buffer exchange and removal of excess heme and then MdCPR-NAPDH was used as electron supplier. The reaction was scanned spectroscopically from 750nm – 350nm in 90µL in a quartz cuvette and the biliverdin release was monitored by following alterations in absorbance between 650-700 nm.

3.4 Discussion

Despite the damage that free heme can cause to a hematophagous insect very little is known about protective mechanisms against heme toxicity in blood feeding insects, particularly about HO. Since biglutaminyl-biliverdin IXα and dicysteinyl-biliverdin IXγ have been isolated respectively from *Ae. aegypti* (Pereira *et al.*, 2007) and *R. prolixus* (Paiva-Silva *et al.*, 2006) as the final products of heme degradation, it has been proposed that HOs provide a protective mechanism against heme toxicity in blood feeding insects, and that they might hold distinct biochemical features from those observed in humans. This Chapter provides evidence that GmmHO also has heme oxygenase activity with key biochemical differences with mammalian HO.

In *G. m. morsitans*, a strong green colour was clearly visible by the naked eye in the posterior region of the insect digestive tract (Figure 3.1) and in Malpighian tubules (data not shown) 72-96 hours following a blood meal. The green colour is characteristic of biliverdin production. Furthermore, HPLC analysis of blood during this period showed a corresponding increase in heme concentration followed by formation of a product (Figure 3.3) with identical retention time as biliverdin IXα. Taken together this data is strongly suggestive of HO activity. Similar production of green pigment has been observed in *Ae. aegypti* (Pereira *et al.*, 2007), although considerably earlier (~24-48 hours) than observed in the Tsetse fly. This could be related to physiological differences in HO production such as more rapid induction of HO gene expression or higher enzyme levels, or it may be biochemically associated with different rates of heme oxidation and biliverdin production.

While HO has been confirmed as an active mechanism in *G. m. morsitans*, there was a considerable difference in the maximal concentration of heme present (3.1 mM) in the intestinal lumen and the amount of biliverdin produced (0.67 µM) (Figure 3.2). Unless biliverdin is extremely rapidly excreted, which seems unlikely, this large discrepancy indicates that GmmHO is probably not the major mechanism responsible for heme degradation. Thus other heme protective mechanisms are active in the insect. One of the possibilities would be the elimination of heme in its intact or aggregated form. Heme polymerization has been observed in the obligatory blood feeder insect *Rhodnius Prolixus* (Oliveira *et al.*, 1999) and proposed as a putative first defense barrier against the toxicity of blood-meal derived heme. This is supported by

the observation that haematin is one of the five main components (6%) of *G. m. morsitans* faeces 24 hours following a single blood meal (Bursell, 1965), however it is not clear in which form heme is excreted by the fly.

Several forms of HO-heme complex can be produced *in vitro,* which present distinct absorption spectres that serve as a signature for tracking modes of heme binding and ligand discrimination. The ferric HO-heme (Figure 3.4) complex of truncated GmmHO presented an absorbance spectrum with a Soret peak of 396 nm and α/β peaks of respectively of 599 and 576 nm. Those values are considerably shifted in comparison to ferric HO-heme complex of rat HO1 homologue (RnHO1) which presents typical spectres such as Soret maximum absorption around 404 nm and α/β peaks around 631 and 500 nm.

The Ferric heme-HO complex of *D. melanogaster* (DmHO) presented some spectroscopic discrepancies in comparison to mammalian HO (Zhu *et al.*, 2003). Electron paramagnetic resonance (EPR) studies have shown that DmHO binds differently to human HO-1 with iron heme in a penta-coordinated state high spin state rather than the classical six-coordinated (Schuller *et al.*, 1999). This means that histidine was not acting as the proximal ligand to heme iron in DmHO (Zhu *et al.*, 2003). Spectroscopical analysis (Figure 3.4) suggests that GmmHO binds heme iron differently to DmHO and humans HO. Whilst in human HO the heme iron is in a six-coordinated way, in DmHO it is a penta- coordinated, affecting in the isomers produced by the HO. Further analysis such as EPR are necessary to confirm such features

In general, when studying the catalytic activity of HOs, the detection methods normally employed follow spectroscopic changes indicative of biliverdin, bilirubin, CO or iron formation given the appropriate system (Wilks & Schmitt, 1998; Soldano *et al.*, 2014; Spencer, 2016). Assays that monitor the production of bilirubin are the preferred method for measuring HO activity due to the fact the bilirubin production can be easily measured and the kinetics of substrate formation accurately quantified. However, this is only feasible with mammalian HOs since there is a known enzyme, biliverdin reductase, that converts biliverdin to bilirubin. Thus, the preferred methods to measure insect HO activity is by following formation of biliverdin, CO or iron (Spencer, 2016).

The catalytic activity of HO is dependent on electron transfer from NADPH to HO via CPR. Electrons can also be artificially supplied using ascorbic acid as a

reductant (Zhang *et al.,* 2004). Efforts to clone and express CPR from *G.m. morsitans* were unsuccessful. However, CPRs are highly conserved across species. Therefore, housefly CPR (MdCPR), which shares 86% amino acid sequence identity with GmCPR was used instead.

When using NADPH/MdCPR as reducing system, the absence of correspondent peaks to release of biliverdin (600-700 nm, Figure 3.5A) and free iron (562 nm, Figure 3.5B) after 2 hours of reaction, indicated that GmmHO did not seem to degrade heme, however in the presence of the chelator agent deferoxamine, the formation of biliverdin was visible either when using DmCPR/NADPH (Figure 3.6) or ascorbic acid (Figure 3.7) as source of reducing equivalents.

Despite human HOs degrade heme in vitro independently of iron chelators, desferrioxamine has been used in in vitro experiments with rat HO-1, because in this system the final product is ferric-biliverdin bound to HO, a biliverdin precursor (Yoshida & Kikushi, 1978). This molecule was also used to complete the reaction of HOs from Plasmodium falciparum (Okada, 2009), D. melanogaster (Zhu *et al.,* 2004) and A. thaliana (Muramoto *et al.,* 2002), where it seems to support the release of iron from the ferric-BV complex (Yoshida & Kikushi, 1978).

Characterization of AgHO by Spencer (2016) revealed that this enzyme behaved as a canonical HO by binding heme in a 1:1 stoichiometry and presenting similar absorption spectres to rat and human HOs, suggesting that the mode of binding to heme was similar to those occurring in mammals. By contrast, similar shared some with mammals but most features observed were similar to Drosophila HO.

In conclusion, both HPLC investigation of the insect midgut contents and biochemical analysis of recombinant GmmHO indicates that this enzyme is a real HO conserved in *G. m. morsitans*, playing a role in the protection against heme potential damage. Furthermore, the dependence on iron chelator, distinct spectroscopic features and apparent slower rate suggests that this HO works differently from those reported from mammals however further investigation is needed.

CHAPTER 4 – FUNCTIONAL MAPPING OF GMMHO

4.1. INTRODUCTION

HO genes are expressed among several organisms, including animalia, plantae and bacteria (Yoshida & kikushi, 1977; Zhu *et al.*, 2000; Schuller *et al.*, 2001; Gohya *et al.*, 2006). In humans, these heme binding proteins are well characterized, presenting 2 isoforms named HO1 and HO2. The isoenzymes share about 43% homology at the amino acid level (Cruse & Maines, 1988) and differ in tissue distribution and regulation (Pahanian *et al.*, 1999). Whilst HO1 is ubiquitously distributed among human tissues, its expression is also strongly triggered by a variety of stimuli (Shibahara *et al.*, 1978 Tenhunen *et al.*, 1979; Keyse & Tyrrell, 1989; Takahashi *et al.*, 1996), HO2 is constitutively expressed, with particularly high levels in the testis and brain, where it protects neurons from oxidative damage (Sun *et al.*, 1990; Kumar & Bandyopadhyay, 2005).

A debatable subject in the study of HOs is the subcellular localization of those enzymes. Traditionally known as an endoplasmic reticulum-anchored enzyme, HOs have also been reported in mitochondria (Bansal *et al.*, 2014), caveolae (Kim *et al.,* 2004) and nuclei (Lin *et al.*, 2007; Giordano *et al.*, 2000), reflecting the complexity and plasticity of those enzymes.

Despite the extensive knowledge gathered about human HOs in the last five decades, very little information is known about those enzymes in invertebrates, especially hematophagous insects. HO has been studied in the non-hematophagous fly *D. melanogaster,* in which HO has been shown to act as a signal protein in response to DNA damage caused by oxidative stress (Ida *et al.*, 2013) and was shown to be necessary for the normal development of *D. melanogaster* tissues (Cui *at al.*, 2008). Concerning hematophagous insects, Spencer (2016) has shown that *An. gambiae* HO shares some biochemical features with mammalian HOs particularly in the mode of binding of the enzyme to heme and dissociation constant value. Furthermore, the functional analysis of HO by chemical inhibition affected the abundance of egg laying in a dose dependant manner, indicating that it likely plays a role in reproduction.

In this chapter, studies have been carried out to describe the tissue distribution and expression pattern of GmmHO in the tsetse Fly. We show that in the blood

sucking insect *G. m. morsitans,* HO is ubiquitously expressed in most tissues with and increased expression levels in reproductive tissues and oenocytes, and can be induced following a blood meal in the midgut and in the fat body.

4.2 MATERIAL AND METHODS

4.2.1 Animals and tissue handling

G. m. morsitans (Westwood) male and female flies were obtained from an established colony at the Liverpool School of Tropical Medicine around 0-24 hours following emergence, separated in individual groups cages according to the desired experiment and maintained at optimum conditions (RH 65-75%; 27°C ± 2°C) until dissection. Using dissecting tweezers, all dissections were performed under binocular stereo light scope. The flies were kept on ice for 10-15 minutes before their digestive tract, fat body (+oenocytes), reproductive tissues or other desired organ or body part was dissected in PBS pH 7.4 with protease inhibitor cocktail (Sigma-Aldrich), snap frozen in liquid nitrogen and kept in -80 until use.

4.2.2 Antibodies

Two sets of primary anti-GmmHO antibodies against were used:

(1) Rabbit polyclonal antibodies against GmmHO (created by David Technologies by injecting 1 mg of recombinant Δ250GmmHO followed by affinity purification of blood serum).

(2) Hen polyclonal antibodies against GmmHO (created by David Technologies by injecting 1 mg of recombinant GmmHOΔ250 followed by affinity purification from eggs laid by the hen injected with recombinant protein).

For western blots, secondary antibodies conjugated to HRP (horse radish peroxidase) and specific for rabbit and hen IgG were purchased from ThermoScientific. For immunostaining studies, Secondary antibodies specific for rabbit (Alexa 488, green) and hen IgG (Alexa 594, red) conjugated to fluorescent dyes were purchased from ThermoFisher.

4.2.3 Determination of protein content by Bradford method

As described in section 2.2.21

4.2.4 Sample preparation for western blotting

Dissections were performed in ice-cold PBS pH 7.4. Tissues were immediately macerated in PBS pH 7.4 in the presence of a protease inhibitor cocktail (Sigma-Aldrich), centrifuged at 15.000 g and the protein content of the supernatant of the homogenate was measured by Bradford assay (Biorad). When appropriate, the pellet was resuspended in Laemmli buffer. Aliquots with 10 μg of samples were added to Laemmli buffer (2X) containing 5% β-mercaptoethanol, heated at 100°C for 10 min and loaded onto a 12.5 % polyacrylamide gel.

4.2.5 Protein electrophoresis and western blotting

As described in section 2.2.22 and 2.22.23

4.2.6 Immunohistochemistry methods

Dissections of tsetse fly tissues were performed in a watch glass containing cold PBS pH 7.4 in the presence of protease inhibitor cocktail (Sigma-Aldrich). The tissues were fixed (4% paraformaldehyde, 1x PBS pH 7.5, 2mM $MgSO_4$, 1 mM EGTA) for 30-45 min at room temperature, blocked for 2 hours (1%BSA, 0.1% Triton X-100, 1x PBS, pH 7.5), incubated with primary antibody overnight and exposed to appropriate secondary antibody for 2 hours. Between each step, successive washings with PBS were performed to improve quality of staining. All samples were also incubated with DAPI for 1 min to stain the nuclei.

4.2.6 Fluorescent microscopy

After fixation, blocking and incubation steps with DAPI and antibodies, the tissues were mounted in microscope slides using 15-20 μL of mounting media and covered with coverslips, which were glued to the slides using polish nail to ensure the samples would not move during analysis. Images of samples showing tissues marked with antibodies specific to HO and CPR, as well as with the nuclei marker DAPI were taken using a Carl Zeiss Axio Observer.Z1 confocal microscope at room temperature with objectives between 10 – 63x depending on the tissue or desired magnification.

Immersion oil was used for 40-63 x objectives. Identical laser settings (Alexa 488: excitation 488 nm, emission 516 nm; Alexa 594: excitation 561 nm, emission 659 nm; DAPI: excitation 405, emission 459) were used. Capture and extraction was carried out with Zen 2.3 lite software.

4.2.7 RNA and cDNA preparation

Tsetse fly tissues were dissected in cold PBS pH 7.4, snap frozen and maintained at -80°C until RNA extraction, which was carried out using the RNAqueous® Micro Kit from Thermofisher, followed by treatment with Turbo DNA-free kit (Ambion) to remove genomic DNA contamination according to manufacturer's instructions. To synthetize cDNA for real time polymerase chain reaction (RT-PCR), total RNA (4 µg) and oligo-dT (20) primers were used to carry out reserve transcription using the Superscript IV First Strand Synthesis kit from Thermofisher Scientific. All steps were carried out using appropriate precautions to maintain purity and integrity of samples.

4.2.8 Quantitative PCR

The design of specific primers for quantitative RT-PCR was carried out using Primer3Plus (http://www.bioinformatics.nl/cgi-bin/primer3plus/primer3plus.cgi). The primers were designed to be between 19 - 22 base pairs (bp), with Tm values ranging from 59.0°C to 61.0°C. The size of the PCR products was set within the range 120–260 bp. Quantitative real-time PCR was performed using SYBR Green Supermix III (Agilent) using an MX3005 and the associated MxPro software (Agilent). Each 20µl reaction contained 10 µl SYBR Green Supermix, 0.5 µM of each primer and 1µl of 1:10 diluted cDNA. Standard curves were produced using cDNA from the whole fly. qPCR was performed with the following conditions: 3 minutes at 95°C, with 40 cycles of 10 seconds at 95°C and 10 seconds at 60°C, followed by a melting curve analysis from 55 to 95°C. All amplification efficiencies of designed primers were within acceptable range (90-120%), following MIQE guidelines (Bustin et al., 2009). Primers specific for tsetse Actin and Rp32 were used as reference genes (Table 4.1).

Table 4.1 – qPCR primers

Gene	Accession entry	Sequence	Efficiency (%)
GmmHO forward primer	GM004329	GCCAGCCGTCAAGAAATA	96.8
GmmHO reverse primer	GM004329	GTGCCATCATACGCTTCTT	-
GmmActinC forward	GMOY007085	CTGGTATTGCTGATCGTATGCAA	110.7
GmmActinC reverse	GMOY007085	TGGAAGGAGCCAAGGCG	-
GmmRpl32 forward	GMOY001799	ATTGCTCACGGCGTGTCA	101.3
GmmRpl32 reverse	GMOY001799	AGCTCTTTCAACAATATCTTTTCGC	-

4.3 RESULTS

4.3.1 Tissue distribution of GmmHO

Antibodies raised against recombinant GmmHO (Chapter 2) in chickens and rabbits were used to determine the tissue distribution of GmmHO in tsetse flies. As discussed in chapter 2, Western blotting analysis indicated that antibodies raised in rabbit were more sensitive (~100x) in recognizing recombinant HO, thus used for initial immunolocalization experiments.

To assess the specificity of GmmHO antibodies, the affinity-purified antibodies were tested against unfed tsetse flies' midguts, with recombinant GmmHO as a positive control and AgCPR as a negative control. As shown in Figure 4.1, no signal was detected in midgut homogenates. Signal was detected against the recombinant GmmHO indicating low concentration of GmmHO in the midgut. Given that the blood meal is digested in the midgut, with concomitant release of heme, high levels of GmmHO were expected. The possibility that GmmHO would be induced by blood feeding was therefore examined.

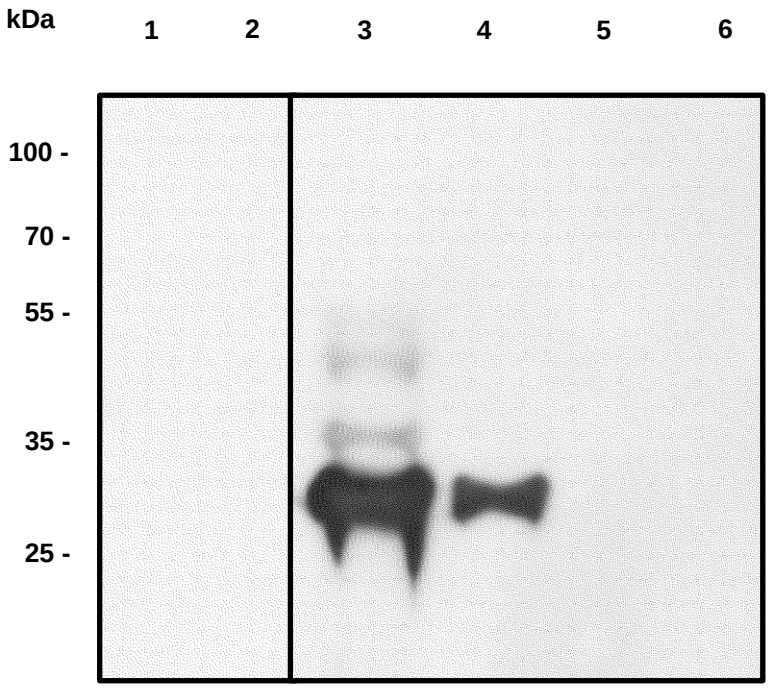

Figure 4.1 – **Reactivity of antiGmmHO to tsetse fly tissues and recombinant enzymes**. (1) Two digestive tract equivalents (2) One digestive tract midgut (3) Recombinant GmmHO - 1 µg (4) Recombinant GmmHO – 0.1 µg (5) Recombinant AgCPR - 1 µg (6) Recombinant AgCPR - 1 µg. Samples were boiled in Laemmli buffer, separated on 12.5% acrylamide-SDS gel and blotted using anti-GmmHO antibodies raised in rabbit. Molecular weight marker (kDa, PageRuler+ Prestained Protein ladder from ThermoFisherScientific) is shown on the left side. The gel was subjected to a voltage of 60mV until the dye front had moved into the resolving gel, after which time the voltage was increased to 90mV. After that, the samples were transferred onto (PVDF) membrane at 90 V for 45 minutes. The membrane were then incubated for 2 hours in 5% skimmed milk powder at 4°C. The following day the membranes were probed at room temperature with of anti-GmmHO polyclonal antibodies raised in rabbit (1:8,000), washed with PBS and then incubated with a 1:10,000 dilution of rat anti-rabbit secondary antibody at room temperature for 1 hour. After several washes, the strips were incubated with SuperSignal West Dura (Pierce, UK) peroxidase buffer and luminol/enhancer solution at a 1:1 ratio, and developed by chemiluminescence for 1 minute

To evaluate the effect of a blood meal on GmmHO expression, male and female tissues were dissected before a blood meal and 48-72 hours after a single blood meal (ABM). The presence of GmmHO in other tissues was also examined. Immunoreactive bands were observed in reproductive tissues and carcasses from both sexes (Figure 4.2 and Figure 4.3). However, no signal was detected in the digestive tract after a blood meal (Figure 4.2, lanes 3 and 4).

In male reproductive tissues and carcass, the levels of GmmHO were similar before and after blood feeding, suggesting that GmmHO expression is constitutive in these tissues (Figure 4.2, lanes 1-2 and 3-4). A similar pattern was also found in female tissues (Figure 4.3). The apparent differences observed in immunoreactivity between male and female tissues was related to different time exposures, therefore not an indication of sex-dependant differences in levels of HO expression.

Besides the expected immunoreactive band migrating at ~31 kDa (full size HO), another band was observed at 62 kDa in reproductive tissues from both sexes (Figure 4.2, lines 5 and 6). Similar bands were seen in carcass however the high molecular weight band was not as prominent (Figure 4.2, lines 1 and 2). The higher molecular weight band may be an indication of dimer formation.

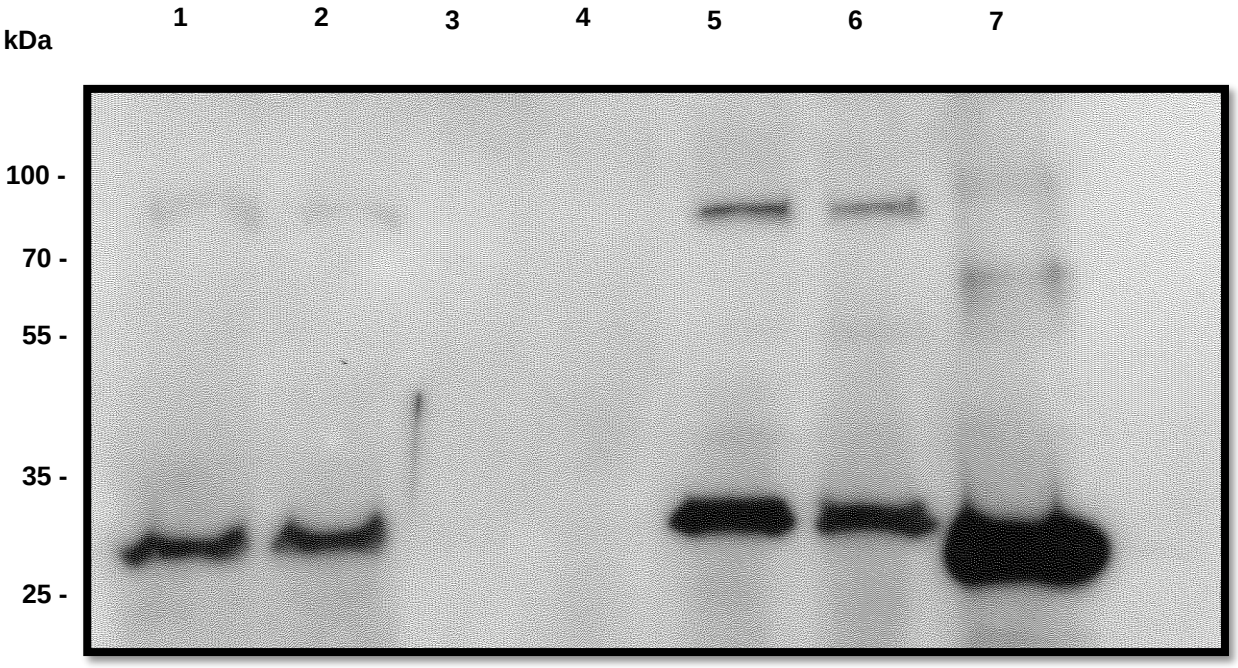

Figure 4.2 – Immunoblot of teneral male tsetse fly before and 72 hours after a single blood meal against anti-GmmHO antibodies raised in rabbit. (1) Carcass before blood meal (2) Carcass after blood meal (3) midgut before blood meal (4) midgut after blood meal (5) reproductive tissues before blood meal (6) reproductive tissues after blood meal (7) Recombinant GmmHO. The tissues were macerated, centrifuged and the supernatant collected. Equal amount of samples were boiled in Laemmli buffer (10 µg protein), separated on 12.5% acrylamide-SDS gel and blotted using anti-GmmHO antibodies raised in rabbit. Molecular weight marker (kDa, PageRuler+ Prestained Protein ladder from ThermoFisherScientific) is shown on the left side. The gel was subjected to a voltage of 60mV until the dye front had moved into the resolving gel, after which time the voltage was increased to 90mV. After that, the samples were transferred onto (PVDF) membrane at 90 V for 45 minutes. The membrane were then incubated for 2 hours in 5% skimmed milk powder at 4°C. The following day the membranes were probed at room temperature with of anti-GmmHO polyclonal antibodies raised in rabbit (1:8,000), washed with PBS and then incubated with a 1:10,000 dilution of rat anti-rabbit secondary antibody at room temperature for 1 hour. After several washes, the strips were incubated with SuperSignal West Dura (Pierce, UK) peroxidase buffer and luminol/enhancer solution at a 1:1 ratio, and developed by chemiluminescence for 5 minutes

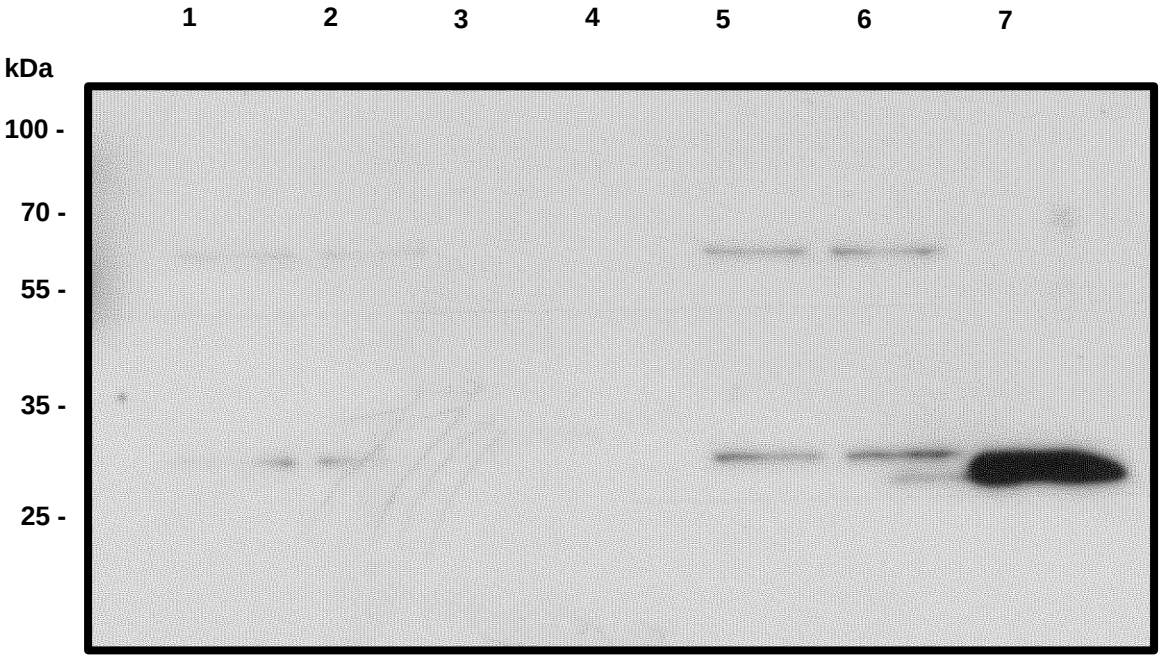

Figure 4.3 – Immunoblot of teneral female tsetse fly before and 72 hours after a single blood meal against anti-GmmHO antibodies raised in rabbit. (1) Carcass before blood meal (2) Carcass after blood meal (3) midgut before blood meal (4) midgut after blood meal (5) reproductive tissues before blood meal (6) reproductive tissues after blood meal (7) Recombinant GmmHO. The tissues were macerated, centrifuged and the supernatant collected. Equal amount of samples (10 µg protein) were boiled in Laemmli buffer, separated on 12.5% acrylamide-SDS gel and blotted using anti-GmmHO antibodies raised in rabbit. Molecular weight marker (kDa, PageRuler+ Prestained Protein ladder from ThermoFisherScientific) is shown on the left side. The gel was subjected to a voltage of 60mV until the dye front had moved into the resolving gel, after which time the voltage was increased to 90mV. After that, the samples were transferred onto (PVDF) membrane at 90 V for 45 minutes. The membrane were then incubated for 2 hours in 5% skimmed milk powder at 4°C. The following day the membranes were probed at room temperature with of anti-GmmHO polyclonal antibodies raised in rabbit (1:8,000), washed with PBS and then incubated with a 1:10,000 dilution of rat anti-rabbit secondary antibody at room temperature for 1 hour. After several washes, the strips were incubated with SuperSignal West Dura (Pierce, UK) peroxidase buffer and luminol/enhancer solution at a 1:1 ratio, and developed by chemiluminescence for 1 minute

Several attempts were made to western blot tsetse fly tissues dissected between 0-48 hours ABM. However, the high amount of blood, especially in the digestive tract, interfered with the analysis (data not shown). Hence, tsetse fly tissues were dissected 48-72 hours ABM when blood was degraded and heme concentration diminished in the digestive tract (Figure 3.2).

To rationalise the absence of a HO immunoreactive signal in the midgut, the method of midgut extraction was changed to include a strong surfactant (Triton X- 100) and a sonication step followed by centrifugation. Both pellet and supernatant fractions from midgut and reproductive tissue were used for blotting against rabbit-GmmHO antibodies. GmmHO was identified in the midgut although it was only detectable in the pellet fraction (Figure 4.4, lanes 2 and 4), but not in the supernatant fraction (Figure 4.4, lanes 1 and 3). By contrast GmmHO was detectable in the supernatant fraction of reproductive tissues and carcass (Fig 4.2). This suggests either different cellular localization and/or expression levels. It was notable that pellets from digestive tract contained a low molecular GmmHO signal in western blots, which suggests possible GmmHO degradation by digestive enzymes present in those tissues. The experiment was repeated with chicken GmmHO antibodies, yielding similar results. The signal was much weaker as expected for the lower chicken antibodies titre. Thus, to analyse the expression in digestive tract the pellet fractions from tissue homogenates were used along with the supernatant fraction.

As described in Chapter 3, high concentrations of biliverdin were seen in the posterior section of the insect digestive tract ~72 hours after a single blood meal (Figure 3.1). Here, we explored the distribution of HO in this organ by sectioning the whole digestive tube in the following parts: proventriculus (PV), crop (CP), anterior gut (AG), bacteriome (BT), midgut (MG), porterior midgut (PG) and hindgut (HG). Similar levels of immmunoreative bands in AM and PG (Figure 4.6) indicated similar GmmHO levels, while the absence of GmmHO signal indicated low levels of the enzyme in the hindgut.

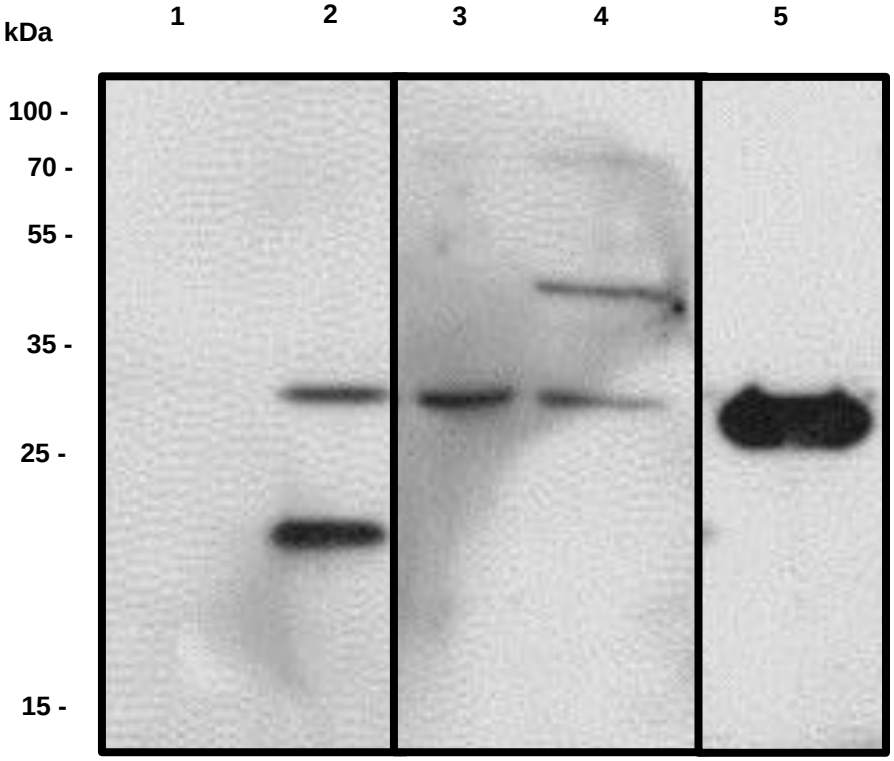

Figure 4.4 - Immunoblot of different extractions of tsetse fly tissues against anti-GmmHO antibodies raised in rabbit. (1) Midgut supernatant (2) Midgut pellet (3) Reproductive tissue supernatant (4) Reproductive tissue pellet (5) Recombinant GmmHO. To improve soluble HO in the samples, the tissues were macerated in the presence of the surfactant Triton X-100, sonicated and centrifuged and both pellet and supernatant were collected. The tissues were macerated, centrifuged and the supernatant collected. Equal amount of samples (10 µg protein), were boiled in Laemmli buffer separated on 12.5% acrylamide-SDS gel and blotted against anti-GmmHO antibodies raised in rabbit. Molecular weight marker (kDa, PageRuler+ Prestained Protein ladder from ThermoFisherScientific) is shown on the left side. The gel was subjected to a voltage of 60mV until the dye front had moved into the resolving gel, after which time the voltage was increased to 90mV. After that, the samples were transferred onto (PVDF) membrane at 90 V for 45 minutes. The membrane were then incubated for 2 hours in 5% skimmed milk powder at 4°C. The following day the membranes were probed at room temperature with of anti-GmmHO polyclonal antibodies raised in rabbit (1:8,000), washed with PBS and then incubated with a 1:10,000 dilution of rat anti-rabbit secondary antibody at room temperature for 1 hour. After several washes, the strips were incubated with SuperSignal West Dura (Pierce, UK) peroxidase buffer and luminol/enhancer solution at a 1:1 ratio, and developed by chemiluminescence for 2 minutes

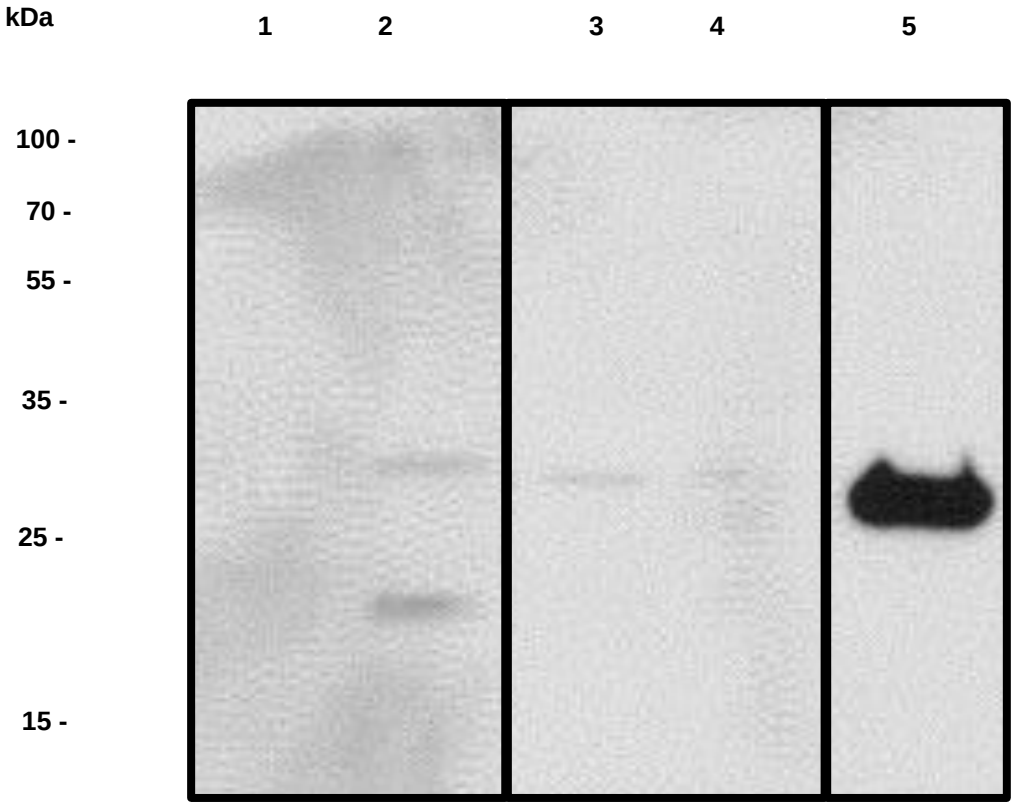

Figure 4.5 - Immunoblot of different extractions of tsetse fly tissues against anti-GmmHO antibodies raised in chicken. (1) Midgut supernatant (2) Midgut pellet (3) Reproductive tissue supernatant (4) Reproductive tissue pellet (5) Recombinant GmmHO. To improve soluble HO in the samples, the tissues were macerated in the presence of the surfactant Triton X-100, sonicated and centrifuged and both pellet and supernatant were collected. The tissues were macerated, centrifuged and the supernatant collected. Equal amount of samples (10 µg protein), were boiled in Laemmli buffer separated on 12.5% acrylamide-SDS gel and blotted against anti-GmmHO antibodies raised in rabbit. Molecular weight marker (kDa, PageRuler+ Prestained Protein ladder from ThermoFisherScientific) is shown on the left side. The gel was subjected to a voltage of 60mV until the dye front had moved into the resolving gel, after which time the voltage was increased to 90mV. After that, the samples were transferred onto (PVDF) membrane at 90 V for 45 minutes. The membrane were then incubated for 2 hours in 5% skimmed milk powder at 4°C. The following day the membranes were probed at room temperature with of anti-GmmHO polyclonal antibodies raised in chicken (1:1,000), washed with PBS and then incubated with a 1:10,000 dilution of rat anti-chicken secondary antibody at room temperature for 1 hour. After several washes, the strips were incubated with SuperSignal West Dura (Pierce, UK) peroxidase buffer and luminol/enhancer solution at a 1:1 ratio, and developed by chemiluminescence for 2 minutes

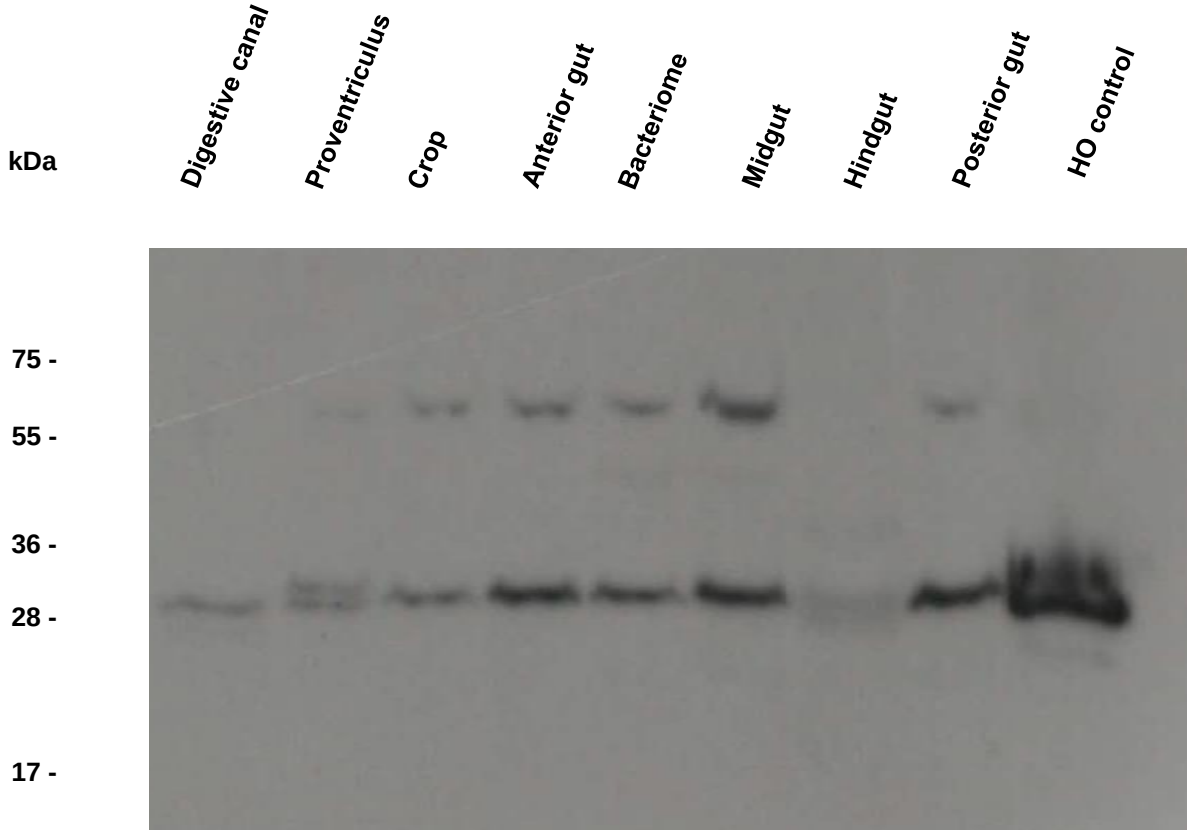

Figure 4.6 - **Western blotting analysis of several sections of tsetse fly digestive tract**. Tissues were boiled in Laemmli buffer, separated on 12.5% acrylamide-SDS gel and blotted using rabbit anti-GmmHO antibody. 3 units of each digestive tract portion from 3 different animals were loaded. Molecular weight marker (kDa) is shown on the left hand side. The tissues were macerated, centrifuged and the supernatant collected. Equal amount of samples (10 µg protein), were boiled in Laemmli buffer separated on 12.5% acrylamide-SDS gel and blotted against anti-GmmHO antibodies raised in rabbit. Molecular weight marker (kDa, PageRuler+ Prestained Protein ladder from ThermoFisherScientific) is shown on the left side. The gel was subjected to a voltage of 60mV until the dye front had moved into the resolving gel, after which time the voltage was increased to 90mV. After that, the samples were transferred onto (PVDF) membrane at 90 V for 45 minutes. The membrane were then incubated for 2 hours in 5% skimmed milk powder at 4°C. The following day the membranes were probed at room temperature with of anti-GmmHO polyclonal antibodies raised in rabbit (1:4,000), washed with PBS and then incubated with a 1:15,000 dilution of rat anti-rabbit secondary antibody at room temperature for 1 hour. After several washes, the strips were incubated with SuperSignal West Dura (Pierce, UK) peroxidase buffer and luminol/enhancer solution at a 1:1 ratio, and developed by chemiluminescence for 2 minutes

Immunofluorescence methods were carried out to provide further information on the tissue distribution of HO in the tsetse fly, as well as cell location. Initially an affinity purified Anti-GmmHO antibodies raised in rabbit was used with a green fluorescent-dye conjugated secondary antibody that targets rabbit IgG (Alexa 488). The blue fluorescent DAPI was used as a DNA marker.

Immunofluorescence analysis of different body parts suggested that HO expression in *G. m. morsitans* was detectable in reproductive tissues, digestive tract and fat body (Figure 4.7). Regarding male reproductive tissues, staining was seen in the testes (Figure 4.7) and accessory glands, as well as in the associated fat body (Figure 4.7). In the digestive tract, high GmmHO staining is observed in the cytoplasm of mid-gut epithelial cells, with distinct non staining of the nuclei identified through DAPI staining (Figure 4.7B). Apart from the hindgut, a similar level of staining was observed all along the extension of the tissue (data not shown).

HO-driven heme degradation requires electrons supplied by an electron-donor, normally CPR. Because tsetse fly CPR antibodies were not available, co-localization of GmmHO with CPR in tsetse organs was examined using antibodies specific for CPR from *A. gambiae* (AgCPR) (Lycett et al, 2006), which share a high degree of identity (85%) and cross-react with GmmCPR. Since AgCPR antibodies were raised in rabbits, co-localization studies with chicken GmmHO antibodies were used.

The co-staining of GmmHO (red) and CPR (green) confirmed that these enzymes are co-expressed in fat body, reproductive tissues and digestive tract (Figures 4.8 and 4.9). Despite the high concentration of chicken anti-HO antibodies used, the GmmHO staining was much weaker than those observed when using rabbit anti-HO, as expected from western blotting results (Figure 4.4 and 4.5). Thus, it was necessary to increase the intensity of the laser at the red excitation wavelength, resulting in high background.

The anterior section of the digestive tract and proventriculus were stained uniformly as shown in Figure 4.8. Staining of the associated fat body can also be observed in the figure. Similar uniform staining also occurred in the reproductive tissues (Figure 4.8). The fluorescence observed in the spermatheca (Figure 4.8, bottom) was not thought to be due to higher levels of GmmHO gene expression since

substantial auto fluorescence in the red spectrum (620-750 nm) was present in this portion of the female reproductive tissue. A similarly high degree of green auto fluorescence was found in the digestive tube.

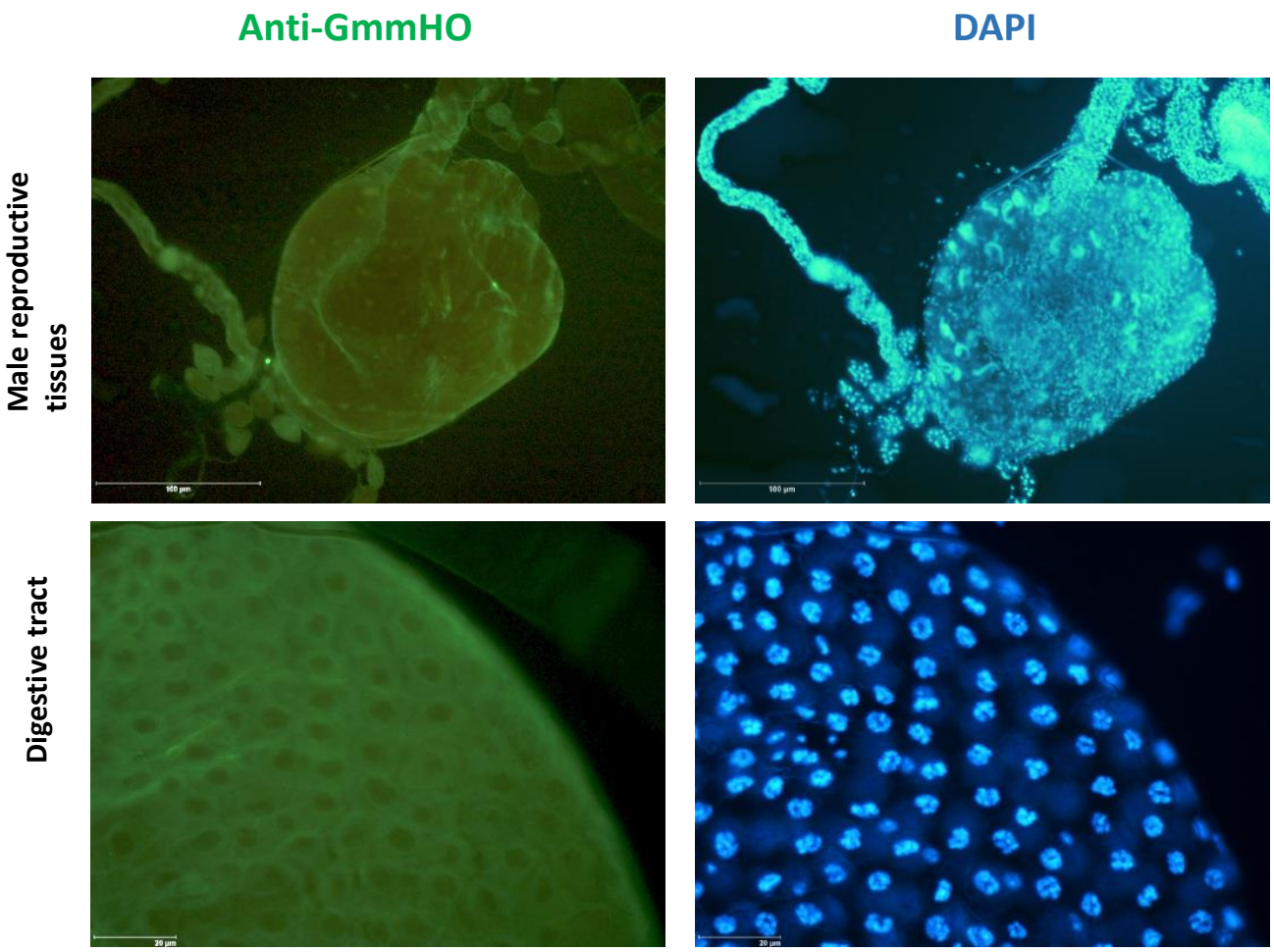

Figure 4.7 – Immunostaining of Tsetse fly reproductive tissues and digestive tract with anti-HO and DAPI marker. The tissues were incubated overnight with 1:200 rabbit anti-GmmHO and counterstained with 1:2000 DAPI to mark nuclei. Other groups with pre-immune and untreated were carried out to rule out auto fluorescence.

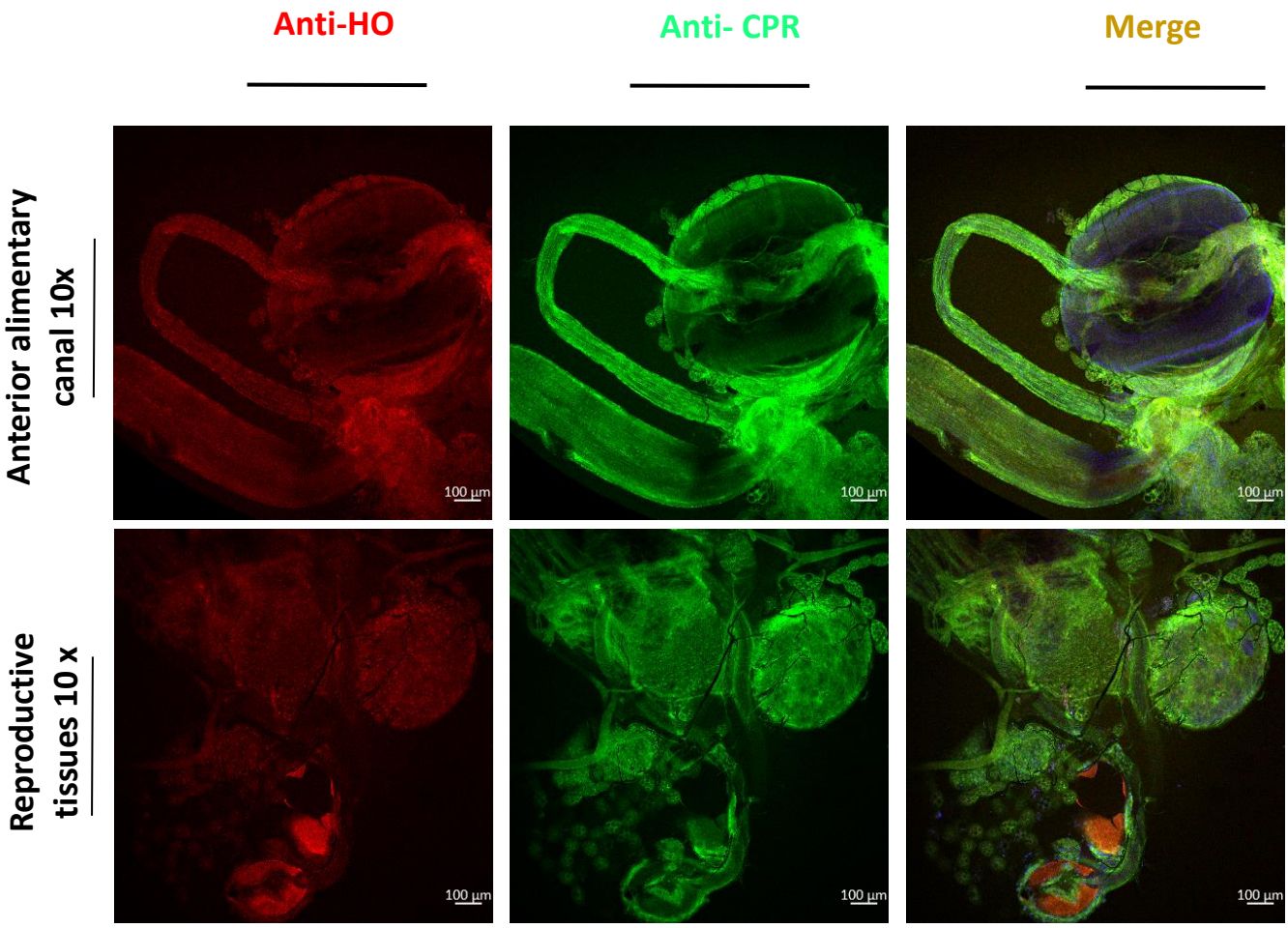

Figure 4.8 – Immunofloresce of tsetse fly tissues marked with hen anti HO and rabbit anti CPR. The tissues were treated overnight with 1:50 GmmHO and anti 1:250 AgCPR and counterstained with 1:2000 DAPI to mark nuclei. Other groups with pre-immune and untreated were carried out to rule out autofluorescence.

4.3.2 Identificaton of Oenocytes

Pioneering work by Tobe et al. (1973) described the cytological changes occurring in fat bodies and milk glands during the gonadatrophic cycle of *G. m. austeni*, another species of tsetse fly. According to the authors, the organization of the fat body in this species consisted of a series of spherical structures covered by a thin layer joining them together in long chains that are intercalated by smaller, denser spheres. Despite being much smaller and quite different morphologically than those observed in higher diptera (Perez, 1910; Wigglesworth, 1965), those cells were proposed to be oenocytes, which are specialised liver-like insect cells that are involved in fatty acid and hydrocarbon metabolism (Makki *et al.*, 2014).

Here, the coupled confocal immunofluorescence techniques showed that the fat body structures in *G. m. morsitans* were not uniformly stained by anti-HO and anti-CPR (Figure 4.9). Instead, some of the cells showed more intense fluorescence. Under high magnification (40x), these were revealed to be smaller and rounder than the weakly stained cells (Figure 4.9 D, E, F). These consistent morphological features are equivalent to those described for proposed oenocytes in *G. m. austeni* (Tobe *et al.*,1973). Furthermore, the high levels of CPR observed is consistent with the high levels observed in other insect oenocytes, including Drosophila and *An. gambiae* (Lycett *et al.*, 2006). Like CPR, GmmHO thus provides a new marker for tsetse fly oenocytes. Importantly, this marker differentiates the different cell types present in the 'fat body', otherwise difficult to distinguish purely by morphology.

Surprisingly, even though the GmmHO and CPR were co-localized in all the tissues analysed, confocal analysis of the oenocytes suggested possible differences in subcellular localization (Figure 4.9). Whilst CPR staining was dispersed throughout the cell, high levels of GmmHO expression were observed in the nuclei, as well as throughout the cytoplasm. CPR and heme oxygenases are normally anchored on the endoplasmic reticulum. In mice fibroblasts for example, a cleaved HO can be found in nuclei under hypoxia conditions (Lin *et al.*, 2007)

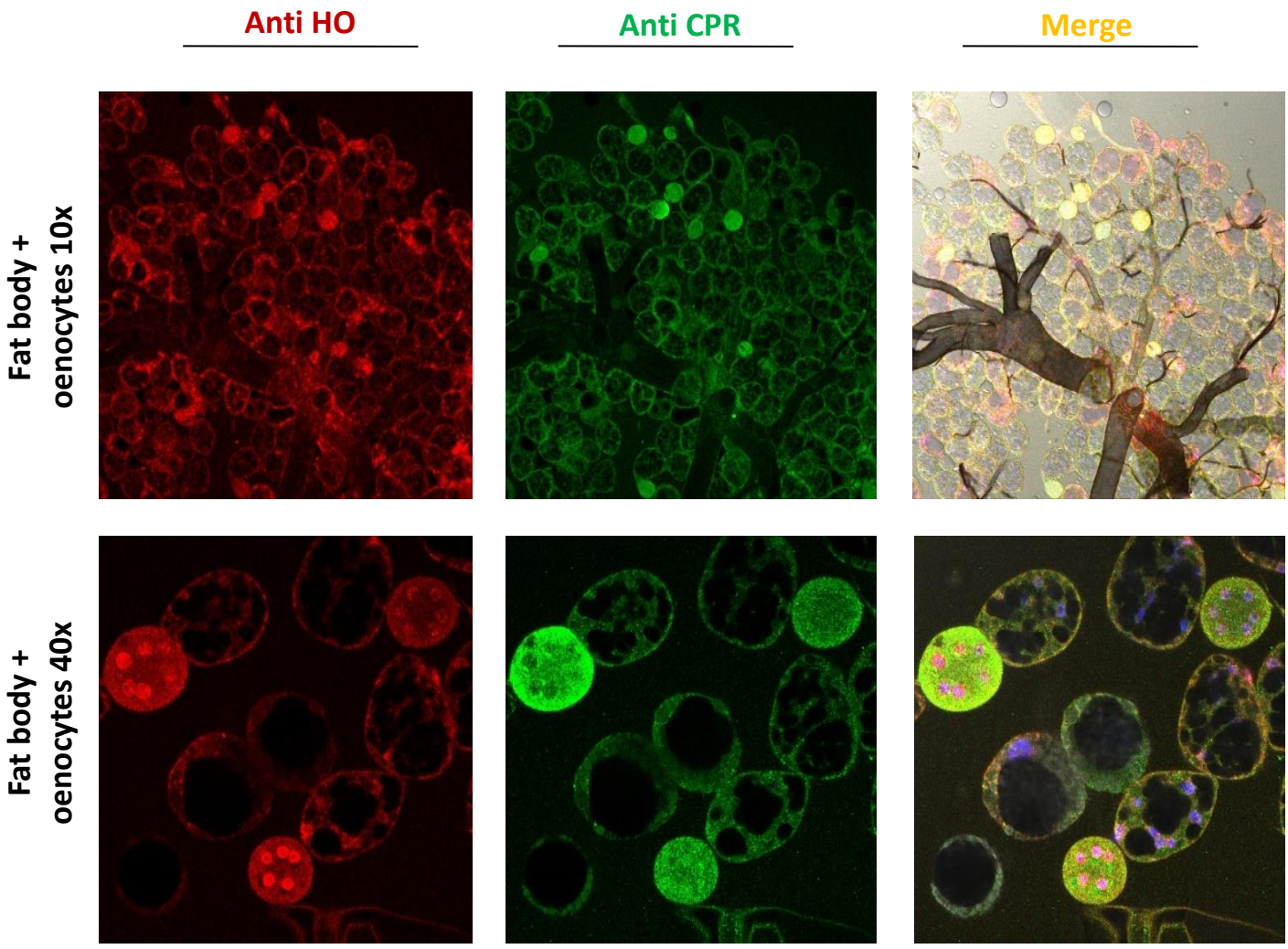

Figure 4.9 – Immunolocalization of HO and CPR in Tsetse flies oenocytes The tissues were treated overnight with 1:50 GmmHO and anti 1:250 AgCPR and counterstained with 1:2000 DAPI to mark nuclei. Other groups with pre-immune and untreated were carried out to rule out autofluorescence.

4.3.3 Effect of a blood meal on GmmHO expression

The levels of HO gene expression in several tissues (reproductive organs, midgut, fat body, flight muscle) of female *G. m. morsitans* was evaluated by qPCR. Relative levels of expression were quantified by comparison with whole body PCR (Figure 4.10). Highest GmmHO transcript levels were observed in reproductive tissues (6.5 x), fat body (1.7 x) and midgut (2.0 x). For flight muscles, GmmHO mRNA levels were basal (~1.0x).

To assess the impact of a blood meal on HO expression, the GmmHO transcript mRNA levels in reproductive tissues, digestive tract and fat body were followed in several time points between 1 to 72 hours after blood feeding. Despite showing the highest levels of HO expression among the tissues analysed (Figure 4.10), GmmHO levels in reproductive tissues were not significantly altered during the first 72h ABM, suggesting that blood meal does not impact the expression of the enzyme in this tissue. In the case of the fat body, which contained oenocytes, the GmmHO levels ABM increased slightly 24 hours post blood meal (2.2 x) before dropping back to basal levels at 48 hours (~1 x), and slightly lower by 72 hours.

The GmmHO mRNA levels in the alimentary canal increased 3.4-fold at 12 hours after a blood meal, reducing to 2.2-fold at 24 hours. This value remaining unchanged until 48 h ABM after which dropped to basal levels (~1.0). This suggests that GmmHO expression may be induced by blood feeding in the digestive tract, strengthening a possible role in heme degradation as a protective response to increased blood levels.

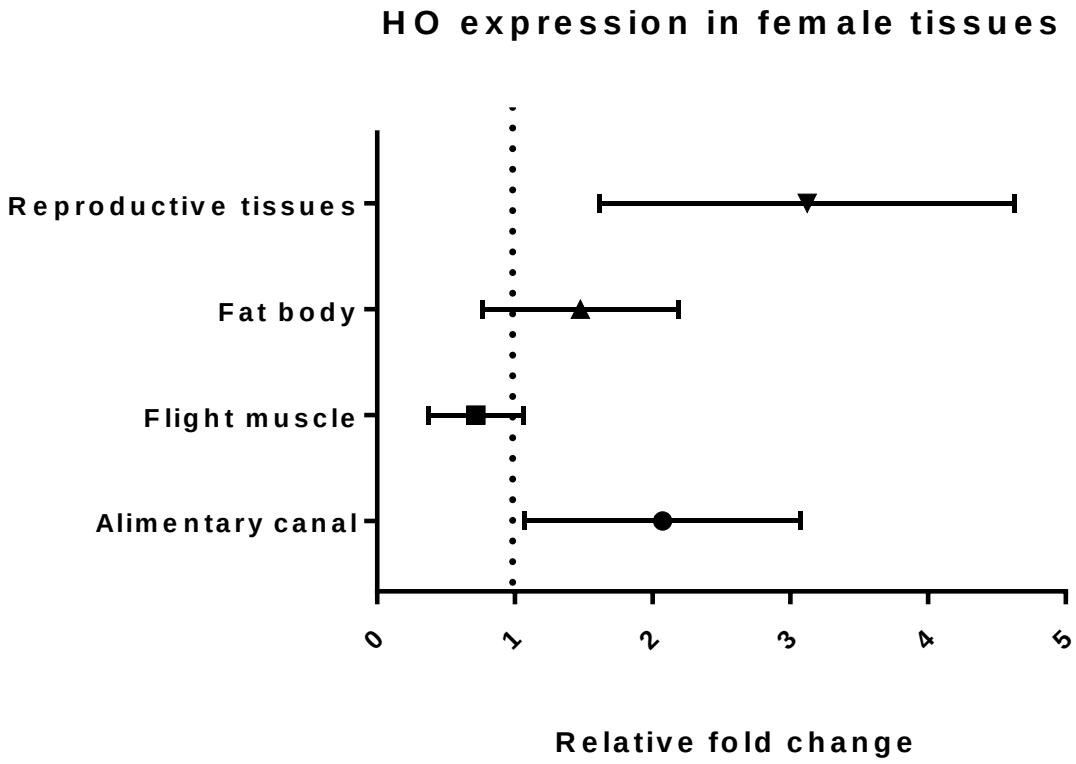

Figure 4.10 – Relative GmmHO mRNA expression levels various female *G. m. morsitans* body compartiments in relation to the whole body. All expression values were calculated against housekeeping genes actin and Rp32. Data representative of three biological replicates, with three technical replicates and are illustrated as average ± SD

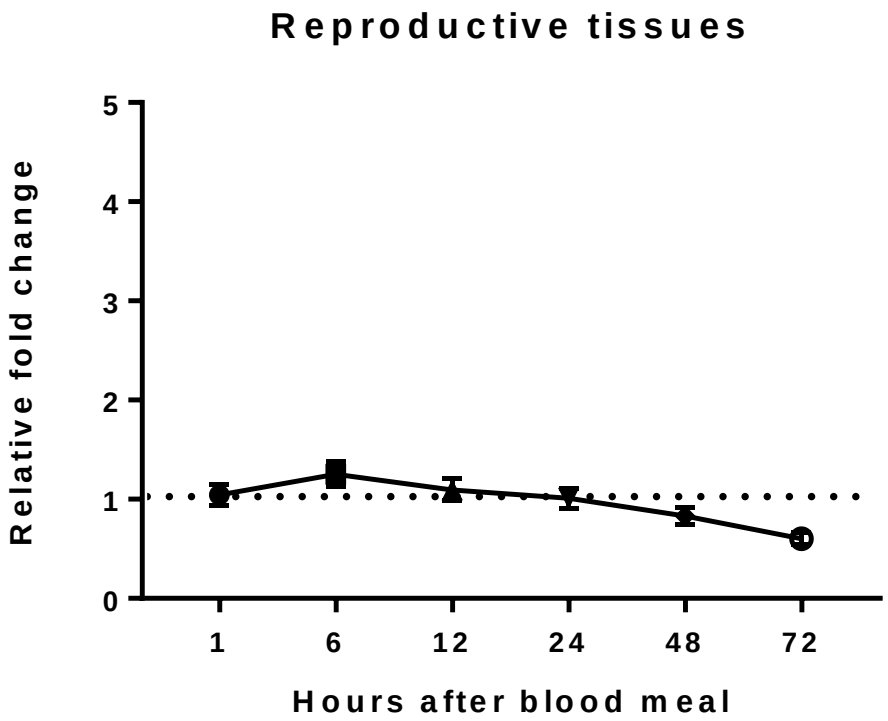

Figure 4.11 – Expression kinetics of GmmHO gene in female reproductive tissues. Relative levels of GmmHO mRNA were analysed in unfed and fed midguts at various time points after blood feeding. All expression calculated against housekeeping genes actin and Rp32. Data representative of three biological replicates, with three technical replicates and are illustrated as average ± SD

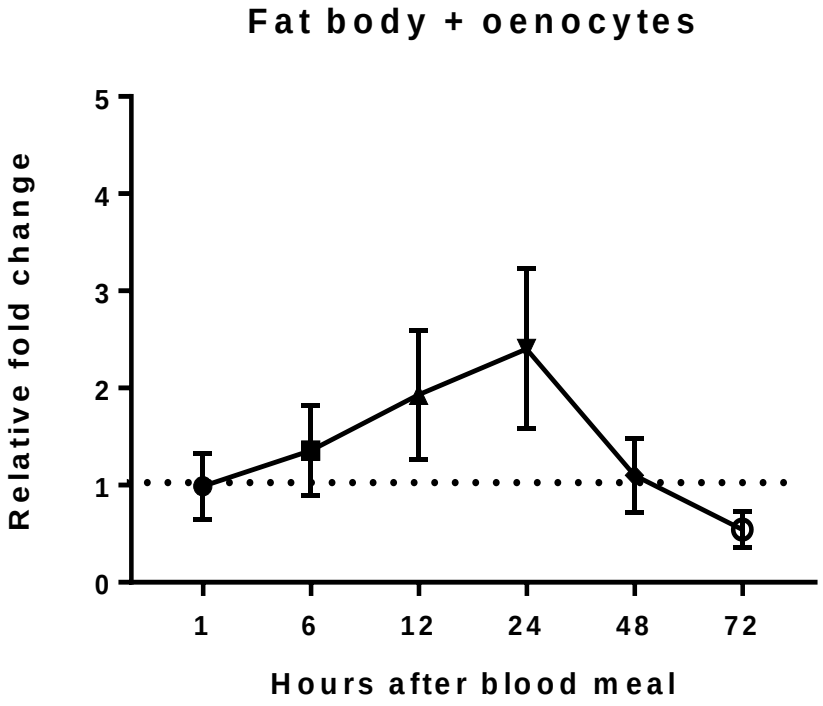

Figure 4.12 – GmmHO expression in various female tsetse fly tissues in relation to the whole body. All expression calculated against housekeeping genes actin and Rp32. Data representative of three biological replicates, with three technical replicates and are illustrated as average ± SD

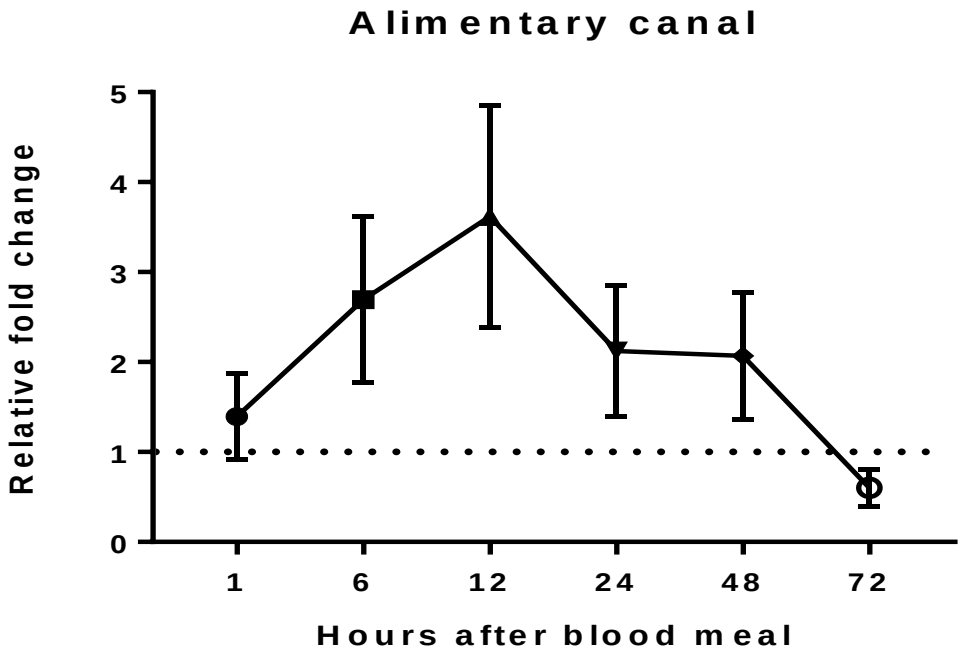

Figure 4.13 – Effect of blood meal in HO expression of Tsetse fly alimentary canal. All expression calculated against housekeeping genes actin and Rp32. Data representative of three biological replicates, with three technical replicates and are illustrated as average ± SD

4.4 DISCUSSION

An extensive amount of research has been dedicated to HOs in humans. Due to its ability in producing equimolar amounts of biliverdin and CO, HOs can control intracellular heme levels and possess anti-inflammatory (Paine *et al.*, 2010; Hualin *et al.*, 2012) and antioxidant (Turkseven *et al.*, 2005; Parfenova *et al.*, 2012) properties, which enables it to participate in a myriad of physiological processes. In particular, the inducible human isoform HO1 is involved in physiological conditions such as cardiovascular diseases (Immenschuh & Schoreder, 2006; Dunn et al., 2014), cancer (Chau, 2015) and organ transplant rejection (Ollinger & Pratschke, 2010). The presence of GmmHO in tsetse fly fat body, midgut, reproductive tissues and carcass, assessed by both western blotting and immunohistochemistry techniques (Figures 4.3 – 4.9) suggests that HO is widely expressed in *G. m. morsitans*. In *R. prolixus*, a modified isomer of biliverdin was isolated from digestive tract and heart of the insect (Paiva-Silva *et al.*, 2006). Likewise, HO activity has been reported in the digestive tract of *Ae. Aegypti* (Pereira *et al.*, 2007). Those studies indicate that HO is present in the heart and digestive tract tissues of hematophagous insects.

In insects, the physiological role of HOs are not well defined. In the fruit fly *D. melanogaster* the silencing of the HO gene results in a 95% mortality in the larval and pupae stages, indicating that this enzyme is essential for the insect survival and normal development of *D. melanogaster* tissues (Cui *at al.*, 2008). Further studies have shown that the abnormalities in eye imaginal disc by tissue specific HO knock down in *D. melanogaster* are linked to a possible role of the enzyme in signalling in the DNA damage pathway which is induced following oxidative stress (Ida *et al.*, 2013).

The immunolocalisation of *G. morsitans* HO to the reproductive tissues in both male and female adult flies suggests that the enzyme may play a role in tsetse fly reproduction. Functional analysis by gene silencing could be used to examine this role in a sex specific manner in tsetse flies. Similarly, an approach could be taken that has been used in other hematophagous insects through classical biochemical inhibition of HO activity by the inclusion of the heme analogues (eg Sn-photoporphirin) in the blood meal. When performed in the Chagas disease vector *R. prolixus*, it led to the impairment of the reproductive capacity of the insect (Caiaffa *et al.*, 2010). Comparable findings were observed with the inhibition of HO in the malaria vector *An.*

gambiae (Spencer, 2016), which resulted in a reduction in oviposition rates. Together, these functional studies strongly suggest that HOs play an important role in the reproduction of blood feeding insects, which is supported by the high expression in tsetse fly reproductive tissues.

The question is what role does HO play in reproduction? The analysis of GmmHO gene expression in the reproductive tissues of tsetse female showed that GmmHO was constitutively expressed with no apparent induction in response to a blood meal between 1- 48h ABM. Heme is the principle substrate for HO, however, CO is also a highly active product of HO activity. Since CO can function as a signalling molecule it may operate through activation/inhibition of several pathways, including those associated with reproduction. There is increasing evidence that CO may play an important signalling role in the female reproductive system in mammals (Němeček *et al.*, 2017). This is supported by the presence of HO in rats and guinea-pigs in the ovaries (Alexandreanu & Lawson, 2003a), uterus and placenta (Ihara *et al.*, 1998; Odrcich *et al.*, 1998; Alexandreanu & Lawson, 2002; Kreiser *et al.*, 2003; Zenclusen *et al.*, 2014), in which the distribution of isoforms differs according to the cell type (Alexandreanu & Lawson, 2003b). The high levels of GmmHO in tsetse fly reproductive organs suggests that HO may have a taxonomically broad role in reproductive activity. Interestingly, the high level of GmmHO staining in reproductive tissues indicates a role in both male and females, thus it is not sex specific.

High levels of HO mRNA (~1.7 fold in relation to the whole body) were found in the heterologous tissues known as fat body (Figure 4.10). Early studies carried out in *G. austeni* described the histological and histochemical characteristic of those tissues that occupy most of the insect abdomen. According to Tobe *et al.* (1973), the fat body in *G. austeni* consists of a series of spherical structures that are covered by a thin layer that unites those spheres together in a series of beads. Furthermore, smaller and denser spheres associated to the fat body were proposed to be oenocytes, specialized liver-like insect cells (Martins and Ramalho-Ortigao, 2012).

The highest levels of GmmHO expression were evident in the oenocytes. This corresponds with high levels of CPR, which have previously been shown to be associated with extremely high levels of CYP4G enzymes involved in cuticular biosynthesis in *Drosophila* (Qiu *et al.*, 2012) and *An. gambiae* (Balabanidou *et al.*,

2016). CPR is the obligate redox partner for both HO and P450s. CPR is also ubiquitously present in all cell types where P450 enzymes function, but generally at low levels in comparison with P450 (Qiu et al, 2012). Thus, the high levels of CPR in oenocytes have previously been explained by the correspondingly high levels of CYP4G enzymes in these cells (Qiu et al, 2012). However, the abundance of HO evident in tsetse fly oenocytes suggest that elevated levels of CPR may also be linked to HO expression. Since P450s are heme containing enzymes, this suggests that high levels of HO may play a critical role regulating safe heme levels in these specialised cells.

While CPR was found mostly in the endoplasmic reticulum a strong HO staining was observed in the nuclei of oenocytes (Figure 4.9). Although HO is classically a membrane anchored enzyme, it has been reported to be located in different cell compartments under certain physiological situations. For instance, cleaved HO-1 has been found in nuclei or other cell compartments (Dunn *et al.*, 2014). This might suggest a more direct non-enzymatic role in transcriptional regulation e.g. protein-protein interactions, although this is speculative at this stage.

The digestive tract in *G. m. morsitans* has a similar organization to those members of muscidae family, being divided in morphologically distinct regions (Billingsley, 1990): Anterior midgut (AM), bacteriome (BT, previously known as mycetome), secretory midgut (SM) and posterior midgut (PM). Here we analysed the enzyme expression in the digestive tract sections described above as well as in crop, proventriculus and hindgut. Our results suggests that HO is expressed in the whole digestive tract (Figure 4.6), especially between anterior midgut and posterior region. This is in accordance with the accumulation of green pigment in the posterior region of the organ shown in Chapter 3. The secretory midgut (or simply midgut), formed by tall columnar cells of irregular height that increase in size after a blood meal (Bohringer-Schweizer, 1977), is where the water is removed from the blood (Leak *et al.*, 2008) and the blood is then digested by an array (Cheeseman & Gooding, 1985) of digestive enzymes. Haemoglobin is thus likely to be broken down in this gut section. Thus, the HO-driven heme breakdown product may occur in the midgut, accumulating in the section following the midgut, the posterior gut. The higher molecular weight band may be an indication of dimer formation. Dimer formation has previously been observed in human HO-1 dimerization driven by the hydrophobic interaction in the C-

terminal transmembrane segment and is implicated in the stabilization of HO-1 in ER (Hwang et al, 2009)

The effect of blood meal in the HO mRNA levels of the female digestive tract (figure 4.13) suggests that HO is an early blood feeding-induced gene in this organ, reaching approximately 3.5 fold expression at 12h ABM. This may be due to the high amounts of heme containing blood (~5.24 mg dry weight), ingested by the female tsetse fly (Bursell, 1965), whose breakdown is likely to cause formation of ROS that may be a threat to homeostasis.

Interestingly, the GmmHO antibodies detected a doublet in the ~31 kDa size range expected for GmmHO in the proventriculus (Figure 4.6). This could be indicative of post translational modification, possibly phosphorylation. Several post translational modifications have been observed in HOs (Dunn *et al.,* 2014). In human brain tissues, for examples phosphorylation has been observed for this enzyme (Barone *et al.*, 2012; Beck *et al.*, 2010) which may be related to specific subcellular localization. However, the occurrence of a post translational modification in GmmHO requires further investigation to confirm this finding.

In summary, our results suggest that HO is a ubiquitous enzyme whose expression can be can be triggered by blood meal in fat body and digestive tract, consistent with a role in defence against blood-derived heme toxicity as well as raising the possibility of involvement in the catabolism of lipids.

CHAPTER 5 – CONCLUSIONS AND FINAL REMARKS

5.1 HEME DEGRADATION BY THE ENZYME HEME OXYGENASE IS AN ACTIVE DETOXIFICATION MECHANISM in *G. morsitans morsitans*

Heme is a ubiquitous biological compound involved in several relevant physiological processes either as a cofactor or prosthetic moiety of hemoproteins (Smith and Witty, 2002). Although an essential element, heme in its free form can be highly toxic (Kumar & Bandyopadhyay, 2005). For hematophagous arthropods this is particularly problematic since they consume large volumes of blood, often several times their own unfed body weight (Lehane, 2005). Such organisms have thus developed several heme detoxification mechanisms such as heme sequestration by the peritrophic matrix (Pascoa et al, 2002; Davenport *et al.*, 2006), heme binding with (Dansa-Petretski *et al.*,1995; Maya-Monteiro *et al.*, 2000), heme polymerisation (Oliveira *et al.*, 1999; Silva *et al.*, 2007) and degradation by heme oxygenase (Spencer, 2016). The latter, although extensively studied in humans has not been well studied in insects.

In this thesis (Chapters 2 and 3) it has been shown that tsetse flies contain an active heme oxygenase, thus a potential enzymatic heme detoxification pathway . GmmHO was cloned directly from tsetse female tissues using primers specific for the putative coding sequence available in database (Acession number GMOY004329, VectorBase). This yielded a gene with exact amino acid sequence to the data base sequence, apart from ~10% of the clones that contained a serine to proline substitution at the amino acid position 171.

The activity observed for recombinant GmmHO was verified by HPLC analysis of female tsetse digestive tract contents (Figure 3.2 and 3.3), which showed that after a single blood meal the concentration of heme rises immediately after a blood meal and then decreases. Concomitantantly, the biliverdin concentration rises, peaking at 48h ABM. These results, however, also show that heme concentration in the insect midgut were about 100x higher than the highest concentration observed for the biliverdin isomers, suggesting that either heme is being rapidly excreted or other heme detoxification processes are the major contributors to heme excretion and detixification in the insect.

In the dengue fever vector *Ae. aegypti*, an integral type I peritrophic matrix (PM) AeIMUCI has been shown to possess dual functions in binding chitin as well as large amounts of heme *in vitro* (Davenport *et al.*, 2006). This strongly suggests that the PM protein is capable of capturing blood derived heme to defend the insect against toxic effects of the compound. The tsetse fly *G. m.morsitans* possesses a 3-layered type II peritrophic matrix (Lehane *et al.*, 1996), which is continuously secreted by a specialized group of cells in the proventriculus either before or after a blood meal. Rose *et al.* (2014) investigated the proteomic composition of the tsetse fly peritrophic matrix, identifying nearly 300 proteins, several of which were peritrophins. Two of the most abundant (GmmPer108 and GmmPer66) present mucin-like domains, which may play a similar role to AeIMUCI as a first barrier defence against heme, although this has yet to be confirmed experimentally.

Polymerisation of blood derived heme is another mechanism that may explain the low levels of biliverdin observed in the tsetse fly digestive tract. Early studies (Bursell, 1965; Langley, 1966) on blood digestion in the *G. m. morsitans* digestive tract suggests that high concentrations of hematin (heme) produced by haemoglobin digestion are excreted by the fly. However it is not clear in which form the porphyrin is excreted. Transmission electron microscopy (TEM) analysis of the lumen content from the Chagas disease vector *R. prolixus*, has revealed that large amounts of electron-dense aggregates with similar spectroscopical characteristics to hemozoin (Oliveira *et al.*, 1999) are present in the insect, and its formation is induced by the perimicrovillar membrane (Silva *et al.*, 2007). Similar analysis of tsetse midgut contents and faeces would determine if a similar event is occurring in *G. m. morsitans*.

Overall, the data demonstrates that GmmHO is an active heme oxygenase. However, although it may contribute to heme detoxification in the tsetse fly, it is not the principle mechanism of heme detoxification. Instead it may operate as part of an orchestrated process in the organism aimed at minimising the risks of a blood based diet.

5.2 GMMHO SHARES BIOCHEMICAL FEATURES WITH *DROSOPHILA MELANOGASTER*

Unlike mammals (Tenhunen *et al.*, 1969), insects HOs have only relatively recently been cloned and characterized (Zhang et al., 2004; Spencer, 2016). The fruit fly *D. melanosgaster* HO shows marked differences to canonical HOs such as non-alpha IX biliverdin regiospecificity and a slower degradation rate. By contrast, AgHO shares quite similar biochemical features to mammals HOs such as mode of binding and Soret peaks similar to those observed in mammals.

Analysis of the GmmHO-heme complex produced absorption spectra most similar to those seen in DmHO. Furthermore, there was a requirement for the iron chelator desferrioxamine to release iron from biliverdin-HO complex (Yoshida & Kikushi, 1978). This suggests that GmmHO shares similar biochemical features to DmHO, and an indication that GmmHO has not evolved specific structural or functional adaptations for hematophagous behaviour. However, further comparative studies are required to test this conclusively.

5.3 GmmHO IS A UBIQUITOUS GENE HIGHLY EXPRESSED IN OENOCYTES AND DIGESTIVE TRACT AND MAY PLAY OTHER ROLES

What role does HO play in the tsetse fly (and by extension hematophagous insects) was a major question addressed in this study. The role of microsomal HOs was believed to be solely involved in the breakdown of heme from senescent hemoglobins (Tenhunen, 1969; Khan & Quigley, 2011). However, further studies in human HOs have shown the enzymes to be linked to a broader array of physiological roles (Maines and Gibbs, 2005). In hematophagous insects studies have indicated that those enzymes are linked to detoxification of blood derived heme (Graca-Souza *et al.*, 2006) and reproduction (Spencer, 2016).

The involvement of HO in the breakdown of heme derived from hemoglobin has been supported by the presence of biliverdin isomers in the lumen content of *R. prolixus* (Paiva-Silva, 2006) and *Ae. aegypti* (Pereira *el al.*, 2007). However, the HOs associated with the production of these heme degradation products have not been cloned or characterized. Here HO activity in the insect digestive tract in tsetse flies has been corroborated by the accumulation of biliverdin pigment in the lumen of the posterior section of the midgut organ by HPLC analysis as well as positive immunoreactive signals to GmHO antibodies in the anterior, mid and posterior sections of the gut. These results are in agreement with previous descriptions of blood degradation in the tsetse fly (Bursell *at al.*, 1965). Importantly, this is the first time that both HO tissue distribution and *in vivo* activity have been confirmed in a hematophagous insect. Additionally, the increase in mRNA levels in the first few hours following a single blood meal provides support to the idea that HO contributes in the defence against heme toxicity.

In this thesis the tissue distribution of HO in an insect has been demonstrated for the first time. Most importantly this has presented further evidence for a key role in reproduction. In tsetse flies, GmmHO is highly expressed in the reproductive tissues of both adult male and female tsetse flies. It has not been demonstrated if GmmHO is constitutively expressed. However, expression levels did not seem to be induced by blood feeding, thus if induction of GmmHO occurs, it must be by another mechanism. Although the presence of GmmHO in these tissues suggests that heme oxygenase activity plays an active role in reproduction, this still needs to be further confirmed by

gene silencing experiments. Taking into consideration the adenotrophic viviparity of *G. m. morsitans*, further comparisons with *An. gambiae* are merited since inhibition of heme oxygenase activity inhibits egg production (Spencer, 2016). This may point to common reproductory biochemical pathways that might be targetted for the development of strategies to control tsetse fly and other insect populations.

Another major finding has been the observation that GmmHO is highly expressed in oenocytes. This corresponds with high levels of its obligate redox partner, CPR. Previous work with *An. gambiae* and *D. melanogaster* has suggested that such high levels of CPR are related to high levels of P450 to support cuticular hydrocarbon biosynthesis (Lycett *et al.* 2006; Qiu *et al*, 2012). Thus the demonstration that oenocytes also express extremely high levels of HO adds a new perspective on the functional roles and interactions between P450s, HO and their common redox partner CPR. Until now, it has been difficult to morphologically separate oenocytes from the fat bodies in tsetse flies. Thus, the production of GmmHO antibodies and demonstration of high levels of GmmHO in these cells has provided a diagnostic marker for future studies of oencytes in testse flies.

The induction of expression in the fat bodies with attached oenocytes by a single blood meal also provided convincing evidence that HO may be implicated in other physiological events such as the metabolism of lipids (Gutierrez et al., 2007) and tyrosine (Tobe *et al.*, 1973), specially taking in consideration the close dietary-nutrient metabolic relationship between oenocytes and fat body observed in insects (Tobe *et al.*, 1973; Makki et al., 2014).

Taken together, the results strongly indicate that, GmmHO is not restricted to one function alone, but by degrading heme, generating by-products potentially involved in signalling and protection against ROS and being highly expressed in several tissues, is engaged in an array of physiological events.

5.4 Future perspectives

Here, we showed that GmmHO is an active HO detoxification pathway present in several organs of *G. m. morsitans*, sheding light into the degradation of heme group in blood feedings. Unfortunately, due to time limitations some experiments were not performed however our work has opened possibilities that would contribute to a wider understanding of the nature of insect HOs, particularly in bood feeding insects. Some of those include:

1) Test the inducibility of GmmHO by heat and chemical inducers – a trait commonly observed in mammals HO1 homologues
2) Further understand the role of GmmHO in reproduction by dsRNA knockdown of the gene – expected phenotype on reproduction
3) Analysis of recombinant GmmHO by electron paramagnetic resonance (EPR) in order to understand the differences in terms of heme binding in comparison to other heme oxygenases

6 – REFERENCES

Aksoy, S. (2008). Transgenesis and the management of vector-bome disease / edited by Serap Aksoy. Springer Science+Business Media, New York 187pp. ISBN 978-0-387-78224-9

Alexandreanu, I. C., & Lawson, D. M. (2002). Effects of chronic administration of a heme oxygenase substrate or inhibitor on progression of the estrous cycle, pregnancy and lactation of Sprague-Dawley rats. Life Sciences, **72**, 2, 153–62.

Alexandreanu, I. C., & Lawson, D. M. (2003a). Heme oxygenase in the rat anterior pituitary: immunohistochemical localization and possible role in gonadotropin and prolactin secretion. Experimental Biology and Medicine **228,** 1, 64–9.

Alexandreanu, I. C., & Lawson, D. M. (2003b). Heme oxygenase in the rat ovary: immunohistochemical localization and possible role in steroidogenesis. Experimental Biology and Medicine **228**, 1, 59–63.

Balabanidou, V., Kampouraki, A., MacLean, M., Blomquist, G. J., Tittiger, C., Juárez, M. P, Mijailovskyd, S. J., Chalepakis, G., Anthousi, A., Lynd, A., Antoinee, S., Hemingway, J., Ranson, H., Lycett, G., Vontas, J. (2016). Cytochrome P450 associated with insecticide resistance catalyzes cuticular hydrocarbon production in Anopheles gambiae. Proceedings of the National Academy of Sciences of the United States of America **113**, 33, 9268–73.

Bansal, S., Biswas, G., & Avadhani, N. G. (2014). Mitochondria-targeted heme oxygenase-1 induces oxidative stress and mitochondrial dysfunction in macrophages, kidney fibroblasts and in chronic alcohol hepatotoxicity. Redox Biology **2**, 273–283.

Barone, E., Di Domenico, F., Sultana, R., Coccia, R., Mancuso, C., Perluigi, M., & Butterfield, D. A. (2012). Heme oxygenase-1 posttranslational modifications in the brain of subjects with Alzheimer disease and mild cognitive impairment. Free Radical Biology and Medicine **52**(11), 2292–2301.

Barrett, M. P., Burchmore, R. J., Stich, A., Lazzari, J. O., Frasch, A. C., Cazzulo, J. J., & Krishna, S. (2003). The trypanosomiases. The Lancet **362**(9394), 1469–1480.

Beale, S. I., & Yeh, J. I. (1999). Deconstructing heme. Nature Structural Biology **6**, 10, 903–905.

Beck, K., Wu, B. J., Ni, J., Santiago, F. S., Malabanan, K. P., Li, C., Wang, Y., Khachigian, L.M. Stocker, R. (2010). Interplay Between Heme Oxygenase-1 and the Multifunctional Transcription Factor Yin Yang 1 in the Inhibition of Intimal HyperplasiaNovelty and Significance. Circulation Research, **107**, 12, 1490-1497.

Bhatt, S., Weiss, D. J., Cameron, E., Bisanzio, D., Mappin, B., Dalrymple, U., Battle K., Moyes C.L., Henry A., Eckhoff P.A., Wenger E.A., Briët O., Penny M.A., Smith T.A., Bennett A., Yukich J., Eisele T.P., Griffin J.T., Fergus C.A., Lynch M., Lindgren F., Cohen J.M., Murray C.L.J., Smith D.L., Hay S.I., Cibulskis R.E., Gething, P. W. (2015). The effect of malaria control on Plasmodium falciparum in Africa between 2000 and 2015. Nature, **526**, 7572, 207–211.

Billingsley, P. F. (1990). The Midgut Ultrastructure of Hematophagous Insects. Annual Review of Entomology, **35**(1), 219–248.

Bouteille, B., & Buguet, A. (2012). The detection and treatment of human African trypanosomiasis. Research and Reports in Tropical Medicine, **3**, 35-45.

Braz, G. R. C., Moreira, M. F., Masuda, H., & Oliveira, P. L. (2002). Rhodnius heme-binding protein (RHBP) is a heme source for embryonic development in the blood-sucking bug Rhodnius prolixus (Hemiptera, Reduviidae). Insect Biochemistry and Molecular Biology, 32, 4, 361–367.

Brun, R., Blum, J., Chappuis, F., Burri, C., Loko, L., & Mpia, B. (2010). Human African trypanosomiasis. Lancet **375**, 9709, 148–159.

Bursell, E. (1965). Nitrogenous waste products of the tsetse fly, Glossina morsitans. Journal of Insect Physiology, **11,** 7, 993–1001.

Chau, L.-Y. (2015). Heme oxygenase-1: emerging target of cancer therapy. Journal of Biomedical Science, **22**, 1, 22.

Cheeseman, M. T., & Gooding, R. H. (1985). Proteolytic enzymes from tsetse flies, Glossina morsitans and Glossina palpalis (Diptera: Glossinidae). Insect Biochemistry, **15**, 6, 677–680.

Chu, G. C., Katakura, K., Tomita, T., Zhang, X., Sun, D., Sato, M., Sasahara, M.; Kayama, T. Yoshida, T. (2000). Histidine 20, the crucial proximal axial heme ligand of bacterial heme oxygenase Hmu O from Corynebacterium diphtheriae. The Journal of Biological Chemistry, **275**, 23, 17494–17500.

Clark, M. K., & Dahm, P. A. (1973). Phenobarbital-Induced, Membrane-Like Scrolls In The Oenocytes Of Musca Domestica Linnaeus. The Journal of Cell Biology, **56**, 870–875.

Cornejo, J., Willows, R. D., & Beale, S. I. (1998). Phytobilin biosynthesis: cloning and expression of a gene encoding soluble ferredoxin-dependent heme oxygenase from Synechocystis sp. PCC 6803. The Plant Journal : For Cell and Molecular Biology, **15**, 1, 99–107.

Cruse, I., & Maines, M. D. (1988). Evidence suggesting that the two forms of heme oxygenase are products of different genes. The Journal of Biological Chemistry, **263**, 7, 3348–53.

Dansa-Petretski, M., Ribeiro, J. M. C., Atella, G. r. C., Masuda, H., & Oliveira, P. L. (1995). Antioxidant Role of Rhodnius prolixus Heme-binding Protein. Journal of Biological Chemistry, **270**, 18, 10893–10896.

Devenport, M., Alvarenga, P. H., Shao, L., Fujioka, H., Bianconi, M. L., Oliveira, P. L., & Jacobs-Lorena, M. (2006). Identification of the Aedes aegypti peritrophic matrix protein AeIMUCI as a heme-binding protein. Biochemistry, **45**, 31, 9540–9549.

Dunn, L. L., Midwinter, R. G., Ni, J., Hamid, H. A., Parish, C. R., & Stocker, R. (2014). New Insights into Intracellular Locations and Functions of Heme Oxygenase-1. Antioxidants & Redox Signaling **20**, 11, 1723–1742.

Fairlamb, A. H. (2003). Chemotherapy of human African trypanosomiasis: current and future prospects. Trends in Parasitology **19**, 11, 488–494.

Fèvre, E. M., Coleman, P. G., Welburn, S. C., & Maudlin, I. (2004). Reanalyzing the 1900–1920 Sleeping Sickness Epidemic in Uganda. Emerging Infectious Diseases **10**, 4, 567–573.

Giordano, A., Nisoli, E., Tonello, C., Cancello, R., Carruba, M. O., & Cinti, S. (2000). Expression and distribution of heme oxygenase-1 and -2 in rat brown adipose tissue: the modulatory role of the noradrenergic system. FEBS Letters **487**, 2, 171–175.

Gohya, T., Zhang, X., Yoshida, T., & Migita, C. T. (2006). Spectroscopic characterization of a higher plant heme oxygenase isoform-1 from Glycine max (soybean): coordination structure of the heme complex and catabolism of heme. FEBS Journal, **273**, 23, 5384–5399.

Gozzelino, R. (2016). The Pathophysiology of Heme in the Brain. Current Alzheimer Research, **13**, 2, 174–84.

Graca-souza, a., Maya-monteiro, c., Maiva-silva, g., Braz, g., Paes, m., Sorgine, m., Oliveira, m.f., Oliveira, p. (2006). Adaptations against heme toxicity in blood-feeding arthropods. Insect Biochemistry and Molecular Biology, **36**, 4, 322–335.

Hagan, H. R. (1951). Embryology of the Viviparous Insects. Science (Vol. 115). New York: Ronald Press. 472p. ISBN 13: 9781258400071

Hayashi, S., Omata, Y., Sakamoto, H., Higashimoto, Y., Hara, T., Sagara, Y., & Noguchi, M. (2004). Characterization of rat heme oxygenase-3 gene. Implication of processed pseudogenes derived from heme oxygenase-2 gene. Gene, **336**, 2, 241–250.

Hualin, C., Wenli, X., Dapeng, L., Xijing, L., Xiuhua, P., & Qingfeng, P. (2012). The Anti-inflammatory Mechanism of Heme Oxygenase-1 Induced by Hemin in Primary Rat Alveolar Macrophages. Inflammation, **35**, 3, 1087–1093.

Hwang, H.-W., Lee, J.-R., Chou, K.-Y., Suen, C.-S., Hwang, M.-J., Shieh, R.-C., & Chau, L.-Y. (2009). Heme oxygenase-1 exists as dimers in endoplasmic reticulum. The FASEB Journal, **23**, 1, 875.3-875.3.

Immenschuh, S., & Schröder, H. (2006). Heme oxygenase-1 and cardiovascular disease. Histology and Histopathology, **21**, 6, 679–85.

Ishikawa, S., Tamaki, S., Ohata, M., Arihara, K., & Itoh, M. (2010). Heme induces DNA damage and hyperproliferation of colonic epithelial cells via hydrogen peroxide produced by heme oxygenase: A possible mechanism of heme-induced colon cancer. Molecular Nutrition & Food Research, **54**, 8, 1182-1191.

Keyse, S. M., & Tyrrell, R. M. (1989). Heme oxygenase is the major 32-kDa stress protein induced in human skin fibroblasts by UVA radiation, hydrogen peroxide, and sodium arsenite. Proceedings of the National Academy of Sciences of the United States of America, **86**, 1, 99–103.

KIM, H. P., Wang, X., Galbiati, F., Ryter, S. W., & Choi, A. M. K. (2004). Caveolae compartmentalization of heme oxygenase-1 in endothelial cells. The FASEB Journal, **18**, 10, 1080–1089.

Klotz, I. M., & Klotz, T. A. (1955). Oxygen-Carrying Proteins: A Comparison of the Oxygenation Reaction in Hemocyanin and Hemerythrin with That in Hemoglobin. Science, **121**, 477–480.

Kreiser, D., Kelly, D. K., Seidman, D. S., Stevenson, D. K., Baum, M., & Dennery, P. A. (2003). Gestational pattern of heme oxygenase expression in the rat. Pediatric Research, **54**, 2, 172–188.

Kumar, S., & Bandyopadhyay, U. (2005). Free heme toxicity and its detoxification systems in human. Toxicology Letters, **157**, 3, 175–188.

Kutty, R. K., & Maines, M. D. (1981). Purification and characterization of biliverdin reductase from rat liver. The Journal of Biological Chemistry, **256**, (8), 3956–62.

Lara, F. A., Lins, U., Paiva-Silva, G., Almeida, I. C., Braga, C. M., Miguens, F. C., Oliveira, P.L., Dansa-Petretski, M. (2003). A new intracellular pathway of haem detoxification in the midgut of the cattle tick Boophilus microplus: aggregation inside a specialized organelle, the hemosome. The Journal of Experimental Biology, **206**, 10, 1707–15.

Leak, S. G. A., Ejigu, D., & Vreysen, M. J. B. (2008). COLLECTION OF ENTOMOLOGICAL BASELINE DATA FOR TSETSE AREA-WIDE INTEGRATED PEST MANAGEMENT PROGRAMMES Joint FAO/IAEA Programme of Nuclear Techniques in Food and Agriculture Vienna, Austria.

Lehane, M. J., & Lehane, M. J. (2005). The biology of blood-sucking in insects. Cambridge University Press. 336p. ISBN-13: 9780521836081

Lemon, S. M., & Institute of Medicine (U.S.). Forum on Microbial Threats. (2008). Vector-borne diseases : understanding the environmental, human health, and ecological connections : workshop summary. National Academies Press.

Lightning, L. K., Huang, H., Moenne-Loccoz, P., Loehr, T. M., Schuller, D. J., Poulos, T. L., & de Montellano, P. R. O. (2001). Disruption of an Active Site Hydrogen Bond Converts Human Heme Oxygenase-1 into a Peroxidase. Journal of Biological Chemistry, **276**, 14, 10612–10619.

Liu, Y., Moënne-Loccoz, P., Loehr, T. M., & Ortiz de Montellano, P. R. (1997). Heme oxygenase-1, intermediates in verdoheme formation and the requirement for reduction equivalents. The Journal of Biological Chemistry, **272**, 11, 6909–17.

Lockey, K. H. (1988). Lipids of the insect cuticle: origin, composition and function. Comparative Biochemistry and Physiology Part B: Comparative Biochemistry, **89**, 4, 595–645.

Loder, P. M. (1997). Size of blood meals taken by tsetse flies (Glossina spp.) (Diptera: Glossinidae) correlates with fat reserves. Bulletin of Entomological Research, **87**, 547–549.

LODER, P. M. J., HARGROVE, J. W., & RANDOLPH, S. E. (1998). A model for blood meal digestion and fat metabolism in male tsetse flies (Glossinidae). Physiological Entomology, **23**, 1, 43–52.

Louis, F. J., Simarro, P. P. (2005). Rough start for the fight against sleeping sickness in French Equatorial Africa. Medecine Tropicale : Revue Du Corps de Sante Colonial, **65**, 3, 251–7.

Ma, W. C., Denlinger, D. L., Järlfors, U., & Smith, D. S. (1975). Structural modulations in the tsetse fly milk gland during a pregnancy cycle. Tissue & Cell, **7**, 2, 319–30.

Maines, M. D. (1988). Heme oxygenase: function, multiplicity, regulatory mechanisms, and clinical applications. FASEB Journal : Official Publication of the Federation of American Societies for Experimental Biology, **2**, 10, 2557–68.

Maines, M. D., Gibbs, P. E. M. (2005). 30 some years of heme oxygenase: From a "molecular wrecking ball" to a "mesmerizing" trigger of cellular events. Biochemical and Biophysical Research Communications, **338**, 1, 568–577.

Martins, G., & Ramalho-Ortigão, J. (2012). Oenocytes in insects. Inver Surv J **9**, 139–152.

Maya-Monteiro, C. M., Daffre, S., Logullo, C., Lara, F. A., Alves, E. W., Capurro, M. L., Zingali, R., Almeida, I.C., Oliveira, P. L. (2000). HeLp, a Heme Lipoprotein from the Hemolymph of the Cattle Tick,Boophilus microplus. Journal of Biological Chemistry, **275**, 47, 36584–36589.

McCoubrey, W. K., Huang, T. J., & Maines, M. D. (1997). Isolation and characterization of a cDNA from the rat brain that encodes hemoprotein heme oxygenase-3. European Journal of Biochemistry, **247**, 2, 725–32.

Miller, Y. I., Altamentova, S. M., & Shaklai, N. (1997). Oxidation of Low-Density Lipoprotein by Hemoglobin Stems from a Heme-Initiated Globin Radical: Antioxidant Role of Haptoglobin. Biochemistry **36**, 40, 12189–12198.

Muramoto, T., Tsurui, N., Terry, M. J., Yokota, A., & Kohchi, T. (2002). Expression and biochemical properties of a ferredoxin-dependent heme oxygenase required for phytochrome chromophore synthesis. Plant Physiology **130**, 4, 1958–66.

Němeček, D., Dvořáková, M., & Sedmíková, M. (2017). Heme oxygenase/carbon monoxide in the female reproductive system: an overlooked signalling pathway. International Journal of Biochemistry and Molecular Biology **8**, 1, 1–12.

Nettleship, J. (n.d.). OPPF-UK Standard Protocols: Insect Expression. Retrieved from https://www.oppf.rc-harwell.ac.uk/OPPF/protocols/sop/OPPF-UK SOP Insect Expression 20161006.pdf

Okada, K. (2009). The novel heme oxygenase-like protein from Plasmodium falciparum converts heme to bilirubin IXα in the apicoplast. FEBS Letters, **583**, 2, 313–319.

Oliveira, M. F., Silva, J. R., Dansa-Petretski, M., de Souza, W., Lins, U., Braga, C. M. S., Masuda, H., Oliveira, P. L. (1999). Haem detoxification by an insect. Nature **400**, 6744, 517–518.

Öllinger, R., Pratschke, J. (2010). Role of heme oxygenase-1 in transplantation. Transplant International, **23**, 11, 1071–1081.

Omata Y., Noguchi M. (1998) A Spectroscopic Study on the Intermediates of Heme Degradation by Heme Oxygenase. In: Ishimura Y., Shimada H., Suematsu M. (eds) Oxygen Homeostasis and Its Dynamics. Keio University Symposia for Life Science and Medicine, vol 1. Springer, Tokyo 522p, ISBN 978-4-431-68476-3

Paine, A., Eiz-Vesper, B., Blasczyk, R., & Immenschuh, S. (2010). Signaling to heme oxygenase-1 and its anti-inflammatory therapeutic potential. Biochemical Pharmacology **80**, 12, 1895–1903.

Paiva-Silva, G. O., Cruz-Oliveira, C., Nakayasu, E. S., Maya-Monteiro, C. M., Dunkov, B. C., Masuda, H., … Oliveira, P. L. (2006). A heme-degradation pathway in a blood-sucking insect. Proceedings of the National Academy of Sciences **103**, 21, 8030–8035.

Panahian, N., Yoshiura, M., & Maines, M. D. (1999). Overexpression of heme oxygenase-1 is neuroprotective in a model of permanent middle cerebral artery occlusion in transgenic mice. Journal of Neurochemistry **72**, 3, 1187–203.

Parfenova, H., Leffler, C. W., Basuroy, S., Liu, J., & Fedinec, A. L. (2012). Antioxidant Roles of Heme Oxygenase, Carbon Monoxide, and Bilirubin in Cerebral Circulation during Seizures. Journal of Cerebral Blood Flow & Metabolism 32, 6, 1024–1034.

Pascoa, V., Oliveira, P. L., Dansa-Petretski, M., Silva, J. R., Alvarenga, P. H., Jacobs-Lorena, M., & Lemos, F. J. A. (2002). Aedes aegypti peritrophic matrix and its interaction with heme during blood digestion. Insect Biochemistry and Molecular Biology **32**, 5, 517–23.

Pentreath, V. W. (1995). Trypanosomiasis and the nervous system. Transactions of the Royal Society of Tropical Medicine and Hygiene **89**, 1, 9–15.

Pentreath, V. W., Baugh, P. J., & Lavin, D. R. (1994). Sleeping sickness and the central nervous system. The Onderstepoort Journal of Veterinary Research **61**, 4, 369–77.

Pereira, L. O. R., Oliveira, P. L., Almeida, I. C., & Paiva-Silva, G. O. (2007). Biglutaminyl-biliverdin IX alpha as a heme degradation product in the dengue fever insect-vector Aedes aegypti. Biochemistry **46**, 23, 6822-9.

Riveron, J. M., Chiumia, M., Menze, B. D., Barnes, K. G., Irving, H., Ibrahim, S. S., Weedall, G.D., Mzilahowa, T., Wondji, C. S. (2015). Rise of multiple insecticide resistance in Anopheles funestus in Malawi: a major concern for malaria vector control. Malaria Journal **14**, 344.

Rosano, G. L., & Ceccarelli, E. A. (2014). Recombinant protein expression in Escherichia coli: advances and challenges. Frontiers in Microbiology **5**, 172,

Rose, C., Belmonte, R., Armstrong, S. D., Molyneux, G., Haines, L. R., Lehane, M. J., Wastling, J., Acosta-Serrano, A. (2014). An Investigation into the Protein Composition of the Teneral Glossina morsitans morsitans Peritrophic Matrix. PLoS Neglected Tropical Diseases **8**, 4, e2691.

Ryter, S. W., Tyrrell, R. M. (2000). The heme synthesis and degradation pathways: role in oxidant sensitivity. Heme oxygenase has both pro- and antioxidant properties. Free Radical Biology & Medicine **28**, 2, 289–309.

Sassa, S. (2004). Why Heme Needs to Be Degraded to Iron, Biliverdin IXα, and Carbon Monoxide? Antioxidants & Redox Signaling **6**, 5, 819–824.

Saunders, D. S., & Dodd, C. W. H. (1972). Mating, insemination, and ovulation in the tsetse fly, Glossina morsitans. Journal of Insect Physiology **18**, 2, 187–198.

Schmitt, T. H., Frezzatti, W. A., & Schreier, S. (1993). Hemin-Induced Lipid Membrane Disorder and Increased Permeability: A Molecular Model for the Mechanism of Cell Lysis. Archives of Biochemistry and Biophysics **307**, 1, 96–103.

Schuller, D. J., Wilks, A., Ortiz de Montellano, P. R., & Poulos, T. L. (1999). Crystal structure of human heme oxygenase-1. Nature Structural Biology **6**, 9, 860–867.

Shibahara, S., Yoshida, T., & Kikuchi, G. (1978). Induction of heme oxygenase by hemin in cultured pig alveolar macrophages. Archives of Biochemistry and Biophysics **188**, 2, 243–250.

Silva, J. R., Mury, F. B., Oliveira, M. F., Oliveira, P. L., Silva, C. P., & Dansa-Petretski, M. (2007). Perimicrovillar membranes promote hemozoin formation into Rhodnius prolixus midgut. Insect Biochemistry and Molecular Biology **37**, 6, 523–531.

Smith, A. G., & Witty, M. (2002). Heme, chlorophyll, and bilins : methods and protocols. Humana Press. 340p. ISBN 978-1-59259-243-2

Soldano, A., Yao, H., Rivera, M., Ceccarelli, E. A., & Catalano-Dupuy, D. L. (2014). Heme-iron utilization by Leptospira interrogans requires a heme oxygenase and a plastidic-type ferredoxin-NADP+ reductase. Biochimica et Biophysica Acta (BBA) - General Subjects **1840**, 11, 3208–3217.

Spencer, C. (2016). Molecular characterisation of Anopheles gambiae haem oxygenase. PhD thesis. University of Liverpool. 167p

Steverding, D. (2008). The history of African trypanosomiasis. Parasites and Vectors **1**, 3

Sun, Y., Rotenberg, M. O., & Maines, M. D. (1990). The Journal of biological chemistry. Journal of Biological Chemistry **265**, 8212–8217.

Takahashi, K., Hara, E., Suzuki, H., Sasano, H., & Shibahara, S. (1996). Expression of heme oxygenase isozyme mRNAs in the human brain and induction of heme oxygenase-1 by nitric oxide donors. Journal of Neurochemistry **67**, 2, 482–9.

Takahashi, S., Wang, J., Rousseau, D. L., Ishikawa, K., Yoshida, T., Host, J. R., & Ikeda-Saitot, M. (1994). THE JOURNAL OF BIOLOGICAL CHEMISTRY Heme-Heme Oxygenase Complex STRUCTURE OF THE CATALYTIC SITE AND ITS IMPLICATION FOR OXYGEN ACTIVATION **269**, 2, 1010–1014.

Tenhunen, R., Marver, H. S., & Schmid, R. (1969). Microsomal heme oxygenase. Characterization of the enzyme. The Journal of Biological Chemistry **244**, 23, 6388–94.

Tijet, N., Helvig, C., & Feyereisen, R. (2001). The cytochrome P450 gene superfamily in Drosophila melanogaster: annotation, intron-exon organization and phylogeny. Gene **262** 1, 189–98.

Tobe, S. S., Davey, K. G., & Huebner, E. (1973). Nutrient transfer during the reproductive cycle in Glossina austeni newst.: Histology and histochemistry of the milk gland, fat body, and oenocytes. Tissue and Cell **54**, 633–650.

Tobe, S. S., & Langley, P. A. (1978). Reproductive Physiology of Glossina. Annual Review of Entomology, **23**, 1, 283–307.

Turkseven, S., Kruger, A., Mingone, C. J., Kaminski, P., Inaba, M., Rodella, L. F., … Abraham, N. G. (2005). Antioxidant mechanism of heme oxygenase-1 involves an increase in superoxide dismutase and catalase in experimental diabetes. AJP: Heart and Circulatory Physiology, **289**, 2, H701–H707.

Vincent, S. H. (1989). Oxidative effects of heme and porphyrins on proteins and lipids. Seminars in Hematology **26**, 2, 105–13.

Wheeler, W. M., & Morton, W. (1892). Concerning the Blood-Tissue of the Insecta. Psyche: A Journal of Entomology **6**, 190, 216–220.

WHO | Trypanosomiasis, human African (sleeping sickness). (2017). WHO. Available on the Internet at: http://www.who.int/mediacentre/factsheets/fs259/en/ (accessed on: 21 march 2017)

WHO | Vector-borne diseases. (2016). WHO. Available on the Internet at: http://www.who.int/mediacentre/factsheets/fs387/en/ (accessed on: 21 march 2017)

Wilks, A., & Schmitt, M. P. (1998). Expression and Characterization of a Heme Oxygenase (Hmu O) from Corynebacterium diphtheriae. The Journal of Biological Chemistry **273**, 9, 837–841.

WILSON, S. G., MORRIS, K. R., LEWIS, I. J., & KROG, E. (1963). The effects of trypanosomiasis on rural economy with special reference to the Sudan, Bechuanaland and West Africa. Bulletin of the World Health Organization, **28**, 5–6, 595–613.

Yoshida, T., Kikuchi, G (1977). Heme oxygenase purified to apparent homogeneity from pig spleen microsomes. Journal of Biochemistry, 81(1), 265–8.

Yuda, M., Hirai, M., Miura, K., Matsumura, H., Ando, K., & Chinzei, Y. (1996). cDNA cloning, expression and characterization of nitric-oxide synthase from the salivary glands of the blood-sucking insect Rhodnius prolixus. European Journal of Biochemistry **242**, 3, 807–12.

Zenclussen, M. L., Linzke, N., Schumacher, A., Fest, S., Meyer, N., Casalis, P. A., & Zenclussen, A. C. (2014). Heme oxygenase-1 is critically involved in placentation, spiral artery remodeling, and blood pressure regulation during murine pregnancy. Frontiers in Pharmacology **5**, 291.

Zhang, X., Sato, M., Sasahara, M., Migita, C. T., & Yoshida, T. (2004). Unique features of recombinant heme oxygenase of Drosophila melanogaster compared with those of other heme oxygenases studied. European Journal of Biochemistry **271**, 9, 1713–1724.

Zhu, W., Wilks, A., & Stojiljkovic, I. (2000). Degradation of heme in gram-negative bacteria: the product of the hemO gene of Neisseriae is a heme oxygenase. Journal of Bacteriology **182**, 23, 6783–90.